Investigation of molecular polarizabilities and derivatives in halomethanes

by

Gulshan. M. Sharma, B.Sc., M.Sc., Bombay University

A Thesis

submitted to the department of Chemistry

in partial fulfillment of the requirements

for the degree of

Master of Science

December 1993

Brock University

St. Catharines, Ontario

to my parents☺

ABSTRACT

The research undertaken was to obtain absolute Raman intensities for the symmetric stretching vibrations of the methyl halides, CH_3X with (X=F, Cl, Br), by experiment and theory.

The intensities were experimentally measured using the Ar+ ion gas laser as excitation source, a Spex 14018 double monochromator and a RCA C-31034 photomultiplier tube as detector. These intensities arise from changes in the derivative of the polarizability ($\partial \bar{\alpha}'$), with respect to vibration along a normal coordinate (∂q_i). It was intended that these derivatives obtained with respect to normal coordinates would be converted to derivatives with respect to internal coordinates, for a quantitative comparison with theory.

Theoretical numerical polarizability derivatives for the stretching vibrations are obtained using the following procedure. A vibration was simulated in the molecule by increasing and decreasing the respective bond by the amount ±0.005Å for the C-H bonds and ±0.01Å for the C-X (X=F, Cl, Br) bond. The derivative was obtained by taking the difference in the polarizability for the equilibrium geometry and the geometry when a particular bond is changed. This difference, when divided by the amount of change in each bond and the number of bonds present results in the derivative of the polarizability with respect to internal coordinate i.e., $\Delta\alpha/\Delta r$. These derivatives were obtained by two methods: 1} *ab initio* molecular orbital calculation and 2} theory of atoms in molecules (AIM) analysis.

Due to errors in the experimental setup only a qualitative analysis of the results was undertaken relative to the theory. Theoretically it is predicted that the symmetric carbon-halogen stretch vibrations are more intense than the respective carbon-hydrogen stretch, but only for the methyl chloride and bromide. The carbon fluorine stretch is less intense than the carbon-hydrogen stretch, a fact which is attributed to the small size and high electronegativity of the fluorine atom. The experimental observations are seen to agree

qualitatively with the theory results. It is hoped that when the experiment is repeated, a quantitative comparison can be made.

The analysis by the theory of atoms in molecules, along with providing polarizabilities and polarizability derivatives, gives additional information outlined below. The theory provides a pictorial description of the main factors contributing to the molecular polarizability and polarizability derivative. These contributions are from the charge transfer and atomic dipole terms i.e., transfer of charge from one atom to another and the reorganization of atomic electronic charge distribution due to presence of an electric field. The linear relationship between polarizability and molecular volume was also observed.

ACKNOWLEDGEMENTS

I would like to express my greatest thanks to Dr. Gough, for her guidance, advice and encouragement during my research work and thesis preparation. She made me feel like I was working with her rather than for her. It was a novel experience for both of us, and I am honoured to be very first graduate student among the many more to come. I have learnt a lot both on the personal and academic front. Thanks again, this was an experience I shall always remember.

The members of my committee, Dr. Moule for his patience and encouragement and Dr. Miller for his advice.

I would like to acknowledge Jim Ross, Tony and their "band of merry men", for all the techinical assistance and major improvements on the laser system.

My friends cum "councellors'" without whom I would never have made it. A mention of the few names: 'Janam', Kats&Peter, Othilla, He Xiau, Maria Luisa and the many others, who I may have encountered and those who have always been around me.

Finally, I wish to acknowledge the Chemistry Department of Brock University, for the financial support for the two years of my studies, and the members, for their advice in my work.

TABLE OF CONTENTS

LIST OF TABLES

Page

LIST OF FIGURES

Page

1: INTRODUCTION-

The main theme of this research was to determine absolute Raman intensities of the stretching vibrations of the halomethanes, namely methyl fluoride, methyl chloride and methyl bromide. These intensity measurements are obtained experimentally and theoretically. In the following we consider, the importance of studing Raman intensities, a review of the previous work done, and a brief description of the work undertaken for this thesis.

1.1: INTENSITIES IN RAMAN SPECTROSCOPY -

Historically the Raman effect was discovered in 1928, by C. V. Raman. This technique is helpful in determining the stereochemistry of new molecules, in the determination of the frequencies of the normal modes of vibration and from this to estimate the force constants involved. These force constants provide insight into the magnitude of the forces holding the molecules together. The basic principles of the Raman phenomenon are explained in Sec.2, and at this point we consider a brief description.

The Raman effect is a scattering phenomenon. Further the property of a sample which determines the degree of scattering is the polarizability. The polarizability is a measure of the degree to which electrons in the molecule can be displaced relative to the nuclei or it can be defined as the ease of charge redistribution. The changes in charge distribution which are usually obtained with respect to nuclear coordinates, can be related to intensities of various spectra, i.e., dipole moment derivatives to infra-red intensities, and molecular polarizability derivatives to vibrational Raman intensities.

Intensities in Raman trace scattering spectra derive from changes in the mean molecular polarizability, given by $\partial\bar{\alpha}$, with respect to displacement along some vibrational coordinate, given by ∂q_i. The Raman intensities are explicitly explained in Section 2.4.

The initial purpose for proposing various intensity models was that the mass independent polarizability derivatives could be expressed in the form of some other parameters which could be transferable between similar molecules. A detailed discussion of the different intensity models is given in Ref. 1, and in the following a list of the different models will be provided. 1} Valence-optical (VO) theory formulated in 1941 by Wolkenstein[2]. Further details of this theory are outlined in Sec. 1.2. 2} Atomic dipole interaction model proposed by Silberstein in 1917[3] and revived by Applequist[4] in 1977. The model considered an empirical partitioning of the polarizability made up of atomic contributions. It was suggested that the polarization of one atom contributes to the polarizability of the other atoms in terms of a dipole-induced dipole model.

1.2: BOND POLARIZABILITY MODEL or (VO) [5, 6]

The Raman intensities have most frequently been described by the bond polarizability model also known as the valence optical theory of intensities (V.O.T). It was introduced by Wolkenstein[2] and Eliashevich[7], and developed by Long[8].

The theory is based on the concept of additivity of molecular properties. This theory postulated that the derived molecular polarizability is made up of contributions due to stretching and change of orientation of the individual bonds of the molecule. The basic assumption of this theory stated that the polarizability of a bond is not affected by a change of bond orientation. The hypothesis was supported by J.Tang and A.C.Albrecht[9], through theoretical arguments.

The main reason for the proposal of this theory was: that if the Raman intensities of a given normal vibration could be related to the properties of a single structural unit, the chemical bond, then they could produce electro optical parameters in terms of bond polarizability derivatives, which could be transferred from one molecule to another for the prediction of Raman intensities, this concept being in analogy with group frequencies. Further the theory involved two assumptions: 1} that the total molecular polarizability can

be expressed as the sum of individual bond polarizabilities which are diagonal in their respective bond coordinate systems. 2} that bond interaction was neglected using zero order approximation i.e., stretching of an individual bond was taken to be independent of the other bonds and of changes in orientation. A compact formulation for the computation of Raman tensors for a vibrating molecule as a function of bond polarizability is described in Ref. 10. They proposed an easier computational method and also showed the dependence of the intensities on the L matrix. This dependence, will be explained later.

Calculations have been performed on two of the molecules of our interest namely, the methyl chloride and methyl bromide, whose Raman intensities were interpreted in terms of the bond polarizability model. They[11, 12] were also successful in showing the flaws of this approach. It is only recently that a new theory has been developed which is shown to be a good substitute for the bond polarizability model, though it may be applied effectively to small molecules, only. The details of this (Theory of Atoms in Molecules) will be considered in Section 5. This theory has been shown to explain the Raman intensities in a clear pictorial manner[13].

Absolute Raman intensities also referred to as Raman cross sections have previously been studied primarily in "the pre-laser era" and a description of the work done has been explained in Ref. 14. In the following we review Raman intensity measurements performed on the methyl chloride and bromide.

1.3: LITERATURE REVIEW -

Experiment-

The following is a description of the intensity measurements recorded previously. The frequencies, intensity values and a brief description of the apparatus employed, will be included.

In 1952[15] relative intensity measurements of a number of gases were taken, which included methyl chloride and methyl bromide. They also showed the inadequacy of the bond polarizability model, unfortunately during this period there was no substitute and this model was used even with the discrepancies. All the work done thereafter also applied the bond polarizability model proclaiming it to be convenient. A brief preview of the apparatus employed will be described, detailed description is found in Ref 15.

The source employed was a set of high intensity mercury lamps, with water cooled electrodes. Cooling was essential as there was observed to be an increase of several-fold in the intensity without a large increase in vapor density. A solution of sodium nitrite was used to isolate the Hg 4358 Å line from the higher frequencies in the mercury spectrum. A thickness of 1 cm of this solution saturated at 25^{o}C transmits 90% of Hg 4358 Å, but only 5% of Hg 4078 Å and 1% of Hg 4047 Å. Further the faint mercury lines appearing at 5000 Å were eliminated by saturating the sodium nitrite solution with rhodamine-B. Advantages associated with use of the lamp at an intensity of Hg 4358 Å included the following, a linear increase in intensity with current up to 15 amperes, no appreciable broadening of the spectral lines, and a very stable operation i.e. the intensity of Hg 4358 Å is not noticeably reduced over a period of 1000hr.

The lamp was started by heating with a bunsen burner and applying a voltage between two starting electrodes. Five lamps were employed and were symmetrically arranged about the tube. Since the scattered light was unpolarized the transmission of the spectrograph was identical for both the isotropic and anisotropic parts.

The Raman tube was made of standard wall Pyrex tubing 35 mm in diameter, withstanding gas pressure up to 12 atmospheres. The tube was placed inside a vacuum flask. The temperature was controlled with the aid of a chromel wire wound in the open coil on the tube, and measured by thermocouples placed at five points along the tube. The Raman spectra were photographically recorded with a double prism glass spectrograph employing two inter changeable cameras. The photographic plates were calibrated for

intensities by recording the spectrum of a Kipp and Zonen standard tungsten band lamp. A Leeds and Northrup recording microphotometer was incorporated to measure the intensities. The Raman shifts were determined from the separation of the bands from the moderately exposed lines at 4180 Å, 4916 Å, and 5026 Å. The relative intensity calculations were obtained by using the equation:

$$i_\lambda = C(45\alpha'^2 + 13\gamma'^2)$$

where - i_λ = relative intensity

C = constant

α = isotropic contribution to tensor

γ = anisotropic contribution to tensor

The terms α'^2 and γ'^2 were evaluated in terms of bond polarizability model which, as stated earlier, was proposed by Wolkenstein. They were successful in showing that the rate of change of bond polarizability is strongly dependent on the nature of the neighbouring bonds. This was found to be apparent when a comparison of the intensities of the bands characteristic of the CH_3 group were compared.

It was obseved that the intensity of the symmetric deformation, designated as ν_2, was not observed in methyl chloride but was easily seen in methyl bromide. They concluded that the intensity of a particular band is dependent on the neighbouring bonds. The frequencies and relative intensities are as depicted in Table 1.1.

The absolute Raman intensity measurements of a number of gases including the methyl chloride and methyl bromide were recorded in 1958, by the photoelectric method[16]. This method has been explicitly explained in Ref 17, and a brief mention of the important components and methodology is as follows:

The source used was six water cooled Toronto-type mercury lamps, each having a current of 20 amperes. The Raman photoelectric spectrometer, built by White Development and Co. was incorporated, which had a dispersing element of 30,000 lines per inch plate replica grating. Detection was by means of a 1P21 photo multiplier used at

TABLE 1.1

Frequencies and relative intensities for methyl chloride and methyl bromide

Molecule	Mode	Frequency (cm^{-1})	Intensity[a] (i_λ)
CH_3Cl	$\nu_1(A)$	2965.5± 0.6	221± 4
	$\nu_2(A)$	1370(liquid)	-
	$\nu_3(A)$	725.3 ±0.6	126 4
	$\nu_4(E)$	3043 ±1	189± 6
	$\nu_5(E)$	1473 ±2	55 ±4
	$\nu_6(E)$	1012± 2	11± 4
CH_3Br	$\nu_1(A1)$	2972± 1	172±4
	$\nu_2(A1)$	1309 ±1	11± 2
	$\nu_3(A1)$	609± 1	188± 2
	$\nu_4(E)$	3068 4	133± 9
	$\nu_5(E)$	1456± 4	57 ±2
	$\nu_6(E)$	956± 5	0.4

[a] Ref- 15 where, $i_\lambda = C(45\alpha'^2 + 13\gamma'^2)$

TABLE 1.2

Absolute intensities of the stretching modes of methyl chloride and methyl bromide

Molecule	Mode	Frequency (cm^{-1})	Intensity[a] $g_j(45\alpha_j'^2 + 7\gamma_j'^2)$ ($cm^4 g^{-1}.N.10^{-32}$)
CH_3Cl	$\nu_1(A)$	$\Sigma\nu_{C-H}$	150
	$\nu_3(A)$	725	17
CH_3Br	$\nu_1(A)$	$\Sigma\nu_{C-H}$	125
	$\nu_3(A)$	609	25

[a] Ref 16

room temperature. The multiple reflection gas cell provided by White Development and Co, was one meter long. The gas pressures were taken to be at 1 to 2 atmospheres. The frequencies, which included only the stretching modes, and intensity values, are as in Table 1.2.

Absolute intensities and depolarization ratios, for the halogen substituted methanes in the gaseous phase were also obtained by W. Holzer in 1968[11]. These measurements were recorded using the apparatus which consisted of the following components: four strong mercury arcs, a 1 meter mirror glass tube, a Steinheil GH spectrometer and photoelectric recording material. The gas pressure ranged from 0.7 to 2 atm. with 2.8 cm^{-1} spectral slit width of the spectrometer. The wavelength of the exciting line was at 4358 Å .

Absolute intensity measurements obtained from Ref. 11 and 16, which employed the photoelectric method, were calculated from the intensities relative to the H_2 J=1-3 rotational line and the value of the polarizability anisotropy for H_2, $\gamma o=0.310$ $Å^3$. (Tables 1.2 and 1.3). From Placzek's polarizability theory[18], absolute intensities were determined as:

$$I_{abs.} = g_i(45(\bar{\alpha}_i')^2 + 7(\gamma_i')^2)$$

Where g_i is the degeneracy of the vibration, α'_i is the isotropy and γ'_i the anisotropy of the derived polarizability tensor with respect to the normal coordinates of the i^{th} vibration. Depolarization calculations for methyl chloride and bromide were obtained from Ref. 11, and are as listed in Table 1.3.

Absolute intensities of all the fundamental bands of methyl chloride and its deuterated analogue were measured in the gas phase, in 1981[19]. The samples were obtained commercially (Merck, Sharp and Dohme). The spectra were recorded at room temperature with a Jarrell-Ash 25-300 Raman laser spectrometer. The 488.0 nm line of the Ar+ laser, operated at a power of 0.5W, was used as the exciting source. A single

TABLE 1.3

Absolute intensities and depolarization ratios for the methyl chloride and methyl bromide

Molecule	Mode	Wavenumber (cm^{-1})	Intensity[a] $g_j(45\alpha_j'^2 + 7\gamma_j'^2)$ ($cm^4g^{-1}.N.10^{-32}$)	ρ
CH_3Cl	$\nu_1(A)$	2965.5	135	0.03
	$\nu_2(A)$	-	-	-
	$\nu_3(A)$	725	21	0.50
	$\nu_4(E)$	3043	135	0.90
	$\nu_5(E)$	1473	-	-
	$\nu_6(E)$	-	-	-
CH_3Br	$\nu_1(A1)$	2971	107	0.0
	$\nu_2(A1)$	1304	2.2	0.5
	$\nu_3(A1)$	608	29	0.37
	$\nu_4(E)$	2819	14.5	0.05
	$\nu_5(E)$	1450	26	0.75
	$\nu_6(E)$	927	2	-

[a] Ref. 11

N: Avogadro Number

ρ-Depolarization ratio

pass, 90^{o} scattering geometry was used with the electric vector of the incident light perpendicular to the direction of observation. The collecting system consisted of a photographic objective of f/0.95 and a lens to focus the scattered light onto the spectrometer slit, with a magnification of 9. A polaroid analyzer was placed in between these two lenses and a scrambler was placed in front of the entrance slit. The gas pressure was monitored, by means of a pressure transducer placed inside the cell. This was essential to counteract the strong adsorption of these molecules. The absolute intensities were evaluated with the nitrogen band at 2331 cm^{-1} (Table 1.4).

Absolute infra-red intensities were obtained for the methyl chloride and bromide. Analysis of these data was not undertaken, but details of results obtained are given in Refs. 20, 21. No intensity data i.e., Raman or infra-red, was obtained for the methyl fluoride.

In conclusion it may be stated that for all previous data, Raman intensities were analyzed on the basis of the bond polarizability model. They showed the inadequacy of the model, namely that the Raman intensity of a particular bond is strongly dependent on the neighbouring bonds within the molecule.

Theory-

Theoretical calculations of molecular polarizabilities were performed for the methyl fluoride and methyl chloride (Ref. 22). The calculations were performed with the Dunning basis set using spd functions and the results will be considered in Section 6. No previous theoretical computation was performed for the methyl bromide. Further, no previous calculations of polarizability derivatives, by the methodology opted in this work i.e., theoretical simulation of a stretching vibration, was performed for any of these molecules. The analysis by the theory of atoms in molecules (AIM), has previously not been undertaken for these molecules.

TABLE 1.4

Absolute intensities and depolarization ratios for the methyl chloride

Molecule	Mode	Wavenumber (cm^{-1})	Intensity[a] (S_i)	ρ
CH_3Cl	ν_1(A)	2972	99.5	0.023
	ν_2(A)	1349	0.6	0.55
	ν_3(A)	735	13.3	0.169
	ν_4(E)	3045	50.2	-
	ν_5(E)	1470	6.1	-
	ν_6(E)	1014	0.78	-

[a] Ref. 19

S_i : scattering coefficient defined as $S_i = g_i(45(\bar{\alpha}_i')^2 + 7(\gamma_i')^2)$

ρ-Depolarization ratio

The theoretical computations in this thesis are similar to those performed for a number of hydrocarbons[13, 23, 24] i.e., methane, ethane, propane and cyclohexane. Hence it was thought appropriate to include a summmary of the results obtained. The results obtained are significant as we would like to investigate the reproducibility of the trends obtained.

Further, not only were they successful in showing the validity of the theoretical computation, relative to the available experimental data but they also illustrated the flaws in the interpretation of Raman intensities on the basis of the bond polarizability model.

The calculated polarizabilities were within a 20% error, relative to experimental data, but of importance was the trend exhibited by all the hydrocarbons. The *ab initio* MO calculations were performed with the D95**[23] basis, which will be explained shortly. With the AIM analysis some of the trends observed are outlined below. The Raman intensities were seen to vary with bond orientation within the molecule. Further, they were able to obtain charge transfer and atomic dipole contributions to the polarizability and polarizability derivatives. These terms will be explained in Sec. 5. The following are some of the conclusions drawn on analysis by the AIM theory[13]:

1} Charge density reorganization was observed to occur specifically on the atoms which constituted the bond.

2} The changes in the charge transfer tensor are not localized to the carbon-hydrogen bond being stretched, but there is a transfer of charge from one end of the molecule to another.

3} Maximum polarizability for a molecule occurs along the length of the chain and increases with increasing chain length.

4} Origin of the polarizability derivatives are predicted to vary with chain length, bond position and conformation. This positional dependence was not obtained in the bond polarizability model, which was therefore stated to be inappropriate to molecules of large size.

5} A molecule in an electric field behaves as a dielectric material. The electrons undergo small displacements as the molecule is not freely conducting.

6} Good correlation was observed between molecular volumes and molecular polarizabilities.

1.4: THIS WORK -

With the advent of the laser in 1960, recording Raman spectra of samples in the gaseous phase has taken an upward swing. Intensity measurements using the laser were performed only for the methyl chloride[19]. Because of the good relationship between previous experiment and theoretical results, and on the basis of the above conclusions drawn, it was thought appropriate to adopt the same methodology for different molecules. Thus we sought this advantage and intended to determine absolute intensities of methyl halides and deuterated samples in the gas phase. The series of methyl halides and deuterated counterparts were considered appropriate as these molecules are small enough to perform computations, along with providing a significant trend in the series.

The primary focus of this research was to observe the changes in the Raman intensities i.e., the polarizability derivatives, for the methane molecule, when one of the hydrogens is replaced by a heavy atom. Comparison of all results obtained will be made relative to methane, substituent effects will be studied, and reasons proposed. Further, we wish to ascertain if previous conclusions drawn are reproducible.

The series of methyl halides i.e., CH_3X (X=F, Cl, Br) form a "simple" series of closely related compounds wherein trends may be observed with respect to physical and chemical properties. The variations in these properties will be strongly dependent on the characteristics of the halogen atom. There is significant concern regarding fluoro-chloro carbons, for environment safety, however the work undertaken does not lead to any help for environment purposes. The halogen atoms belong to group VII A of the periodic table. The properties of individual halogens will not be considered, as they may be

obtained elsewhere[25]. We consider some properties important for this work: 1} the electronegativity, which decreases from F to Cl to Br, 2} the polarizability which increases as the atomic size increases. This property is very important for Raman intensities and will be focussed on all through the discussion, Sec. 6. A note about the individual methyl halides:

The methyl fluoride is stated to be the least reactive, which is due to the high electronegativity of 4, and small size (only slightly larger than hydrogen) of the fluorine atom i.e., the C-F bond is quite stable as are the C-H bonds. The main use of methyl fluoride is for commerical purposes, however it is stated to be narcotic in high concentrations.

The methyl chloride and bromide are listed as 'hazardous air pollutants" as defined by the 1990 clean air act amendments. The electronegativities of chlorine and bromine are 3 and 2.8, respectively. Methyl chloride is primarily used in manufacture of silicone, synthetic rubber and methyl cellulose. The methyl bromide is useful in extermination of insects and rodent pests and for fumigation of food commodities e.g., dried fruits, grain nuts etc.

Experiment-

A brief description of the experimental setup employed for recording the spectra is as given below and will be followed by the theoretical computations performed. As the molecules under study are active in the infrared and in the Raman, spectra by both methods were obtained and the setups are as follows.

For recording Raman spectra, the experimental setup included the following essential components: an Ar+ ion gas laser as the source operating at 515.4nm, a Spex 14018 double monochromator and a RCA C31034 photomultiplier tube as detector. The infrared spectra were recorded on a Bomem MB-120 FTIR instrument. A detailed explanation of the setup for Raman measurements is more important, and is explicitly

explained in Section 3. Comparison of the band positions obtained via the two methods i.e., FTIR and Raman, and with the values reported in the literature is made. Details of the theory of FTIR may be obtained in Refs. 26 and 27.

Theory-

The theoretical calculations were performed via two methods:

1} *ab initio* molecular orbital calculation at the HF level, with the D95** basis set, {(4s2p/2s) Dunning[28] contraction of the (9s5p/4s) Huzinaga[29] basis} for CH_3F and CH_3Cl and the LANLIDZ[30, 31] basis set, {D95V on first two row elements and ECP+DZ on other row atoms}, for CH_3Br, using the GAUSSIAN 90[32] package for all calculations. Polarizability and polarizability derivatives were computed for different values of the inter nuclear distances. Details of the theory involved, methodology and discussion may be obtained in Section 4.

Further, *ab initio* molecular orbital computation provides information with respect to assigning frequencies to the normal modes, intensities of the bands, and depolarization ratios, which may then be compared with experimental results, to test the validity of the computation. Comparison was also made with the literature results and is as explained in Section 6.

2} Atoms in molecules (AIM) calculations were performed on the wave function obtained by *ab initio* MO calculation, employing the PROAIM[33] program. These calculations along with providing polarizabilities and polarizability derivatives, also give insight as to the actual charge transfer and atomic dipole change occurring on each atom. This provides a very clear picture of the factors influencing the intensity of the individual Raman bands. Details of theory, calculation methods and results are as described in Section 5. Recovery of the information provided in the *ab initio* molecular orbital wave function, is ascertained.

Comparison is also made with experimental results where ever available.

2: THEORY OF RAMAN SPECTROSCOPY-

The Raman theory has been explained clearly on the basis of classical and quantum mechanics[34, 35]. In the following is outlined a brief description of the basic phenomenon, quantum and classical explanations, intensities in Raman spectra and finally Raman depolarization ratios.

2.1: RAMAN PHENOMENON-

The Raman effect is a scattering phenomenon, wherein monochromatic light, of frequency ν_0, is incident on a sample, and a very small part of the light is scattered in a direction different from the incident beam. The spectrum, when observed, is found to consist of a high proportion of light of frequency ν_0, the Rayleigh line, whose intensity is proportional to the fourth power of the incident light. In addition to the Rayleigh line a pattern of lines of shifted frequency are observed, which constitute the Raman spectrum, (Fig. 2.1). These shifts are independent of the incident frequency and are characteristic of the species giving rise to the scattering. The lines on the low frequency side of the exciting line are known as the Stokes lines and those on the high frequency side are the anti-Stokes lines. The phenomenon may be understood explicitly from the ongoing explanation.

Considering monochromatic light consisting of photons of energy $h\nu_0$, incident on a molecule, two interactions result. One, wherein the light is scattered at the same frequency whether or not the molecule is vibrating, is an *elastic collision*. The second, wherein the light is scattered at a frequency different from the incident frequency, is an *inelastic collision*. The *inelastic collisions* are of two types: 1} where the light interacts with a particle in the ground state and excites it to a higher level. 2} the instance where the light interacts with a molecule already in the excited level, interaction results in the molecule losing energy to the light and returning to the ground level. The frequencies of the light are given as ν_0-ν_S and ν_0+ν_S and are known as Stokes and anti-Stokes radiation

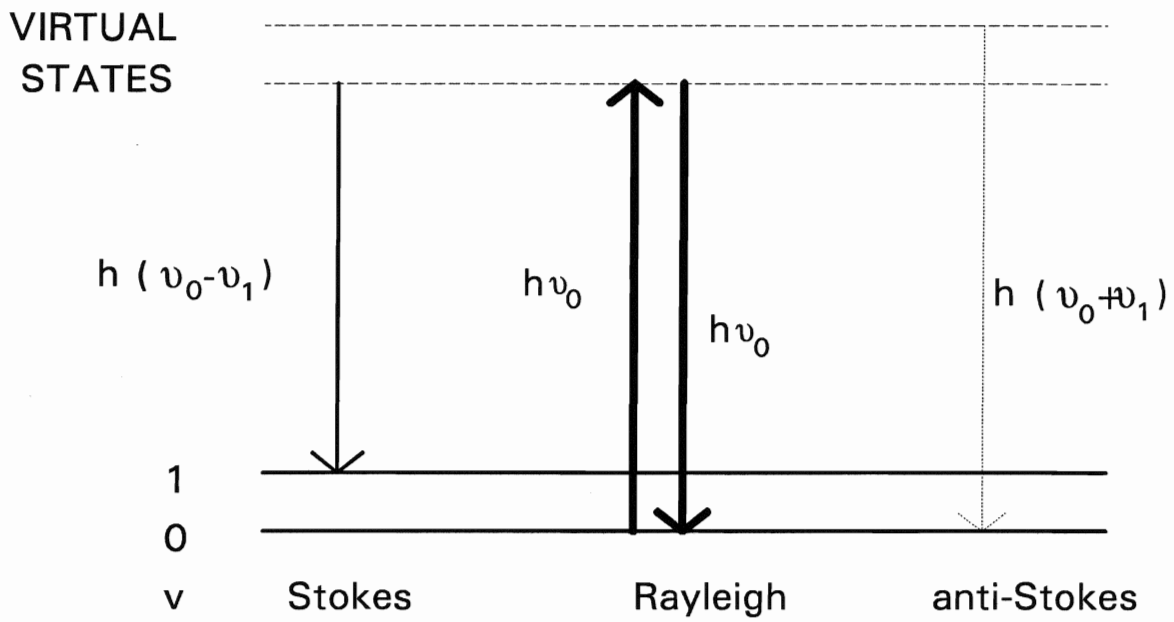

Fig. 2.1- Energy level diagram illustrating the fundamental processes of Raman scattering.$h\upsilon_0$ is the energy. Raman bands appear at $h(\upsilon_0 - \upsilon_1)$ and $h(\upsilon_0 + \upsilon_1)$

respectively. These shifts on either side of the exciting radiation constitute the Raman spectrum while the *elastic collision* is known as the Rayleigh scattering.

2.2: CLASSICAL EXPLANATION-

The Raman effect can be predicted on the basis of classical arguments, and is as follows. The electric field E associated with the wave of frequency ν_0, is written in the form:

$$E = E_0 \cos 2\pi\nu_0 t \qquad (2.01)$$

where E_0 is the amplitude of the electric field oscillations and t is the time.

When this oscillating wave interacts with the polarizable electric field, a dipole is induced in the molecule, whose magnitude is given by the equation:

$$\mu = \alpha E \qquad (2.02)$$

where α is the polarizability of the molecule and varies with the configuration of the molecule i.e., a function of the vibrational or other motions of the nuclei.

The Raman effect results from the interaction of the polarizability with the normal modes, Q, of vibration of the molecules. The normal modes are characteristic modes of vibration wherein, in any one normal mode, every mass performs a nearly simple harmonic motion with the same characteristic frequency ν. All the masses move in phase with one another but with different amplitudes. The number of normal modes is specific depending on the molecule under study, and is generally obtained by the equation: 3N-6 for a non linear molecule and 3N-5 for a linear molecule, where N denotes the number of atoms in the molecule[36, 37].

The different normal modes for the methyl halides are as depicted in Fig. 2.2. The general convention followed to number the distinct frequencies is as follows: The vibrations are arranged by species, usually starting with the totally symmetric and continuing with the remaining non-degenerate species, the doubly degenerate and finally

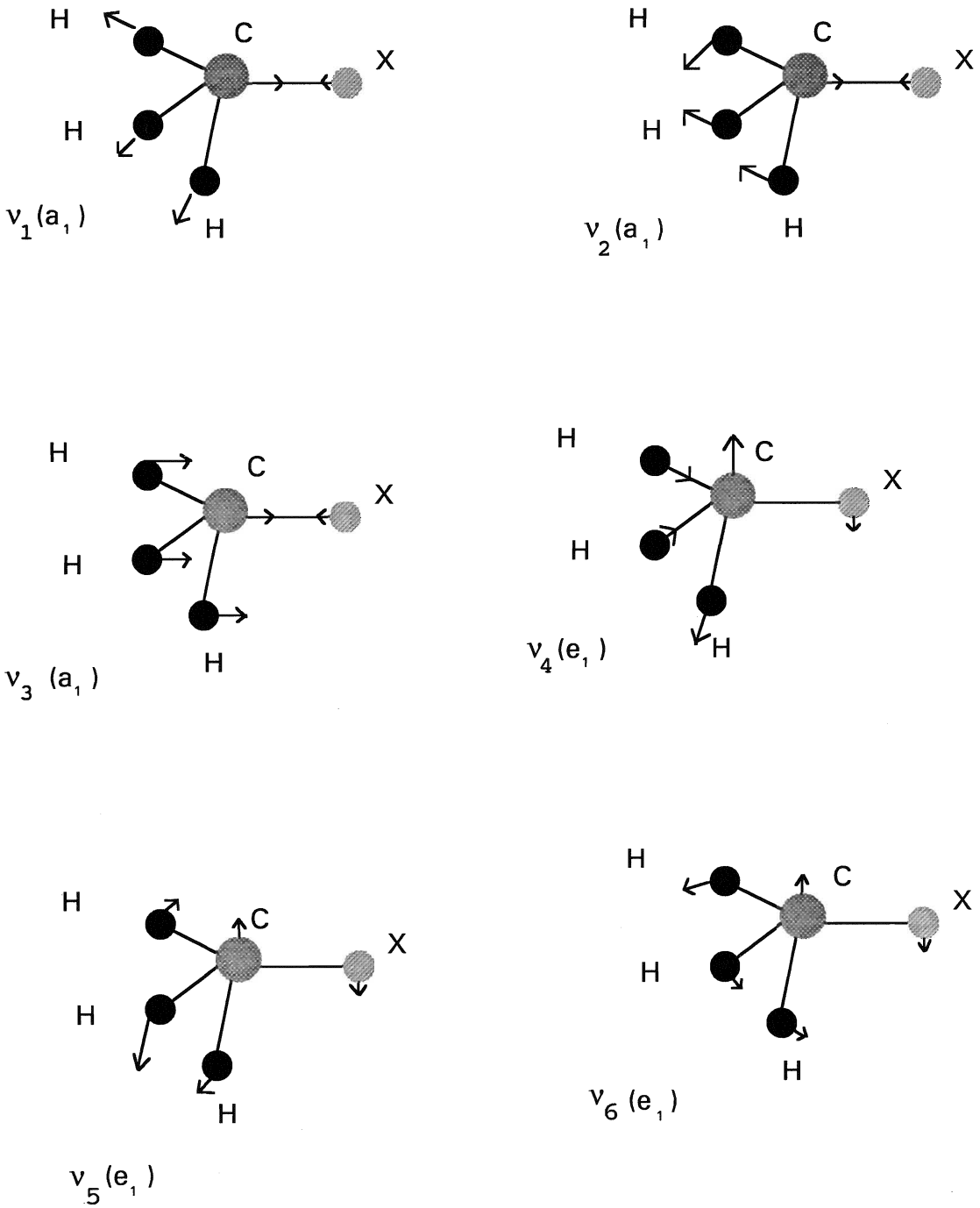

Fig. 2.2- Schematic of normal modes for the methyl halides CH_3X (X=F, Cl, Br)

the triply degenerate[36]. Then within a particular species the frequencies are numbered in order of descending magnitude. Thus, from Fig. 2.2, we have $\upsilon_1 > \upsilon_2 > \upsilon_3$, for the totally symmetric species (A), and $\upsilon_4 > \upsilon_5 > \upsilon_6$, for the doubly degenerate species (E).

The polarizability in terms of the normal modes may be written as:

$$\alpha = \alpha_0 + \frac{\partial \alpha}{\partial Q_k} + \text{.....higher order terms} \qquad (2.03)$$

where the kth normal mode is considered, and α_0 is the polarizability of the molecule for a fixed nuclear configuration. The higher order terms are neglected since all amplitudes of the normal vibrations are very small i.e., harmonic approximation.

The normal coordinates may also be written in their time dependent form and are given as:

$$Q_k = Q_k^0 \cos 2\pi \nu_k t \qquad (2.04)$$

substituting into Eqn. (2.02), we get:

$$\mu = \alpha_0 E_0 \cos 2\pi \nu_0 t + E_0 \left(\frac{\partial \alpha}{\partial Q_k}\right) Q_k^0 \{\cos 2\pi(\nu_0 + \nu_k)t + \cos 2\pi(\nu_0 - \nu_k)t\} \qquad (2.05)$$

The first term corresponds to scattering without change in frequency i.e., the unshifted Rayleigh scattering, whose intensity depends on the molecular polarizability and is observed with all substances. The second and third terms give rise to the Raman scattering: the high frequency term is the anti-Stokes line and the low frequency term, the Stokes line. Further, the Stokes lines are more intense than the anti-Stokes lines. (Fig. 2.1)

The difference in intensity of the Stokes and anti-Stokes radiation is explained from the Boltzman distribution of state populations, which is given as:

$$N_E = N_o \, e^{\frac{-E}{kT}} \qquad (2.06)$$

where N_E is the number of states with energy E, N_0 is the ground state population, k is Boltzman constant and T is absolute temperature.

The Stokes lines originate from scattering when the molecule is excited from the ground level to higher energy level, and the anti-Stokes from a scattering when a molecule in the excited level falls to the ground level. At room temperature the ground state levels will be significantly more populated than those in the excited levels. Hence under the influence of an electromagnetic field, the number of molecules available for Stokes scattering will be greater than that for anti-Stokes scattering, because of the Boltzman distribution factor.

In the general case, we have Ex, Ey and Ez representing the three directions of the electric field, the dipole moment corresponding to these three directions is written as:

$$\begin{aligned} \mu_x &= \alpha_{xx}E_x + \alpha_{xy}E_y + \alpha_{xz}E_z \\ \mu_y &= \alpha_{yx}E_x + \alpha_{yy}E_y + \alpha_{yz}E_z \\ \mu_z &= \alpha_{zx}E_x + \alpha_{zy}E_y + \alpha_{zz}E_z \end{aligned} \tag{2.07}$$

or in matrix notation form we get:

$$\begin{pmatrix} \mu_x \\ \mu_y \\ \mu_z \end{pmatrix} = \begin{pmatrix} \alpha_{xx}\alpha_{xy}\alpha_{xz} \\ \alpha_{yx}\alpha_{yy}\alpha_{yz} \\ \alpha_{zx}\alpha_{zy}\alpha_{zz} \end{pmatrix} \begin{pmatrix} E_x \\ E_y \\ E_z \end{pmatrix} \tag{2.08}$$

The polarizability is obtained in tensor form Eqn. (2.08), and is written as an array of nine components, as depicted above. In all cases the tensor is symmetric i.e., the off diagonal components are related by the following three equations:

$$\alpha_{xy} = \alpha_{yx},\ \alpha_{yz} = \alpha_{zy},\ \text{and}\ \alpha_{xz} = \alpha_{zx}$$

and the number of distinct components is reduced to six.

Two important terms obtained from the tensor are the mean value, $\bar{\alpha}$, and the anisotropy, γ, which are defined as:

$$\bar{\alpha} = \frac{1}{3}(\alpha_{xx} + \alpha_{yy} + \alpha_{zz}) \tag{2.09}$$

and

$$\gamma^2 = \frac{1}{2}\left\{(\alpha_{xx} - \alpha_{yy})^2 + (\alpha_{yy} - \alpha_{zz})^2 + (\alpha_{zz} - \alpha_{xx})^2 + 6(\alpha_{xy}^2 + \alpha_{yz}^2 + \alpha_{zx}^2)\right\} \tag{2.10}$$

The above two terms are commonly known as invariants i.e., their values are unaffected by changes in orientation of the molecule relative to the space-fixed coordinate system.

The selection rule procedures will not be considered in detail, only the result, *that a fundamental is Raman active if there is a change in the polarizability of the molecule during a vibration.* Thus the necessary condition for a particular frequency υ_k to be observed in Raman scattering, may be written in the form:

$$\left(\frac{\partial \alpha_{ij}}{\partial Q_k}\right) \neq 0 \tag{2.11}$$

where i or j = x, y, or z,

i.e., at least one of the components of the derivative of the polarizability tensor with respect to the normal mode is non zero.

2.3: QUANTUM MECHANICAL EXPLANATION-

The preceding classical approach will now be considered in quantum mechanical terminology.

We consider the *transition moment*, denoted as μ_{nm}, for the transition between two states characterized by the wave functions $\psi^{(n)}$ and $\psi^{(m)}$. The transition moment is defined by the following equation:

$$\mu_{nm} = \int \psi^{(n)} \mu \psi^{(m)} d\tau \tag{2.12}$$

where $d\tau$ is the volume element in configurational space, and the integration is extended over the whole of this space.

The transition moment is important as it determines the intensity of the absorption or emission of radiation by the transition in question. Further the intensity is proportional to the square of the transition moment. Substituting Eqn. (2.02), into the above equation we get:

$$\int \psi^{(n)} \mu \psi^{(m)} d\tau = E \int \psi^{(n)} \alpha \psi^{(m)} d\tau \qquad (2.13)$$

Expanding α in terms of the Taylor series expansion, Eqn. (2.03), and substituting in Eqn. (2.13), the equation of the transition moment arising from the induced dipole moment, μ, is given as:

$$\int \psi^{(n)} \mu \psi^{(m)} d\tau = E\alpha_0 \int \psi^{(n)} \psi^{(m)} d\tau + E \sum_k \left\{ \left(\frac{\partial \alpha}{\partial Q_k} \right)_0 \int \psi^{(n)} Q_k \, \psi^{(m)} d\tau \right\} \qquad (2.14)$$

Because of the mutual orthogonality of the eigenfunctions, the first term on the right hand side of Eqn. (2.14) must vanish. Thus the first term corresponds to Rayleigh scattering, without change in frequency, i.e., for n=m, the first term is unity. In the second term, the kth summation represents the contribution of the kth normal mode to the Raman spectrum. The integral term vanishes except when $\Delta\upsilon_k = \pm 1$, i.e., except for transitions associated with the frequency υ_k.

The restricted selection rule which governs whether a particular vibrational frequency is permitted or forbidden in the Raman is dependent on the factor $(\partial\alpha/\partial Q_k)_0$. Therefore we can make the statement that only those modes can be active in Raman scattering which satisfy the condition $(\partial\alpha_{ij}/\partial Q_k)_0 \neq 0$, for at least one component of the molecular polarizability (i or j = x, y or z). This is identical to the classical rule stated above.

2.4: INTENSITIES IN RAMAN SPECTRA-

It is the Raman intensities which are of importance in this thesis, and will be considered in detail. In a Raman scattering experiment, the power of the light scattered in a given direction due to the vibrations occurring in the molecule, is given by the equation:

$$I_{T,i} = N\left(\frac{\partial \sigma}{\partial \Omega}\right)_i I_o \qquad (2.15)$$

where Io is the power density of the incident radiation, $\left(\frac{\partial \sigma}{\partial \Omega}\right)_i$ is the differential scattering cross section for the ith vibrational band, and N is the number of scattering molecules[38]. Further the differential scattering cross section is given as:

$$\left(\frac{\partial \sigma}{\partial \Omega}\right) = \left(\frac{\Pi^2}{90\varepsilon_o}\right)\upsilon_s^4 \left[1 - \exp\left(\frac{-hc\upsilon_i}{kT}\right)\right]^{-1} g_i \left(45\bar{\alpha}'^2 + 7\gamma'^2\right) \qquad (2.16)$$

where υ_S is the wave number of the scattered radiation; g_i is the degeneracy of the vibrational mode; $\bar{\alpha}'^2$ and γ'^2 are the invariants of the derivative of the molecular polarizability with respect to the dimensionless normal coordinate i.e., a single coordinate along which the progress of a single normal mode of vibration can be followed; ε_o is the permittivity of vacuum ($8.8542 \times 10^{-12} CV^{-1}m^{-1}$); and h, c, k, T are Planck's constant, velocity of light, Boltzman's constant, and temperature respectively.

The polarizability invariants $\bar{\alpha}'^2$ and γ'^2, Eqns. (2.09) and (2.10), give rise to the trace and quadrupole spectra respectively, also known as the isotropic and anisotropic spectra. Considering the polarizability properties of the scattered light, these two spectra may be separated[39], using a suitable optical device (Sec. 3). The two polarized components of the scattered light are given as:

$$I_{//} = 45\bar{\alpha}'^2 + 4\gamma'^2 \qquad (2.17)$$

and

$$I_{\perp} = 3\gamma'^{2} \qquad (2.18)$$

where $I_{/\!/}$ denotes the component of the scattered light whose polarization vector is parallel, and $I_{\perp}$, perpendicular , to that of the incident light.

Thus employing a suitable polarization analysis (polarizer), the trace and quadrupole spectra may be separately obtained. Further each of the above mentioned spectra have different characteristics; the trace spectrum is observed only for the totally symmetric vibrational modes i.e., those vibrational motions maintaining the equilibrium symmetry of the molecule, and for transitions between rotational levels having the same angular momentum. The quadrupole spectra on the other hand generally consist of more bands each with complicated rotational structure.

As the focus of this work is the study of the intensities of the symmetric stretching vibrations it is the trace spectra which are of more interest, as will be explained in the following section. There are advantages of working with the trace spectra, namely, the well resolved narrow bands permit the baseline to be determined in a straight forward manner. Further it is not important to make rotational corrections[38].

The absolute intensities (differential scattering cross section) will be experimentally determined employing the apparatus described in the following section, and also theoretically computed via *ab initio* molecular orbital calculations (Sec. 3) and by the theory of atoms in molecules (Sec. 4).

2.5: DEGREE OF DEPOLARIZATION [34] -

Of importance is the *depolarization ratio*, given by the relation:

$$\rho = \frac{I_{\text{perpendicular}}}{I_{\text{parallel}}} \qquad (2.19)$$

substituting values from Eqns. (2.17) and (2.18), the depolarization ratio is given as:

$$\rho = \frac{3\gamma'^2}{45\,\bar{\alpha}'^2 + 4\gamma'^2} \tag{2.20}$$

The depolarization ratio indicates whether the line is polarized or depolarized and hence gives information relative to the symmetry of the normal mode giving rise to the particular vibration. For the special case of isotropic molecule i.e., a molecule whose three principal values of the polarizability are equal, we get $\gamma=0$ (Eqn. 2.10) and $\rho=0$, and the line is completely polarized. A totally symmetric vibration gives rise to ρ values lying in the range $\rho = 0$ to $\rho < 0.75$. The trace $\bar{\alpha}' = 0$ for asymmetric vibration and we get $\rho = 0.75$. The depolarization may also be experimentally measured, by individually measuring $I_{parallel}$ and then $I_{perpendicular}$.

3:RAMAN SETUP -

The set up for recording Raman spectra is as depicted in Fig. 3.1 and the main components are as follows:

3.1: SAMPLES -

The samples, and their isotopically labeled analogues were obtained at 99.9% purity and used without further purification. The CH_3Cl and CH_3Br were commercially obtained from Aldrich Chemical Company, CD_3Cl and CD_3Br were obtained from MSD Isotopes. The CH_3F and CD_3F were provided by Dr. Murphy, who was working at NRC. He has done a significant amount of work in measuring absolute intensities of a series of hydrocarbons[40] and substituted analogues. The samples were obtained in metal and glass cylinders which could conveniently be connected on to the vacuum line.

3.2: LOADING SAMPLE-

The samples were loaded into the cell, on the vacuum line, Fig. 3.2. A pressure of approximately 10^{-5} Torr is maintained in the vacuum line. This is attained with the aid of a fore pump and a diffusion pump.

The sample cell was first pumped down, and spectrum of the empty cell was recorded to check for impurity and also to obtain background spectrum. The cell was then connected onto the vacuum line at the position shown in Fig. 3.2. The sample cylinder was then connected onto the line at the appropriate position, and on opening the respective stop cocks the line was first flushed with the sample, to ascertain that all impurities were removed. During this procedure the valve leading to the sample cell remained closed, so that the sample was flushed through the line and out into the atmosphere, through the fume hood. After this step, the stop cock leading to the cell was opened and sample vapors were allowed to expand into the sample cell. The stop cock was closed and the pressure of sample in the cell was recorded from the pressure read out.

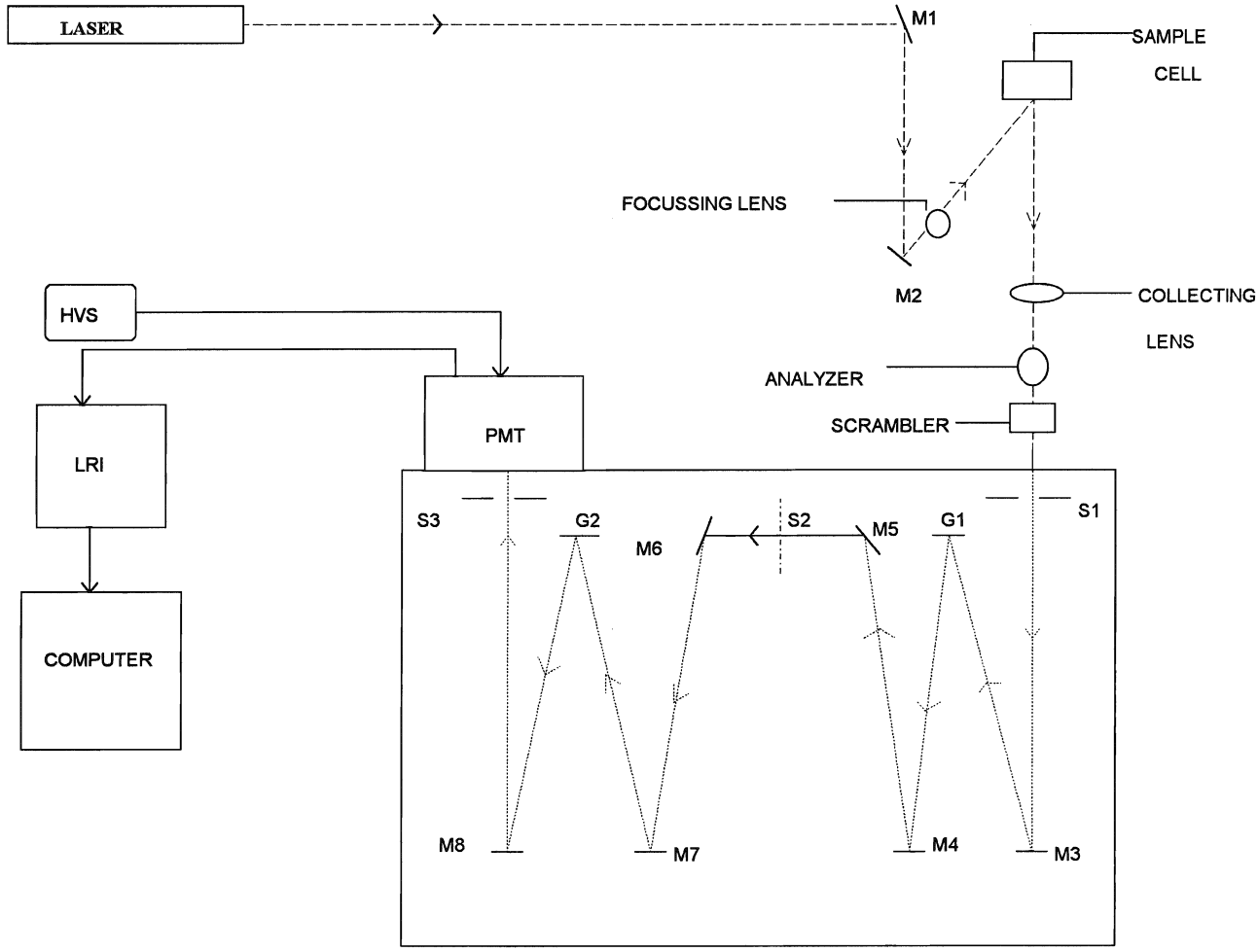

HVS- High Voltage supply

PMT- Photomultiplier tube

LRI - Laser Raman interface

M- Mirror

S- Slit

G- Grating

Fig. 3.1- Schematic of laser Raman setup

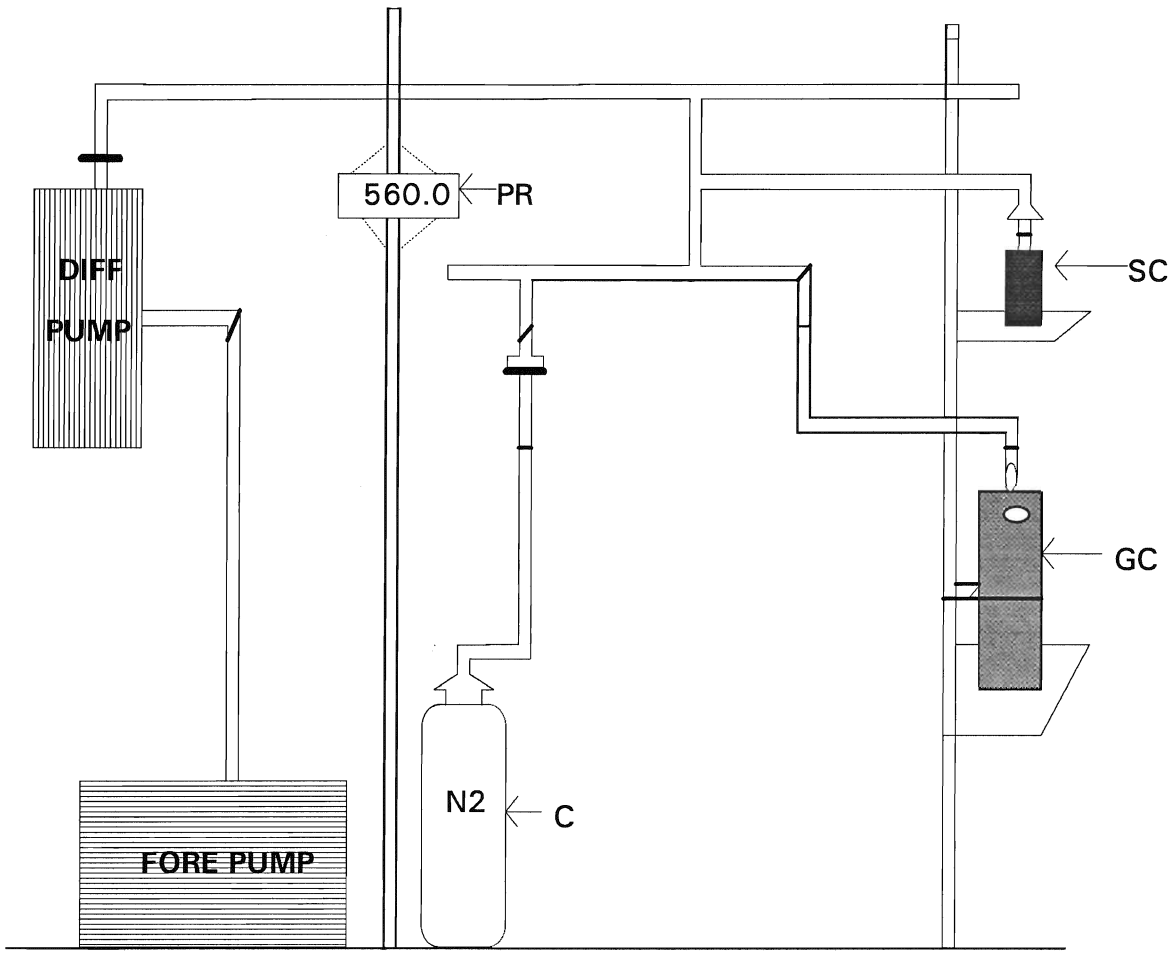

GC- Gas cyclinder

SC- Sample cell

PR- Pressure readout

C-Nitrogen cyclinder

Fig. 3.2- Schematic of vacuum line for loading sample

The pressure read out was a MKS 122AA 01000AB. For a mixture of sample and nitrogen, sample was first loaded into the sample cell , procedure as described above. The stop cock leading to the sample cylinder was shut, and the stop cock connected to the nitrogen cylinder was opened. Nitrogen, which serves as an internal standard, was once flushed through the line and pumped out and then reloaded to a pressure exceeding that of the sample in the sample cell. The cell stop cock was opened and nitrogen was allowed to expand into the cell body. The cell stop cock was closed and the line pressure was recorded. The pressure of nitrogen in the cell was determined by taking the difference of final pressure read out and sample pressure.

3.3: SOURCE -

A high powered Coherent Innova 200 series argon ion gas laser operating at 5W was used. The laser line was taken at 514.5 nm.

3.4: SAMPLE CELL -

To ensure enhancement of the intensity of Raman signal a specially constructed cell was designed[41]. The cell body was cylindrical and the windows mounted at Brewster's angle[42] ($56^{\circ}39'$), i.e., the angle which allows passage of polarized light with minimum reflection. The windows, made of fused silica, were 1" in diameter and 3 mm thick. These were sealed onto the cell body with black wax.

The multipass arrangement was designed by Kiefer et al[41]. This arrangement is as shown in Fig. 3.3. The two mirrors M1 and M2 are coated with a rare earth oxide to give maximum reflectance at 514.5nm. They are arranged in the form of a concentric sphere and have their common center of curvature C located at the center of the gas cell, GC.

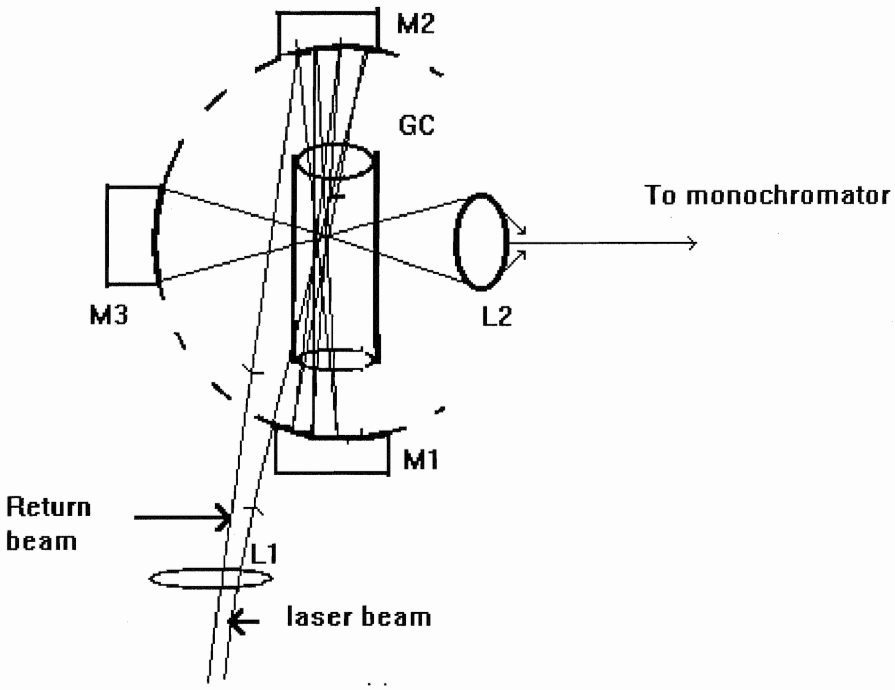

M- Mirror

L- Lens

GC- Gas cell

Fig. 3.3- Schematic of multipass arrangement

The laser beam is focused by lens L1 near the center, C, and then diverges onto mirror M2. After reflection the beam is refocused at C, and then is reimaged onto mirror M1 and the process repeats itself producing a multipass system. By alternating reflections at mirrors M1 and M2, the laser beam passes two focal points on either side of the center of curvature C. The mirror M3 of diameter 5cm collects the back scattered light at 90^{o} thereby further enhancing the intensity. With this arrangement there is a gain factor of approximately 20^{38} compared to a single focused laser beam. However to achieve this, the cell windows and the mirror surfaces have to be extremely clean. The scattered light is collected by lens L2 and focused onto the monochromator entrance slit.

3.5: TRANSFER OPTICS -

The transfer optics include the optics which help the scattered light to be focused onto the slit of the monochromator. The lens, L2 has its focal point at the center of entrance slit. Placed between the lens L2 and the slit are an analyzer and a scrambler.

The analyzer is necessary for determining the polarization properties of the scattered light. It is a high quality photographic polarization filter mounted on a standard photographic mount. It may be oriented either parallel or perpendicular to the direction of scattered light by rotation through 90°. The parallel position gives rise to the intensity denoted as $I_{/\!/}$ and the perpendicular position gives rise to the intensity denoted as $I_{\perp}$, these terms have been explained in the preceding section (2.4).

Spectrometers have different responses for light polarized parallel and perpendicular to the slit. The scrambler is designed to give equal instrument response to parallel and perpendicular polarization. The scrambler or depolarizer is a wedge of birefringent material that scrambles the polarization of the scattered light to avoid problems due to difference in monochromator transmission efficiency for the different polarizations[43]. The scrambler employed was a 25mm square section of quartz having a 1° wedge angle, oriented so that the slit height is parallel to the plane mutually perpendicular to the two

surfaces of the scrambler. There were difficulties encountered with the use of this scrambler and a new scrambler was opted for. This was a calcite sheet.

The functions of the analyzer and scrambler are diagramatically depicted in Fig. 3.4, wherein plane polarized light is incident on the sample cell, and is shown to be along the z direction. The scattered light is observed at right angles to the incident light, and is now seen to be polarized along the x and z direction. The polarizer orientation is taken parallel Fig. 3.4a, and then perpendicular Fig. 3.4b, and we observe parallel and then perpendicular light to be transmitted, respectively. The scrambler then scrambles the light before it enters the spectrometer.

This separation of the parallel and perpendicular components of the scattered light serves two main purposes:

1} The depolarization ratio may be calculated, and degree of depolarization ascertained (Sec. 2.5).

2} Spectra corresponding to parallel and perpendicular intensities may be separately obtained, and on subtracting 4/3 times the latter from the former we get the trace spectra, corresponding only to the symmetric vibrations.

3.6: MONOCHROMATOR -

A double monochromator was incorporated to reduce the amount of stray light reaching the detector. The Spex 14018 double monochromator has a Czerny-Turner double holographic grating, and is built to read the correct wave number, and difference in wave number (Δcm^{-1}), for 1800/grooves/mm grating. The entrance and exit slits are kept equal to obtain maximum throughput. The slit width was taken at 200 to 250 μm to achieve a balance between intensity and resolution.

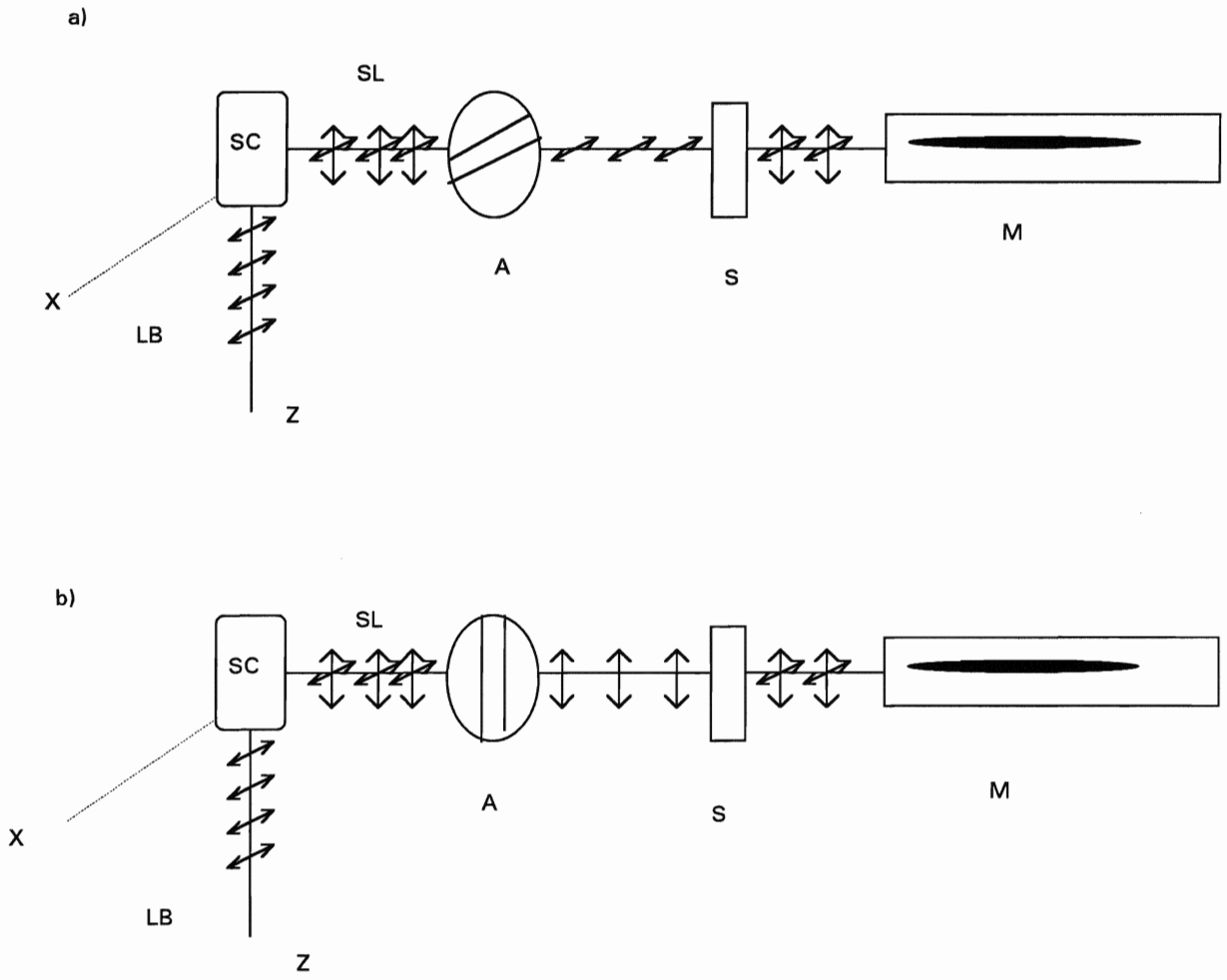

LB-Laser beam

SC- Sample cell

SL-Scattered light

A-Analyser or polarizer

S-Scrambler

M- Monochromator

Fig. 3.4-Polarization arrangements for Raman depolarization measurements

3.7: DETECTOR -

The detector employed was a RCA C 31034-RFSSR photomultiplier (PMT), cooled with the aid of a TE-104TS Peltier cooler whose temperature was set to -20° C.

3.8: LASER RAMAN INTERFACE-

The setup of the lri is as shown in Fig. 3.5 and is described as follows. The PMT cathode is connected to a high voltage supply operating at 1750V. The anode is coupled to a preamplifier. The preamplifier is powered with a 9 pin D cable, connected to the NA11 amplifier. The amplifier out put is connected to a discriminator. The discriminator is equipped with pulse height selectors, and an electronic circuit that rejects not only those pulses with heights below some predetermined level but also those above a preset maximum level i.e., it removes all pulses except those which lie within a limited channel or window. The importance of the discriminator is its ability to reduce detector and amplifier noise. The output from the discriminator is connected to an IBM 386 computer via a bnc COAX cable. The laser Raman interface was setup at Brock University by Tom from the electronic shop.

3.9: COMPUTER-

The spectra were recorded directly on the IBM 386 computer with the aid of laser Raman interface software. The method of recording spectra is explained as follows.

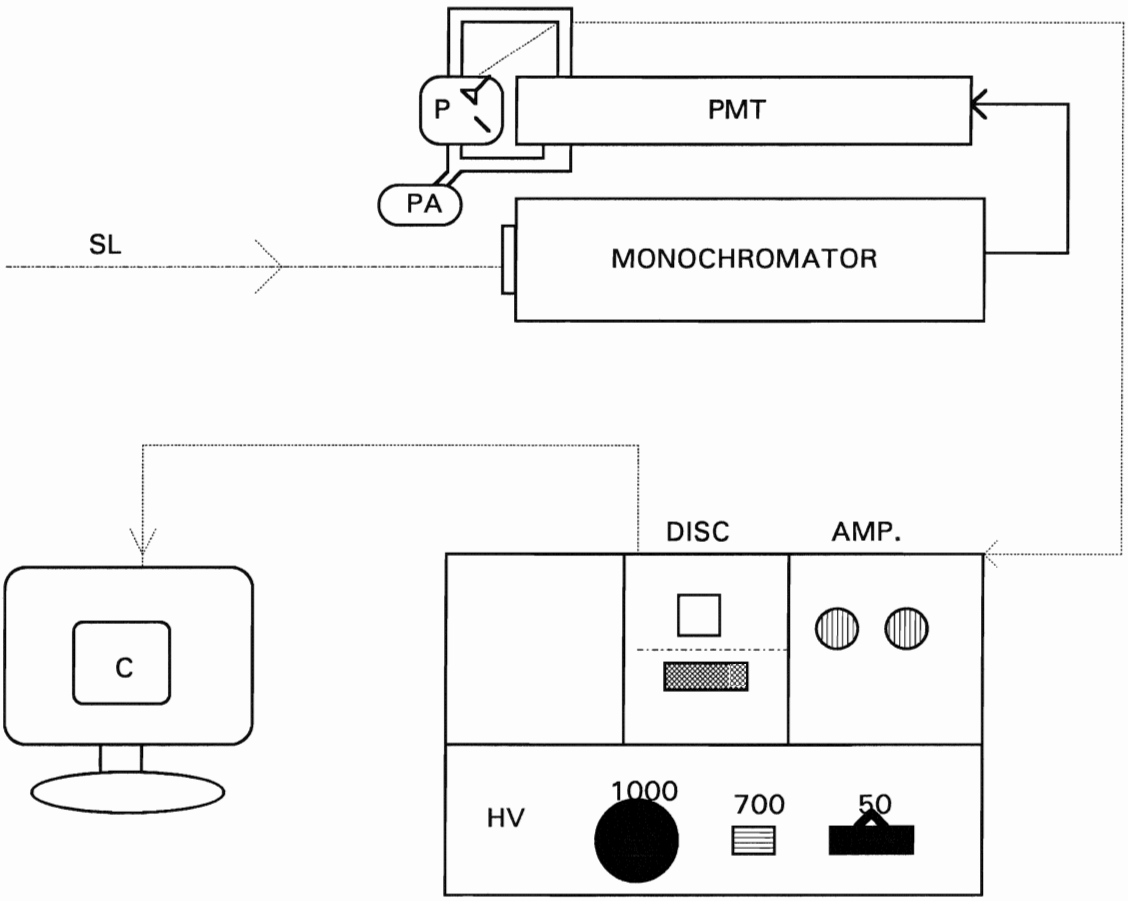

SL-Scattered light

P-Peltier cooler

PMT-Photomultier tube

PA-Pre-amplifier

AMP-Amplifier

DISC.-Discriminator

HV-High voltage

C-Computer

Fig. 3.5- Schematic of laser Raman interface.

3.1.0: RECORDING SPECTRA-

Methodology-

The laser and the Peltier cooler were turned on 45 minutes prior to recording of spectra. The sample cell was attached onto the vacuum line and pumped down. Spectrum of empty cell was recorded, to obtain background spectra of the cell and also to check for impurities The sample was loaded into sample cell by the procedure previously described (Sec. 3.2). A pressure of approximately 600-650 Torr of sample was taken. A check was done to ensure that all windows were extremely clean, which is essential as the smallest dust particle could cause the windows to "smoke". The cell was placed appropriately i.e., ensuring that the laser was away from the black wax surfaces and a maximum number of passes were achieved through the cell, in the path of laser beam. Further the sample cell position is as depicted in Fig. 3.3. The laser was operated at a power of 5 watts, as there are a number of difficulties encountered on operating at higher power, primarily window damage.

As the main modes of interest were those which constituted the totally symmetric vibrations, only these regions were scanned. Thus for each molecule, the regions scanned included the C-H stretch which occurs in the region 2800-2900 cm^{-1}, C-X stretch occurring in the range 600-1000 cm^{-1} and the symmetric deformation in the region 1300-1600 cm^{-1}. Details of the actual frequencies observed and a description of the normal modes will be considered in Section 6.

The cell was then pumped down again, and equal proportions of sample and nitrogen (internal standard), were loaded into the cell. The pressures taken were approximately 250 Torr of each, and spectra were recorded. A procedure as stated above was followed, wherein the regions of interest were scanned. Hence for the N-N stretch the region 2200-2400 cm^{-1} and 2800-2900 cm^{-1} for the C-H, were scanned.

3.1.1: INSTRUMENT STANDARDIZATION-

An integral part of the experimental work involves calibration of the spectrometer response. This has been explained in detail in Ref. 38, and in the following a brief description of the main purpose and procedure will be outlined.

Purpose-

The recording of Raman spectra involves proper optical alignment and intensity measurement. It is important to calibrate the frequency values of the spectrometer and the intensity response. It is known[43] that the detector (PMT) response is not linear with an increase in wave number shift. This is attributed to the decrease in energy of the photons as the wave number decreases. Further the response is seen to be different for the scattered light when the polarizer orientation is taken parallel and then perpendicular.

Procedure-

The instrument intensity response was calibrated by recording the spectrum of a standard lamp, which was a 200W quartz halogen calibrated with the NRC spectroradiometer. The calibration was done against three NRC spectral irradiance standards. The spectral irradiance of the standard are in units of $\mu W\ cm^{-2}\ nm^{-1}$ which are converted into wave number units by multiplying with the square of the wave length[44].

The setup was as directed in the manual, and the transfer optics are the same as in the Raman experiment for recording sample spectra. This is essential as the response is to be determined under identical optics conditions i.e., polarizer and scrambler orientation should be unchanged. It was stated[38] that the calibration result is independent of the polarizer orientation, however our results do not agree. The response was seen to be different for the polarizer orientation taken parallel and then perpendicular, and are as shown in Figs. 3.6 and 3.7.

The calibration function is generated by taking the ratio of the lamp emissivity to the observed lamp signal at the lamp calibration points. Figure 3.8 shows the actual response

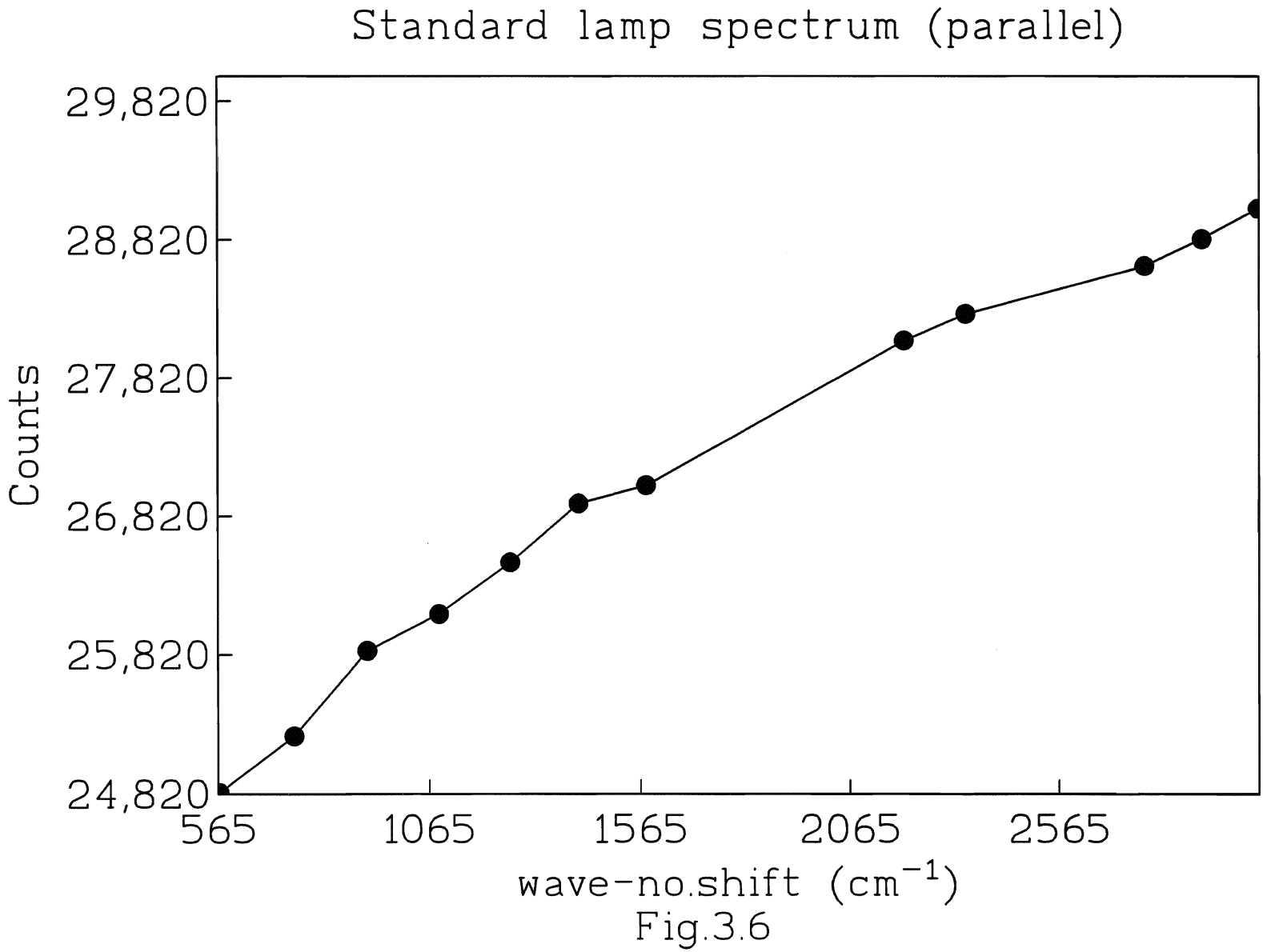
Standard lamp spectrum (parallel)
29,820
28,820
27,820
26,820
25,820
24,820
Counts
565
1065
1565
2065
2565
wave-no.shift (cm^{-1})
Fig.3.6

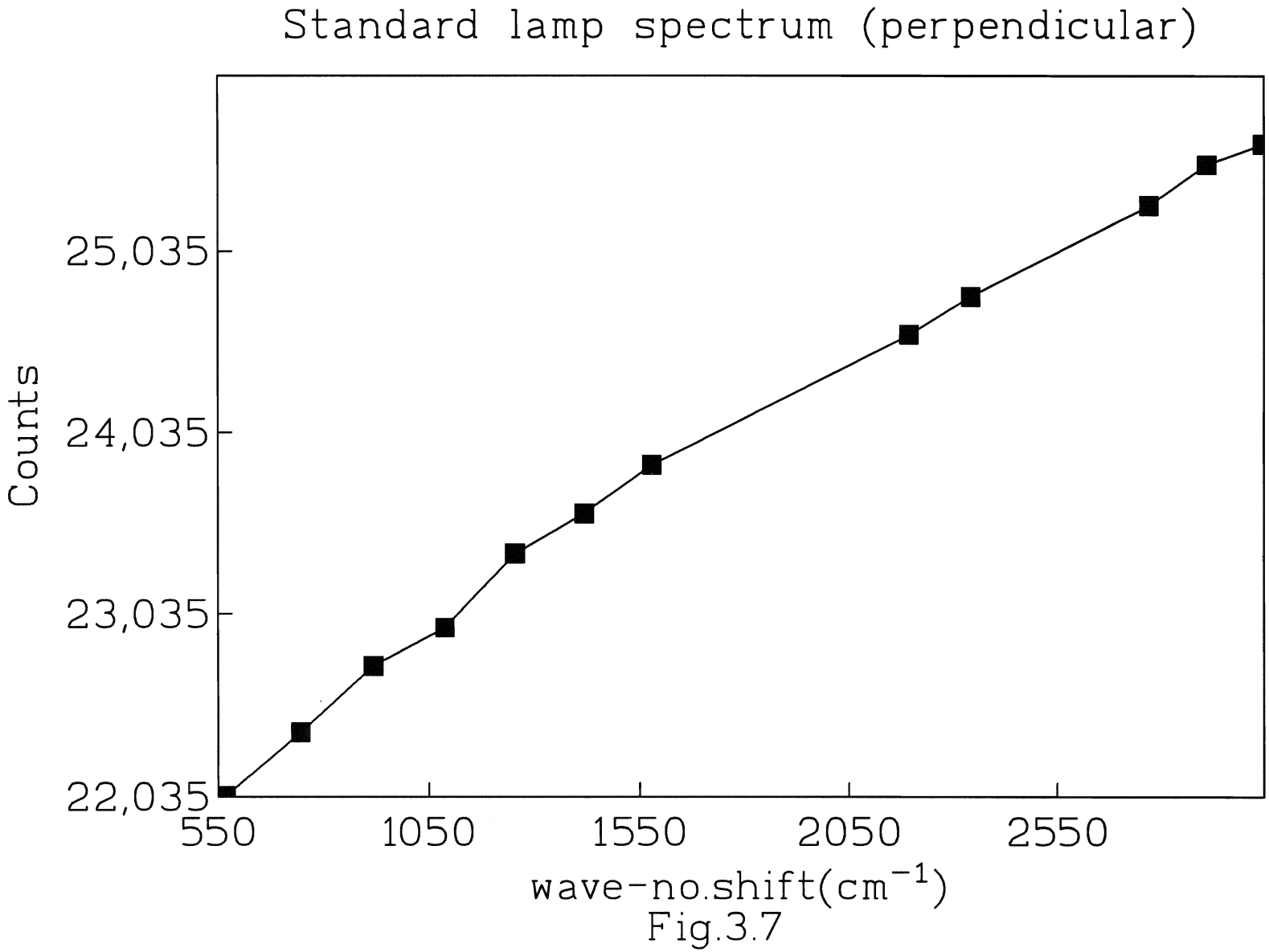
Standard lamp spectrum (perpendicular)
Counts
25,035
24,035
23,035
22,035
550
1050
1550
2050
2550
wave-no.shift(cm^{-1})
Fig.3.7

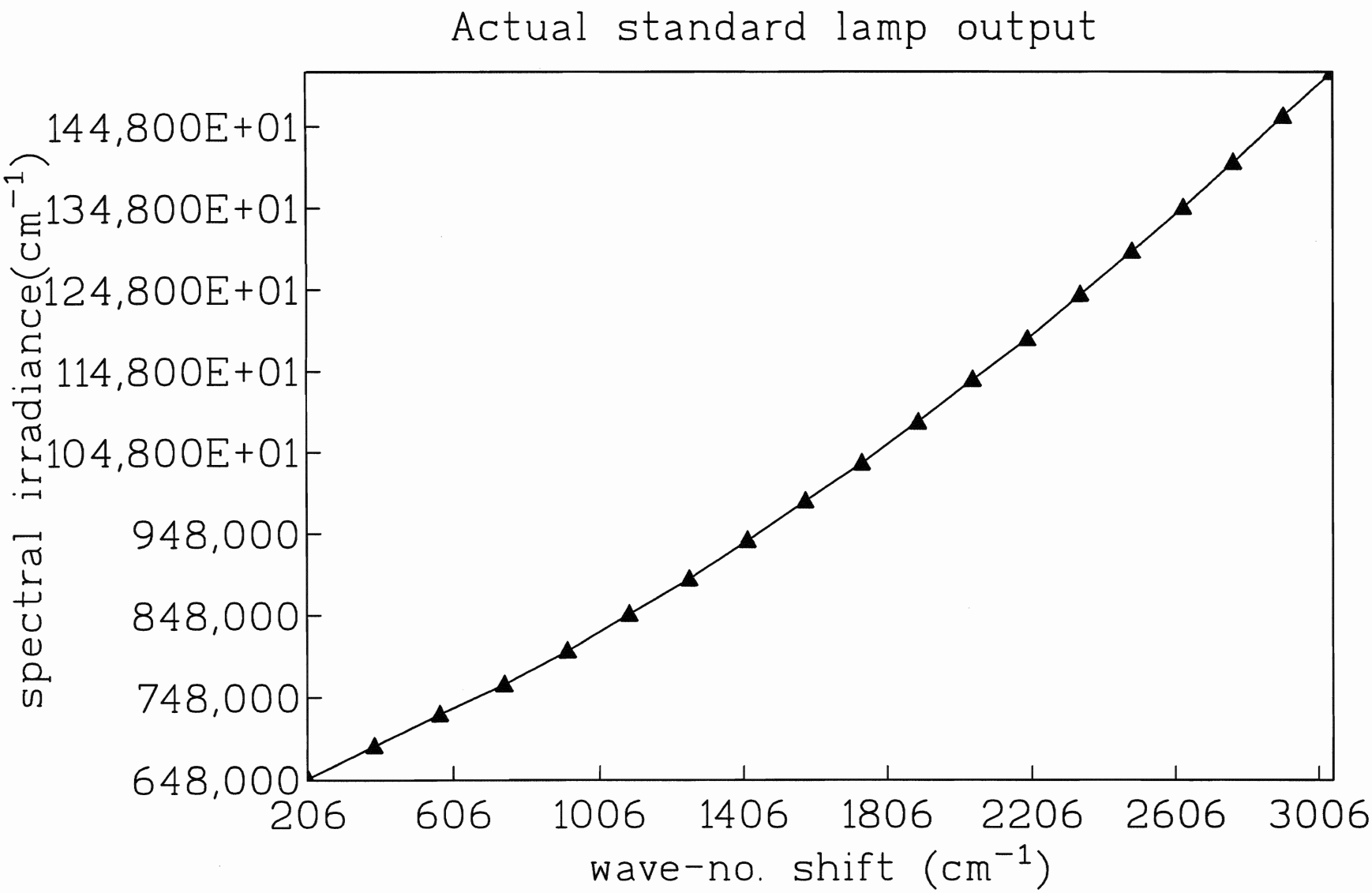
Actual standard lamp output
144,800E+01
134,800E+01
124,800E+01
114,800E+01
104,800E+01
948,000
848,000
748,000
648,000
spectral irradiance(cm^{-1})
206
606
1006
1406
1806
2206
2606
3006
wave-no. shift (cm^{-1})

Fig. 3.8

of the lamp as per manual. Employing a suitable interpolation method the calibration values were obtained which correspond to the experimental spectrum. This procedure was opted for both parallel and perpendicular orientations of the polarizer.

Correction factors were determined for both polarizer orientations and the relative intensities $I_{//}$ and $I_{\perp}$ were obtained. The trace intensity was obtained by multiplying $I_{\perp}$ by the factor 4/3 and subtracting this from the value for $I_{//}$. The value obtained corresponds to the differential scattering cross section for the trace scattering. The reliability of the standardization procedure and the results obtained will be considered in Sec. 6.

3.1.2: CALCULATION OF ABSOLUTE INTENSITIES-

The following is an explanation of absolute intensity measurements, undertaken for the three methyl halides. Calculations were done for each of the three symmetric modes, and the results are as in Sec. 6, along with a discussion.

Spectra were recorded for each region of interest, as stated above, with parallel and perpendicular orientations of polarizer. Hence we obtain spectra which are denoted as $I_{//}$ and $I_{\perp}$. These terms have been explained in Sec. 2.4, and as stated above, we require only the trace scattering. Areas corresponding to $I_{//}$ and $I_{\perp}$ were measured, and on multiplying by the appropriate correction factor, adjusted areas were obtained given as $I_{//}$ and $I_{\perp}'$. Multiplying 4/3 $I_{\perp}'$ and subtracting from $I_{//}$, we obtain areas corresponding to only trace scattering. The above can also be written in the form given below:

$$I_{//} \Rightarrow \text{area} \times \text{correction factor} = I_{//}' \text{ (adjusted area)} \qquad (3.1)$$

$$I_{\perp} \Rightarrow \text{area} \times \text{correction factor} = I_{\perp}' \text{ (adjusted area)} \qquad (3.2)$$

$$I \text{ (trace)} = I_{//}' - 4/3 \, (I_{\perp}') \qquad (3.3)$$

The absolute intensity of nitrogen has been determined[45] in the visible region. The value is (40.8± 0.8) × 10^{-36} m^2/sr, for the 514.5 nm excitation line. Using the above value the absolute intensities of the different symmetric vibrations i.e., C-H stretch, C-H deformation and C-X stretch, for all molecules were obtained. The following procedure was opted for and the results are as in Sec. 6.

As stated earlier a mixture of sample and nitrogen at approximately equal pressures were taken in the cell and spectra recorded. The trace areas were calculated for the respective stretching modes i.e., C-H and N-N, following procedure outlined above. The absolute intensity for the C-H stretch was determined using the following equation:

$$\frac{I_{(trace)_{C\text{-}H}}}{I_{(trace)_{N\text{-}N}}} \times \frac{\text{Pressure of nitrogen}}{\text{Pressure of methyl halide}} \times \text{Absolute value for } N_2 = \text{Absolute value for } C\text{-}H_{CH_3X} \tag{3.4}$$

From Eqn. (3.4), we obtain absolute intensity for the C-H stretch, and using this value the absolute intensity for the C-H deformation and C-X stretch, as given below:

$$\frac{I_{(trace)_{C\text{-}Hdef.}}}{I_{(trace)_{C\text{-}H}}} \times \text{Absolute value for } C\text{-}H = \text{Absolute value for } C\text{-}H_{def.} \tag{3.5}$$

$$\frac{I_{(trace)_{C\text{-}X}}}{I_{(trace)_{C\text{-}H}}} \times \text{Absolute value for } C\text{-}H = \text{Absolute value for } C\text{-}X \tag{3.6}$$

The above calculations were performed for all symmetric modes for methyl bromide, only the C-H and C-Cl stretch for methyl chloride as only these two were seen. For the methyl fluoride calculations were performed for all modes observed, though greater uncertainty exists for the symmetric deformation mode.

All spectra were manipulated and plotted using the program Spectra Calc[46].

4: Ab INITIO CALCULATION-

In the following we consider the basic principles involved in an *ab initio MO* calculation, a general G90 input, and the methodology to obtain different observables namely: frequencies, polarizabilities and numerical polarizability derivatives.

4.1: Basic Principles-

Ab initio is Latin for "from the beginning" and indicates a calculation based on fundamental principles. The theory implies that no experimental information is used in the implementation other than the values of fundamental constants such as speed of light. The model considers the atoms and molecules as a group of positive nuclei and negative electrons which move under the influence of electrostatic coulombic potential. The exact solution to Schrodinger equation has not been attained for a system with more than one electron. Hence to achieve a partial solution a number of approximations need to be introduced.

4.2: BORN-OPPENHEIMER APPROXIMATION[47, 48, 49] -

The initial approximation made in an *ab initio* calculation is the Born-Oppenheimer approximation. The essence of this is that the electrons are much lighter than the nuclei, they move more rapidly than the nuclei. Hence it is considered that the electrons move in a field of fixed nuclei. The total Hamiltonian for N electrons and M nuclei is given as:

$$H = -\sum_{i=1}^{N}\frac{1}{2}\nabla_i^2 - \sum_{A=1}^{M}\frac{1}{2M_A}\nabla_A^2 - \sum_{i=1}^{N}\sum_{A=1}^{M}\frac{Z_A}{r_{iA}} + \sum_{i=1}^{N}\sum_{j>1}^{N}\frac{1}{r_{ij}} + \sum_{i=1}^{M}\sum_{B>A}^{M}\frac{Z_A Z_B}{R_{AB}} \qquad (4.01)$$

The first term is the kinetic energy of the electrons, the second term is the kinetic energy of the nuclei, the third term is the coulomb attraction between electrons and nuclei, the fourth term is the repulsion of electrons, and the fifth term is the repulsion between nuclei. Within the Born-Oppenheimer approximation, the second term is neglected and

the fifth term is treated as a constant. The remaining terms define the electronic Hamiltonian.

4.3: SELF-CONSISTENT FIELD (HF) METHOD[47, 48] -

The basic idea of SCF methods is that each electron moves in an average field due to the nuclei and remaining electrons. The Schrodinger equation involving the electronic Hamiltonian is:

$$H_{elec'}\Psi_{elec'} = E_{elec'}\Psi_{elec'} \tag{4.02}$$

The electronic Hamiltonian operator, $H_{elec'}$, describes the kinetic and the potential energy operators of the system. The electronic wave function is described by the spatial and spin orbitals. The eigen value, $E_{elec'}$, represents the total one electron energies in the SCF field.

The N-electron wave function, Ψ, is approximated to be a linear combination of one-electron wave functions, Φ, :

$$\Psi = \sum_{i=1}^{N} C_{ij}\Phi_i \tag{4.03}$$

where the coefficients C_{ij} are determined such that the total electronic energy is minimized.

The Hartree-Fock method is based on the variational theorem. For an antisymmetric normalized function Φ, the expectation value of the energy is:

$$\langle E \rangle = \frac{\langle \Phi^* | H_{elec'} | \Phi \rangle}{\langle \Phi^* | \Phi \rangle} \tag{4.04}$$

If the chosen wave function, Φ, is the exact wave function, Ψ, then the exact lowest possible energy is obtained. If on the other hand Φ is not Ψ then the calculated energy will be higher than the exact energy. This energy value is subject to the single determinant condition imposed by the (HF) method, and the choice of basis set.

The variational principle is used to obtain optimum orbitals in the single determinant wave function. This is done by selecting a basis set and minimizing E with respect to the coefficients C_{ij}. This leads to the variational condition:

$$\frac{\partial E}{\partial C_{ij}} = 0 \tag{4.05}$$

4.4: BASIS SETS[47, 48] -

In the HF method, the N-electron wave function is constructed from the molecular orbitals in a single determinant. There are two major types of basis functions: the Slater type atomic orbitals (STO), and the Gaussian type atomic orbitals (GTO). The STO's are labeled as hydrogen-like atomic orbitals 1s, 2s, $2p_X$, ..., and are of the form:

$$\Phi_{1s} = (\frac{\zeta_1^3}{\pi})^{\frac{1}{2}} \exp(-\zeta_1 r) \tag{4.06}$$

$$\Phi_{2px} = (\frac{\zeta_2^5}{32\pi})^{\frac{1}{2}} x \exp(\frac{\zeta_2 r}{2}) \tag{4.07}$$

where ζ_1 and ζ_2 are constants determining the size of the orbitals. The integral evaluation using STO's is observed to be time consuming, and hence more commonly used is the other basis function namely Gaussian type. The GTO's include an exponential term of the form $\exp(-\alpha r^2)$, the radial dependence of such functions is similar to those of hydrogen-like 1s function (1s-STO). The GTO's are of the form:

$$g_s(\alpha, r) = (\frac{2\alpha}{\pi})^{\frac{3}{4}} \exp(-\alpha r^2)$$
$$g_x(\alpha, r) = (\frac{128\alpha^5}{\pi^3})^{\frac{1}{4}} x \exp(-\alpha r^2) \tag{4.08}$$

The GTO's provide extremely fast computation and the integrals are easily solved. There are several GTO basis sets and a brief discussion follows:

STO-nG implies that Slater type orbitals simulated by n Gaussian functions are used as basis set. The STO-3G is the minimal basis set, but it has the draw back of being unable to expand or contract its orbitals to fit the molecular environment, hence the use of split-valence or double zeta basis sets. In such basis sets the atomic orbitals consist of an inner compact orbital and an outer diffuse orbital. The size of the atomic orbital that contributes can be varied by the coefficients associated with the compact and diffuse parts. An example of the double-zeta function is the 4-31G basis set. 4-31G implies that there are four Gaussians for the core orbitals, three inner Gaussian valence-orbitals, and one outer valence orbital is used.

In this thesis, the D95 ** basis set was incorporated, this is the (4s2p/2s) Dunning[28] contraction of the (9s5p/4s) Huzinaga[29] basis, with a single polarization function on each atom i.e., a d function (exp =0.75) on the carbon atom and a p function (exp = 1.0) on the hydrogen atoms. The choice of this basis has been explicitly explained in Ref.23. This basis set was feasible only for the CH_3Cl and CH_3F molecules and a different basis set was necessary for the CH_3Br molecule.

4.5: CALCULATIONS FOR CH_3BR MOLECULE-

The D95** basis set has not been parameterized for the Br atom. The other basis sets found feasible included the STO-3G*, LANL1DZ (D95V on first two row elements and ECP+DZ on the other atoms) and the LANL1MB (STO-3G on first row, ECP+MBS on other atoms). Calculations were performed with all the above mentioned basis sets and also with a general basis set[50], specifically written for third row elements, but optimization did not produce reasonable results and hence it was not considered further. The choice of basis set used for further calculations was the LANL1DZ, and the reasons are explicitly considered in Section 6.

The preceding is a description of the basic principles involved in an *ab initio* calculation. To obtain results with the G90 package, a systematic format of the input is essential. The input is explained as follows.

4.6: EXPLANATION OF G90 INPUT-

A detailed explanation may be obtained in Ref. 47, and at this point a brief explanation is provided. The description is similar for all molecules, changes occurring with respect to the name of the molecule and the bond lengths.

The first line is a specification of the output containing the read/write file (rwf), which contains information about the wave function. This file is important as we obtain the wave function from it, required for the AIM calculations.

The next line specifies the task to be performed and the basis set incorporated i.e., the calculation was performed at the Hartree-Fock (hf) level with the D95 ** basis set, to determine the polarizability of the molecule (polar). Other calculations may include: single point calculation, geometry optimization, harmonic frequencies, etc. The term density = all is an essential condition for the program PSIG90[33] to read the rwf. This term allows the charge density to be obtained for the perturbed and unperturbed field. The next line is a description of the molecule, its conformation, type of calculation etc. This line is not processed by the program, but is merely reproduced in the output.

The geometry of the molecule is given in the form of the Z-matrix, details of the procedure are as given in Ref. 26. The 'x' signifies dummy atoms, and are opted for only to simplify the orientation of the molecule. The Cartesian coordinates generated for the dummy atoms are not utilized in the quantum mechanical calculation. From the Cartesian coordinates generated the orientation of the molecule is as given in Fig. 4.1. This is identical for all molecules, only difference is relative to bond lengths. Thus for all molecules we have the carbon at the origin, the halogen directed along the positive z axis. The three hydrogens were labeled as H3, H4 and H5, depending on the position along the

coordinate system. This was merely done for practical purposes and ease of computation understanding, which will be discussed later.

Finally the values of importance, the bond lengths, are given. These were obtained by a previous optimization calculation, with the D95** basis set.

Details of the output will not be considered and may be obtained in Ref. 47. Only the methodology to obtain frequencies, polarizabilities and numerical polarizability derivatives are considered in Sections 4.7-4.10.

4.7: GEOMETRY OPTIMIZATION[47, 52]

A geometry optimization is generally obtained by successively minimizing variables; this is explained as follows.

The sequence of modules resulting in the optimization of the molecular geometry, is as shown in Fig. 4.2. The computation begins with a fixed geometry of the molecule. After an initial geometry and the basis set are specified, the integrals are evaluated and an initial guess is made at the wave function. The SCF equations are solved to obtain the total energy and wave function. Using this wave function, the gradient of the energy, i.e., the derivative of the energy with respect to displacement in the nuclear coordinates, is evaluated. The optimization procedure terminates when the gradient is below some preset limit. If the gradient is larger, then the original geometry is varied by slight change in the bond lengths and bond angles and a new calculation of integrals, SCF energy and energy gradient follows. Further for a system of n variables, between n and 2n gradient cycles are usually needed to find the minimum energy geometry.

At this optimized geometry, further calculations are performed on the molecule, and the values of different observables are obtained. Of significance for our work include

G90 INPUT-

% rwf = CH3f.

p hf/d95** 6D polar density = all

methyl fluoride polarizability calculation, using optimized parameters.

0 1

C

f 1 rcf

x 1 rcx 2 90.0

x 1 rcx 2 90.0 3 120.0 +1

x 1 rcx 2 90.0 3 120.0 -1

h 1 rch 1 90.0 2 180.0

h 1 rch 1 90.0 2 180.0

h 1 rch 1 90.0 2 180.0

rcf - 1.3667

rcx - 1.0251

rhx - 0.3512

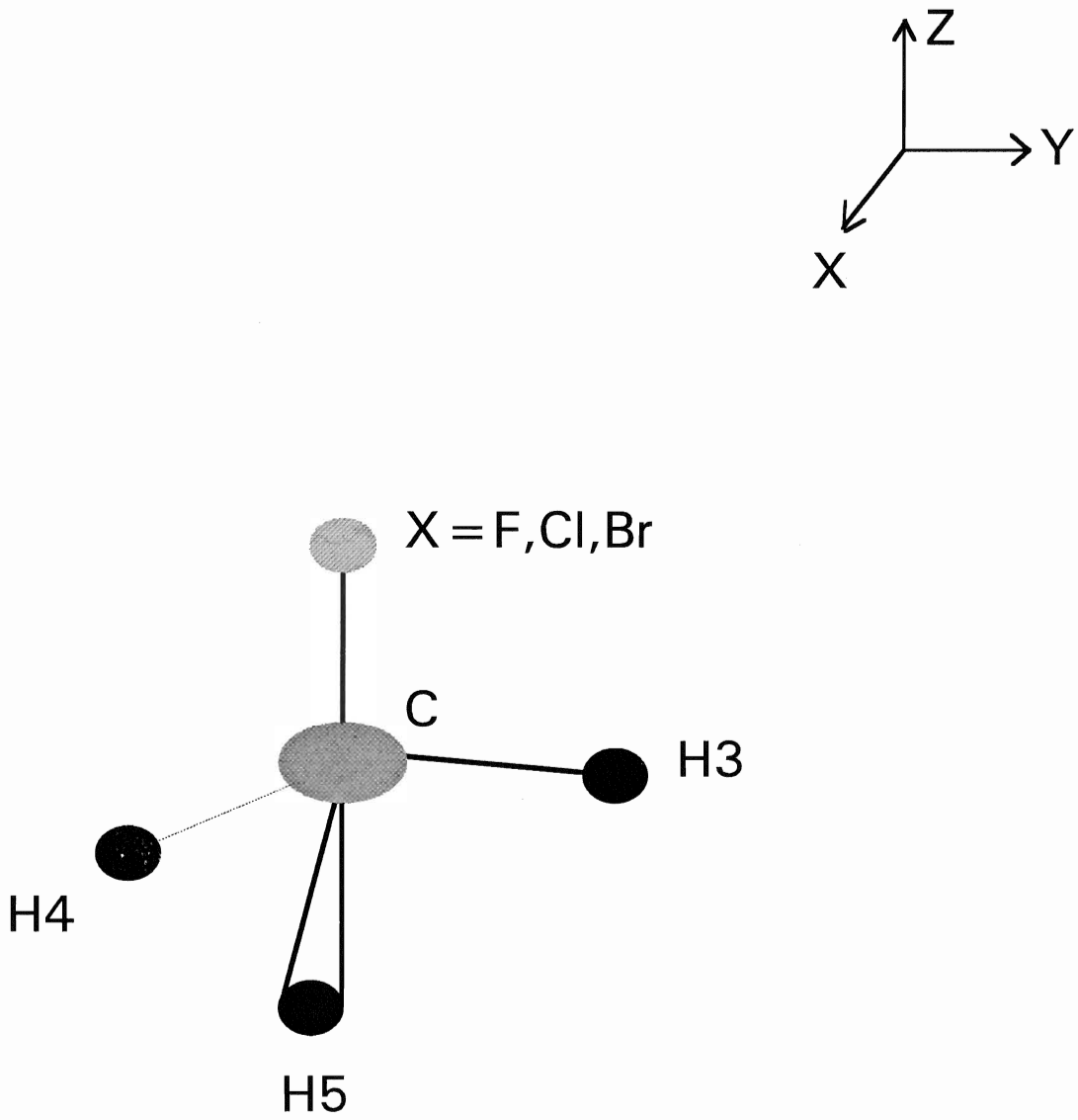

Fig. 4.1-Molecular orientation of the methyl halide

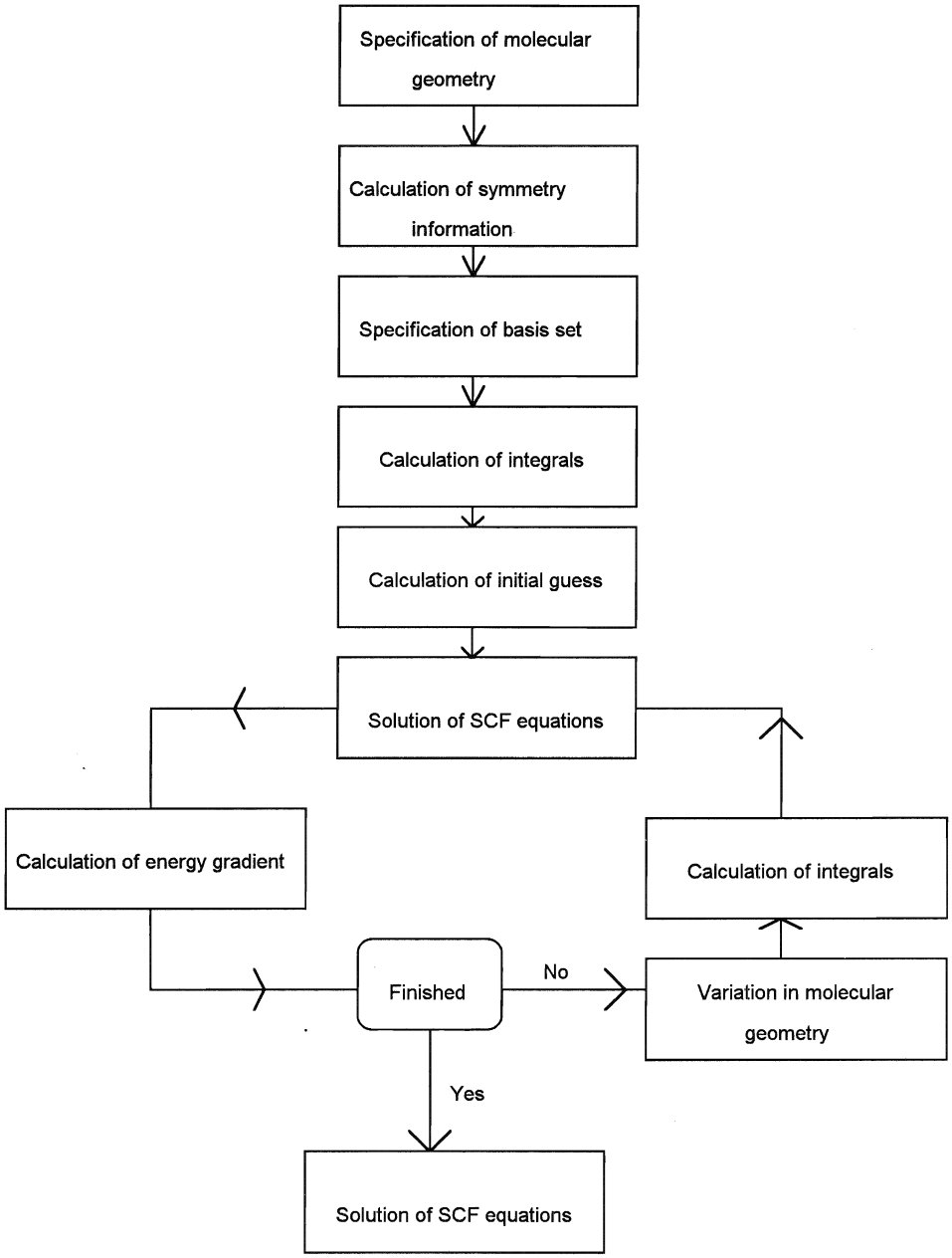

Fig. 4.2- Sequence of modules resulting in the optimization of the molecular geometry

vibrational frequencies, polarizabilities and numerical determination of polarizability derivatives.

4.8: VIBRATIONAL FREQUENCIES[47]-

The vibrational frequencies, within the harmonic approximation, are given as:

$$\upsilon = \frac{1}{2\pi}\left(\frac{f_{ij}}{\mu}\right)^{\frac{1}{2}} \tag{4.09}$$

where μ is the reduced mass $=m_1m_2/(m_1+m_2)$

f_{ij} are the quadratic force constants, which are determined as follows.

Starting with the optimized coordinates, the quadratic force constants i.e., the second derivatives of the potential energy with respect to mass weighted Cartesian displacements, are evaluated at the equilibrium nuclear configuration, and given as:

$$f_{ij} = \left(\frac{\partial^2 V}{\partial q_i \, \partial q_j}\right)_{eq} \tag{4.10}$$

where :

V is the potential energy at the equilibrium geometry

q_i are the mass weighted Cartesian displacement coordinates and

f_{ij} are the quadratic force constants

The f_{ij} may be evaluated by numerical second differentiation,

$$\frac{\partial^2 \mathrm{V}}{\partial \mathrm{q_i} \, \partial \mathrm{q_j}} \cong \frac{\Delta(\Delta \mathrm{V})}{\Delta \mathrm{q_i} \, \Delta \mathrm{q_j}} \tag{4.11}$$

or by numerical first differentiation of analytical first derivatives,

$$\frac{\partial^2 V}{\partial q_i \, \partial q_j} \cong \frac{\Delta\left(\frac{\partial V}{\partial q_j}\right)}{\Delta q_i} \qquad (4.12)$$

The calculation yielded a set of 3N normal modes of motion. Six are zero corresponding to translational and rotational degrees of freedom. Frequencies computed theoretically are compared with the frequencies obtained experimentally via Raman and FTIR, and results are as depicted in Section 6.

The *ab initio* calculation provides further insight regarding infrared and Raman intensities, depolarization ratios and force constants. This information is extremely helpful in assigning frequencies to the respective normal modes, and in predicting the validity of a peak depending on its intensity value. Of significance are the force constants obtained in both internal and Cartesian coordinates, these values are then used for normal mode calculation to obtain the L matrix. The L matrix[36] is essential to relate theoretical intensities obtained via *ab initio* and AIM with experimental intensities.

4.9: POLARIZABILITY CALCULATION[53]-

When a molecule is placed in an external field the nuclei are attracted towards the negative end and the electrons towards the positive end. Thus a dipole is induced in the molecule whose magnitude is proportional to the field strength, and is given as:

$$\mu = \alpha E \qquad (4.13)$$

where μ is the induced dipole, E is the electric field, and α is the proportionality constant or the polarizability.

The polarizability is a measure of the ease of charge redistribution within the molecule. If the charge distribution is mobile then it will redistribute itself until its energy in the external field is minimized.

The dipole moment tends to change in the external field. This change is studied by expanding the moments as a Taylor series, and we obtain:

$$\mu=\mu_e(E=0) + \alpha E + \tfrac{1}{2}\beta' E^2 + \ldots\ldots\ldots\ldots \quad (4.14)$$

where $\mu_e(E=0)$ is the permanent dipole moment, α is the dipole polarizability tensor and β' is the first hyperpolarizability tensor.

The energy, (W), of the charge distribution can be written in terms of the permanent moment as:

$$W = Wo - \mu_e(E=0).E - \tfrac{1}{2} E.\alpha.E - \ldots\ldots \quad (4.15)$$

Further the dipole moment and the polarizability can be related to the energy of the charge distribution, by the following:

$$(\mu_e)_i = -\left(\frac{\partial W}{\partial E_i}\right)_{E=0} \quad (4.16)$$

and

$$\alpha_{ij} = -\left(\frac{\partial^2 W}{\partial E_i \partial E_j}\right)_{E=0} \quad (4.17)$$

The tensor is symmetric, and we get $\alpha_{ij} = \alpha_{ji}$, so that there are not more than six independent components representing the polarizability. As mentioned earlier (Sec. 2), these six components combine to give the isotropic and anisotropic part of the polarizability tensor.

The molecule is rotated so that the principal axes of the polarizability ellipsoid coincide with the geometric coordinate axes, and the tensor is written as:

$$\alpha = \begin{pmatrix} \alpha_{xx} & 0 & 0 \\ 0 & \alpha_{yy} & 0 \\ 0 & 0 & \alpha_{zz} \end{pmatrix} \quad (4.18)$$

For the molecular orientation chosen and due to the symmetry of the molecules, we may write:

$$\alpha_{xx} = \alpha_{yy}.$$

The molecular polarizability is given as one third the sum of the diagonal elements of the polarizability tensor and is of the form:

$$\bar{\alpha} = \frac{1}{3}\left(\alpha_{xx} + \alpha_{yy} + \alpha_{zz}\right) \tag{4.19}$$

4.10: POLARIZABILITY DERIVATIVE-

The polarizability is computed for the equilibrium geometry and for a geometry wherein one or more of the bonds is displaced along the bond axis, to simulate a vibration in the molecule. Since, for the molecules under study, there are two types of bonds, the C-H and the C-X (X = F, Cl, Br), the polarizability is computed by increasing and then decreasing the particular bond by a certain value. Discussion of the choice of bond change for each type of bond type is in Section 6.

The polarizability derivatives are numerically obtained from the difference in the polarizability tensors at the equilibrium geometry and at geometries distorted along the symmetry coordinates for the C-H and C-X, where (X=F, Cl Br), bonds. The numerically obtained polarizability derivatives, $\Delta\alpha$, are divided by Δr, the amount by which each bond is changed, and we can write the derivative in the form:

$$\frac{\Delta\alpha}{\Delta r} = \frac{\alpha_{eq} - \alpha_{ch.}}{\Delta r} \tag{4.20}$$

where - α_{eq} is the polarizability at equilibrium geometry,

$\alpha_{ch.}$ is the polarizability when the respective bond is changed and

Δr is the amount by which the bond is changed.

Further, the individual polarizabilities, for the respective geometries are determined as given in Eqn. (4.19). The derivatives calculated are divided by the number of similar bonds i.e., three for C-H and one for the C-X (X = F, Cl Br), and we get the change in polarizability per bond type.

We obtain the theoretical derivatives with respect to internal coordinates i.e., bond length. As has been explained in Section 2, the Raman intensities are directly proportional to the change in polarizability with respect to the normal coordinates. These are then converted to internal coordinates for comparison with theoretical values.

5: THEORY OF ATOMS IN MOLECULES-

In the following we consider the basic principles of the theory of atoms in molecules, the methodology to obtain polarizabilities and polarizability derivatives and finally a general input explanation for the PROAIM computation.

5.1: BASIC PRINCIPLES-

The theory of atoms in molecules (AIM), was formulated on the basic postulates proposed by Dalton (1808)[48]: that matter is made up of atoms, that atoms of a given element are identical and that atoms preserve their identity in all chemical transformations.

The following is an explanation of the theory (AIM), which will lead to the definition of a quantum subsystem or atom, on the basis of a study of the topological properties of the system's charge distribution. This study also leads to definitions of bonds which link atoms together, structure and structure stability. This has been very efficiently covered in Ref. 54, and at this point the basic principles need to be considered.

The state function, denoted by the symbol (ψ), appears in one of the first postulates of quantum mechanics[48]. The state function is a function of nuclear and electronic coordinates and is denoted as $\psi(x, X, t)$. Of significance is the physical interpretation of the state function i.e., the square of the state function $(\psi)^2$, which is the probability distribution of finding a particle within a given volume element. The probability distribution may also be denoted as $\rho(r, X)$, which is the charge density distribution in real space.

The charge density is commonly written as $\rho(r)$; here r denotes the position vector of an electron. The nuclear coordinate, (X), term may be omitted as all calculations are done within the Born-Oppenheimer approximation[47, 48]. Further, the charge density is a description of the distribution of charge of one electron as determined by an average over the motions of the other electrons i.e., determined by an average over the interactions of all the particles in the system.

There is however a reduction in the amount of information in passing from the state function (a vector in Hilbert space), to the charge density (a distribution function in real space). It is stated[54] that to define an atom in real space and to obtain atomic properties, it is more appropriate to study the charge density. Further, the information contained in the state function is observed to be too much, some of it being redundant because of the indistinguishability of the electrons and also because of the symmetry of their interactions. In describing a system in terms of $\rho(r)$, the properties of a system as observed in real space are obtained and through this a basis for the definition of structure.

Topology is a study of geometrical properties unaffected by continuous change of shape or size. We study the topological features of the charge density i.e., the fluctuations of charge distribution within the molecule. It has been observed[54], by experiment (X-ray diffraction studies on crystals) and by theoretical calculations, that the charge density exhibits maxima only at the positions of nuclei[55]. Since the charge density is a scalar field, it has only magnitude associated with it, and its form is dominated by the forces exerted on it by the nucleus.

It is the display of the gradient vector of the charge density which, by associating magnitude and direction with each point in space, leads to the definition of atoms and molecular structure. The significance of this is that with the gradient vector we are able to observe the direction in which the density is increasing. This point will be considered in the ongoing explanation.

The gradient denoted by the symbol (∇), is written as:

$$\nabla = i(\frac{\partial}{\partial x}) + j(\frac{\partial}{\partial y}) + k(\frac{\partial}{\partial z}) \qquad (5.01)$$

where i, j, and k denote unit vectors along the x, y, and z axes respectively.

The methodology to obtain the *gradient paths* or *trajectories* has been explained in Refs. 54 and 56, and a brief description is sufficient. The paths are obtained by starting at

some arbitrary point, r_o, and taking a step $|\Delta r|$ in the direction indicated by the gradient vector i.e., in the direction of increase in the charge density. The gradient vector field of the charge density, denoted as, $\{\nabla\rho(r_o)\}$, is then calculated The path generated terminates, at the critical points[57], defined next.

The critical points, are defined as the points where the first derivative of the charge density vanishes[57]. At such a point r_c, we obtain the equation:

$$\nabla\rho(r_c) = 0 \qquad (5.02)$$

The critical points are commonly expressed as (w, σ), where 'w' or rank, signifies the number of non zero curvatures of the critical point and 'σ' or signature, is the sum of the signs of the curvatures at the critical point. The rank value is taken to be 3[54, 57], and relative to this value there exist four different values for the signature. We thus obtain four critical points which are of importance for the definition of structure: (3, -1), (3, -3), (3, +1), and (3, +3). The first point is characteristic of a bond critical point which will be discussed below. The other points are characteristic of ring and cage structures which will not be discussed, but may be obtained in Refs. 54, 55, and 57.

Because the charge density exhibits maxima only at the position of the nuclei and the gradient paths terminate at the nucleus, it is termed as an *attractor*. The "space" surrounding the nucleus is the *basin* and may be understood as being the region surrounding the nucleus consisting of the gradient paths. The complete region upto which the paths terminate at a particular nucleus, defines the *basin* of that nucleus. The atomic basin, Ω, is taken to be the union of the surface and the *volume* within. The volume of an atom is determined by the intersection of the atomic surface with an envelope of the charge density of some chosen value[56, 58]. The 0.001[54, 58] au envelope for an entire molecule was found to give good agreement with the van der Waals shapes and sizes of molecules in the gas phase.

As mentioned above, all these paths terminate at the position of the nucleus, except two. There exist two paths which terminate at the (3, -1) critical point, and lead to the formation of the *interatomic surface*[54, 55]. This surface exists between all pairs of bonded nuclei and defines a boundary.

An atom is then defined, in the AIM theory terminology, as being the union of an attractor and its basin. Alternatively the atom is defined in terms of its surface, and is defined as[54]: " the subsystem (atom) satisfies a boundary condition stated in terms of the property of the charge density, i.e., the flux in the gradient vector field of the charge density vanishes at every point on the surface which bounds the subsystem and is given as:

$$\nabla\rho(\mathrm{r})\cdot\, \mathrm{n}(\mathrm{r}) = 0 \qquad (4.03)$$

where n(r) is the unit vector normal to the surface."

It can be stated that any surface in the molecule, satisfying the above boundary condition, is one which defines the surface of an atom. Pictorially a molecule may be seen to be partitioned into a set of disjoint regions or atoms, if the above stated boundary condition is satisfied.

From the definition of an atom we obtain a definition of bonds, which finally leads to molecular structure. The (3, -1) critical point, also referred to as bond critical point[57], is a point found between all pairs of bonded nuclei. There exist two paths, terminating at this point, which signify the boundary surface of the atom i.e., *interatomic surface.* There are also two gradients paths which originate at this point and terminate at the positions of the nuclei situated at either end of this point. The line formed when the paths are taken together is the *bond path* or *atomic interaction line*[54, 55]. These bond paths thus determine which nuclei are bonded in the molecule. The union of these bond paths leads to the formation of *molecular graphs*[54].

For the understanding of atomic properties the discussion above is sufficient and will be terminated at this point, however details of structure and structural stability may be

obtained in Ref. 54. The following is a detailed explanation on how the AIM theory may be applied, with the help of a number of programs, to determine different molecular properties, and in particular the polarizability. Following this will be the general input for the calculation and then the results.

The approach taken in the AIM analysis, for the determination of any molecular property, is to first obtain atomic properties i.e., atomic volumes, atomic dipoles, atomic energies, atomic charge etc. Summation of these properties over all atoms present in the molecule determines the total molecular property for the molecule.

This theory (AIM) has been applied to determine the molecular polarizability which will be obtained by first determining the atomic charges and atomic dipoles, summation of which will lead to the total molecular polarizability. A detailed discussion follows along with appropriate equations.

5.2: DETERMINATION OF MOLECULAR POLARIZABILITY -

When a molecule is placed in an electric field, E, the charge density, ρ, is redistributed. The magnitude of the induced dipole, $\Delta\mu$, depends on the magnitude of the applied field, E, and on the molecular polarizability, α, and is given as:

$$\Delta\mu = \alpha E \qquad (5.04)$$

Within the theory of atoms in molecules the molecular polarizability is obtained as a sum of atomic polarizabilities which are obtained from atomic properties, calculated by the program PROAIM[33].

The molecular wave function obtained from *ab initio* MO calculation is found to contain all the information on the atoms (subsystems Ω). The program PSIG90[33] was used to obtain the perturbed and the unperturbed wave functions from the G90 read/write file. The unperturbed wave function corresponds to a zero electric field, E_0, and the perturbed wave function results from the application of a field strength of 0.009449 a.u.,

applied in x, y, and z directions corresponding to E_x, E_y, and E_z respectively. The program SADDLE[33] was used to determine the critical points from the wave functions, relating to the different fields. The critical points, the points at which the first derivative of $\rho(r)$ vanish, are positions of extrema in the charge density — maxima, minima, or saddle points.

The application of an electric field has two effects[59, 60, 61]: it perturbs the charge distribution over the atomic basin, and this results in the transfer of electronic charge from one atom or grouping of atoms to the other; it also changes the polarizations of the atomic densities. The change in the dipole moment is given as the sum of the these two terms, a charge transfer contribution, $\Delta\mu_c$, and a polarization contribution, $\Delta\mu_p$[61], and is written as:

$$\Delta\mu = \sum_{\Omega}\{\Delta q(\Omega) X_{\Omega} + \Delta M(\Omega)\} = \Delta\mu_c + \Delta\mu_p \qquad (5.05)$$

where- X_Ω is the position vector of the nuclei, $q(\Omega)$ is the net charge on atom Ω, and is given as:

$$q(\Omega) = Z_{\Omega} - N(\Omega) \qquad (5.06)$$

$\Delta M(\Omega)$ is the atomic first moment which provides a measure of the dipolar polarization of the atom's density, written as:

$$M(\Omega) = -\int_{\Omega} r_{\Omega}\rho(r)d\tau \qquad (5.07)$$

with the origin of the position vector r_Ω taken at the nucleus. The changes in these quantities as they appear in Eqn. (5.05), when divided by the field strength, yield the corresponding contributions to the atomic polarizability.

The average value of an observable of the total system is then just the sum of the atomic contributions.

$$\langle A \rangle = \sum_{\Omega} A_{\Omega} \tag{5.08}$$

In the following discussion we consider the calculation of the atomic polarizability. This is obtained by integration over the atomic basin, and the steps outlined below are based on previous calculations[13].

The atomic basin is simplified into the sum of two contributions as stated above: charge transfer and atomic dipole contributions. This is calculated for each atomic basin, Ω, as:

$$(\text{charge transfer})_{i,j,\Omega} = \left[\Delta N_i x_j\right]_{\Omega} = \left\{\left[N(E_i) - N(E_0)\right] \cdot x_j\right\}_{\Omega} \tag{5.09}$$

where x_j is the atom position on the j^{th} axis, ΔN_i is the change in the electron population of that atom for a field is applied in the i^{th} axis, and i, j = x, y, and z. The charge transfer is generated in tensor form, wherein the rows relate to the direction of the applied field and the columns give the three dimensional response. For $x_i = 0$, i.e., the instance when an atom lies in the field perpendicular to the applied field, the change in charge transfer makes no contribution to the diagonal term in the tensor.

The second contribution is due to the rearrangement of electronic charge within an atomic basin in the jth direction, for a field applied in the ith direction:

$$(\text{atomic dipole})_{ij,\Omega} = \Delta\mu_{ij,\Omega} = \left[\mu_j(E_i) - \mu_j(E_0)\right]_{\Omega} \tag{5.10}$$

Thus the atomic polarizability tensor is given by:

$$\left(\alpha_{ij}\right)_{\Omega} = \frac{\left[-\Delta N_i x_j\right]_{\Omega}}{E_i} + \frac{\Delta\mu_{ij,\Omega}}{E_i} \tag{5.11}$$

where the two contributions to the induced dipole have been divided by the magnitude of the field applied along the ith axis, E_i. The total molecular polarizability tensor is obtained as summation over all atomic contributions and is given as:

$$\alpha_{ij}(molecule) = \sum_{\Omega=1}^{n\,\text{atom}} (\alpha_{ij})_{\Omega} \qquad (5.12)$$

The molecular axis orientation chosen for the calculations was such as to place the principle axes of the molecular polarizability along the Cartesian axes of the system. All off diagonal terms cancel on summation, and the molecular orientation (Fig. 4.1) was taken such that we get $\alpha_{xx} = \alpha_{yy} < \alpha_{zz}$ for CH_3Cl and CH_3Br and $\alpha_{xx} = \alpha_{yy} > \alpha_{zz}$ for CH_3F.

5.3: POLARIZABILITY DERIVATIVE-

The derivative of the molecular polarizability with respect to a bond stretch was found from the numerical difference between the polarizabilities calculated for the equilibrium geometry and for the geometry wherein the bond was distorted to simulate a vibration. The wave functions are obtained from *ab initio* (MO) calculations, relative to all the different geometries i.e., C-H increase and decrease and the C-X increase and decrease. The wave functions were analyzed, within the theory of atoms in molecules, in the steps outlined above. Atomic contributions i.e., charge transfer and atomic dipole, were obtained for each geometry, and taking the difference relative to the equilibrium structure the polarizability derivative was numerically obtained and is given as:

$$(\Delta\alpha_{ij})_{\Omega} = (\Delta \text{ charge transfer})_{ij,\Omega} + (\Delta \text{ atomic dipole})_{ij,\Omega} \qquad (5.13)$$

where Δ(charge transfer) and Δ(atomic dipole) are obtained from the difference in the atomic charge transfer and atomic dipole terms, for the distorted geometry and the equilibrium geometry. The molecular polarizabilities and the polarizability derivatives were obtained with the program ALPHA[62], and calculations were performed on a 386 SX IBM-PC compatible.

The results were obtained in tensor form, and all non diagonal terms were either zero or too small to be considered significant. Hence only diagonal terms for the charge transfer and atomic dipole were considered. The polarizability derivatives obtained were then divided by the number of equivalent bonds being displaced. There are three corresponding to the C-H bonds and one for the C-X (X=F, Cl, Br) bond. We thus obtain a derivative of the polarizability with respect to a symmetry coordinate, which is given as:

$$(\frac{\Delta\alpha_{ij}}{\Delta r})_{\Omega} = \frac{(\Delta \text{ charge transfer})_{ij,\Omega}}{\Delta r} + \frac{(\Delta \text{ atomic dipole})_{ij,\Omega}}{\Delta r} \qquad (5.14)$$

This was then converted to the mean of the molecular polarizability and reported in SI units for comparison with experiment.

$$\frac{\Delta\overline{\alpha}}{\Delta r} = \frac{1}{3}(\frac{\Delta\alpha_{xx}}{\Delta r} + \frac{\Delta\alpha_{yy}}{\Delta r} + \frac{\Delta\alpha_{zz}}{\Delta r}) \qquad (5.15)$$

5.4: EXPLANATION OF PROAIM INPUT-

The following is a PROAIM[33, 56] input for the methyl fluoride at the equilibrium geometry. A similar input is used for all molecules, for the different geometries and for the different field directions i.e., E_X, E_Y and E_Z.

The first line is a description of the molecule and the type of calculation i.e., methyl fluoride, equilibrium geometry for the unpertubed wave function (E_0 field) and the fact that this integration is carried out on the carbon atom which is numbered as one. The atom numbering is that opted for in the G90 z matrix orientation, Fig. 4.1.

The second line is the atom symbol with the atom label i.e., 1 for C, 2 for F etc. This is followed by the number of critical points relative to the particular atom i.e., carbon has four bond critical points, fluorine and the hydrogens will have each have one bond critical

point. The coordinates of the associated critical points corresponding to the different bonds in the molecule are obtained by SADDLE, and are as noted.

It is stated[33] that by integrating along the trajectories of $\nabla\rho(x)$, which terminate at the position of the nucleus, the basin of the particular atom is efficiently covered. Further, it is not possible to cross from one atomic basin to the neighboring basin, due to the zero flux surface condition. To exploit this idea requires a coordinate transformation from (x, y, z) to (s, θ, ϕ), where s determines the position of a point along the gradient path which is further defined by an initial set of angular coordinates, θ and ϕ. Hence, the direct determination of atomic surfaces is obtained.

The values of 120 and 96 correspond to the number of phi(ϕ) and theta(θ), planes, respectively. It was found that the best integration results are obtained on taking this many planes, and the recovery of the polarizability, by the AIM theory is approximately 99%+ of G90. Integrations with a value of 96 or 64 for both planes were performed, but the recovery was too low and they were not considered further.

The next input is the size of the beta sphere i.e., the minimum distance between the atom of interest and an associated (3, -1) or bond critical point. The value of this was obtained from SADDLE. For the carbon atom, due to the presence of four critical points, four values were obtained, and the smallest value is assigned as the beta radius. For the remaining atoms there will exist only one value due to the presence of one (3, -1) point. This beta sphere serves the main purpose of performing the integration accurately at the respective atom.

The values of 360 and 141 denote the number points per surface path and the number of gradient paths to be used to approximate each of the interatomic surfaces of the atom, respectively. These path lengths and points per path length are incorporated such that the whole surface is partitioned into non overlapping triangles, details of this algorithm may be obtained in Ref. 56. These values produced better integration as compared with values of 80 and 140.

PROAIM INPUT-

```
CH3f_C1.e0        equi.
    C         1
 4  0    0
6.81238610E-10  -1.08690806E-09  -3.65360912E-01          C 1  F 2
1.63653437E-09   1.20236485E+00  -1.58710365E+00          C 1  H 3
-1.04127851E+00 -6.01182427E-01  -1.58710364E+00          C 1  H 4
1.04127851E+00 -6.01182427E-01  -1.58710364E+00          C 1  H 5

120  96
0.81537
141 360
120
0.001 0.002
```

6: RESULTS AND DISCUSSION-

The following is a discussion of the calculations performed, i.e., G90 and AIM, the results obtained for the individual calculations, and finally a comparison of the polarizabilities and polarizability derivatives from both methods. A comparison will also be made with the experimental data wherever available, either from the literature or work done in our lab.

6.1: AB INITIO COMPUTATION-

In the ongoing we consider the choice of basis set and the results obtained, namely geometric parameters, spectroscopic data (frequencies, intensities, depolarization ratios and normal mode analysis), polarizabilities and polarizability derivatives.

6.1.1: CHOICE OF BASIS SET-

The G90 calculations were performed at the HF level with the D95** basis set. This basis set was found to produce good results as compared with experiment in previous calculations performed[13,23,24] for the methane, ethane, propane and cyclohexane molecules.

The D95** basis is the Dunning[28] contraction (4s2p/2s) of the Huzinaga[29] basis (9s5p/4s), with a single polarization function on each atom, i.e., a p function (exp=1.0) on the hydrogen and a d function (exp=0.75) on the carbon atom. This incorporation of functions of higher quantum number than are required by the atom is called a polarization basis set. These functions provide for displacement of electronic charge away from the nuclear centers, i.e., charge polarization. The reliability of this basis set has been considered in Ref.23, and as this work is a continuation of the previous work it was essential to use the same basis set.

This basis set was not suitable for the methyl bromide, and as has been earlier mentioned (Sec. 3), three different basis sets were considered i.e., STO-3G*, LANL1MB,

LANL1DZ. In the continuing discussion the choice of basis i.e., LANL1DZ, will be explained. This basis was then used for further computation i.e., AIM analysis. It is however inconvenient to compare results obtained by different basis sets quantitatively. Hence, polarizabilities were computed for methyl fluoride and methyl chloride using the LANL1DZ basis, but the error was significantly greater than that with the D95**, and those results were not considered. Further, it is the trend exhibited in the three molecules which will be of more significance and a qualitative analysis will be made.

6.1.2: GEOMETRICAL PARAMETERS-

Table 6.1 depicts the theoretically obtained bond lengths, which are compared with experimentally determined values. The C-F bond length was slightly shorter (0.15 Å) than experimental, and the C-Cl bond length was slightly longer (0.09 Å). For both molecules the C-H bond lengths were shorter than experimental data. Calculations using different basis set at the HF level and with MP2 have previously[47] been performed, and it was seen that incorporating perturbation gives theoretical values closer to that of experimental values. The main purpose of performing the calculations at the HF level is because previous calculations[23] have shown that the polarizability derivatives are over estimated by 6%, but this error cancels out with the static calculation which under estimates the derivatives by 6%.

For the methyl bromide, the geometric parameters obtained with all three bases sets are as depicted in Table 6.2. The STO-3G* basis resulted in the least deviation from experimental values relative to the other two bases, resulting in the bond lengths being shorter. With the LANL1MB and LANL1DZ the C-Br bonds were slightly longer and the C-H bonds slightly shorter. However choice of basis is primarily from the value of theoretical polarizability as compared with experimental polarizability, and will be considered shortly.

TABLE 6.1

Comparison of experimental parameters with D95** basis set

Molecule	Geometrical Parameters	HF/D95** Basis Set (Å)	Experimental [47] (Å)
CH_4	r(CH)	1.085	1.092
CH_3F	r(CF)	1.367	1.383
	r(CH)	1.084	1.095
CH_3Cl	r(CCl)	1.790	1.781
	r(CH)	1.079	1.086

TABLE 6.2

Geometrical parameters and vibrational frequencies obtained with different basis sets, for CH_3Br

Bond Lengths	**HF/STO-3G***	**HF/LANLIMB**	**HF/LANLIDZ**	**Experiment**
C-H (Å)	1.085	1.084	1.074	1.086[a]
C-Br(Å)	1.906	2.035	2.013	1.933[a]
Polarizability	Units ($10^{-40}Cm^2/V$)			
	2.46	2.00	3.38	6.30[b]
Frequencies	Units (cm^{-1})			Ref. 37
$\nu_1(A_1)$	3557.3	3592.3	3164.2	2972.0
$\nu_2(A_1)$	1655.5	1563.4	1520.5	1305.1
$\nu_3(A_1)$	860.8	673.0	574.3	611.0
$\nu_4(E)$	3748.3	3810.5	3275.4	3055.9
$\nu_5(E)$	1787.3	1733.2	1639.7	1445.3
$\nu_6(E)$	1155.3	1106.7	1084.6	952.0

[a] Ref. 47

[b] Ref. 63

For the methyl halides it is observed that the C-H bond length is greatest in methyl fluoride and identical for the methyl chloride and bromide. The carbon halogen bond length increases as the atomic size of the halogen atom increases.

6.1.3: SPECTROSCOPIC DATA-

Previous[47] computations of the frequencies of the methyl fluoride and chloride have been obtained with different basis sets namely the HF/3-21G, HF/6-31G* and the MP2/6-31G. The computed frequencies were approximately 10-15%[47] higher than the observed anharmonic frequencies. Further the frequencies calculated at the MP2/6-31G, were seen to be closer in value with the experimental frequencies, as compared to calculations performed at the HF level. The discrepancies in the calculations were stated to be mainly due to the basis set effects, lack of electron correlation corrections, and the neglect of anharmonicity corrections in the calculated frequencies. Details of these results and the foregoing discussion are found in Ref. 47. Detailed discussion of the results obtained by calculations done in the lab are as follows:

The frequencies calculated theoretically are higher than the literature experimental values, and the frequencies determined in our work i.e., by FTIR and Raman, by 10-15%. (Tables 6.3-{a, b}) The main reason for this is that the frequencies computed are harmonic frequencies compared with the anharmonic frequencies measured. In FTIR all frequencies were observed and the values were very similar to the literature values[37]. In the Raman scattering only the symmetric modes were observed, and these values were nearly similar to the literature value but with a greater deviation than those obtained by FTIR. This deviation in frequency will be considered later in the discussion (Sec. 6.3). The degenerate modes were not observed for any of the molecules, in Raman scattering.

TABLE 6.3
Theoretical and experimental vibrational frequencies
units(cm^{-1})

a}

Molecule	Symmetry of vibration	Mode	FTIR	RAMAN	HF/D95**	Liter.[37]
CH_3F	A_1	ν_1	2963.5	2966.8	3219.9	2964.5
		ν_2	1474.3	1461.8	1623.6	1475.3
		ν_3	1046.1	1047.2	1176.7	1048.2
	E	ν_4	2986	-	3313.8	2982.2
		ν_5	?	-	1619.8	1471.1
		ν_6	1183.1	-	1300	1195.5

b}

Molecule	Symmetry of vibration	Mode	FTIR	RAMAN	HF/D95**	Liter.[37]
CH_3Cl	A_1	ν_1	2965.5	2968.6	3251.59	2966.2
		ν_2	1354.8	-	1514.4	1354.9
		ν_3	731.9	732.6	787	732.1
	E	ν_4	3046.5	-	3314.9	3041
		ν_5	1423.7	-	1604.9	1454
		ν_6	1019.2	-	1116.1	1015

TABLE 6.3

Theoretical and experimental vibrational frequencies units(cm^{-1})

c}

Molecule	Symmetry of vibration	M ode	FTIR	RAMAN	LANL1DZ	Liter.[37]
CH_3Br	A_1	ν_1	2973.2	2972.6	3164.2	2972
		ν_2	1306.1	1306.5	1520.5	1305.1
		ν_3	609.4	610.1	575.3	611.0
	E	ν_4	3060	-	3275.4	3055.9
		ν_5	1414.1	-	1639.7	1445.3
		ν_6	956.5	-	1084.6	952.0

For methyl bromide, no theoretical calculation was found in the literature. Comparison of the frequencies was made with the three different basis sets (Table 2). The LANLIDZ basis resulted in the least error, compared with literature experimental values[37], and the STO-3G* showed the largest deviation. In Table 6.3c, a comparison of frequencies, obtained by FTIR and Raman experiment in our lab, and the LANL1DZ basis, is made with literature experimental values.

As stated above, for the Raman scattering, the frequencies of only the symmetric modes were observed. Thus for all three molecules the symmetric C-H and C-X stretch, designated as ν_1 and ν_3, respectively were easily identified.

Considering the symmetric C-H stretch, these peaks are strongly polarized and the spectra show a distinct Q branch with weak rotational levels (Figs.-6.1, 6.2, 6.3) for methyl bromide, chloride and fluoride respectively. The peak observed at lower intensity at approximately 2800 cm^{-1} is the first overtone corresponding to the ν_2 mode. The intensity of the first overtone is maximum for the methyl fluoride.

The symmetric carbon halogen stretch also shows a distinct Q branch with weak rotational structure. Further there is observed to be an isotopic shift of 6 cm^{-1} for the CH_3Cl (Fig. 6.5) and 8 cm^{-1} for the CH_3Br (Fig. 6.4). These values are in agreement with the literature values. There is an increase in wave number shift from Br to F, but a large decrease in intensity. This is primarily due to the large size and ease of polarization of the bromine atom, which decreases for Cl and then the F atom (Fig. 6.6). This point will be discussed later in the section.

The symmetric deformation, designated as ν_2, was of very weak intensity, and was seen only for the methyl bromide Fig. 6.7. For the methyl chloride this peak was not observed. For the methyl fluoride the fundamental should have appeared at 1475 cm^{-1}, however a peak was observed at 1461 cm^{-1} (Fig. 6.8). There is too large a deviation with the literature value to claim that it may be designated as ν_2 , and hence the assignement is

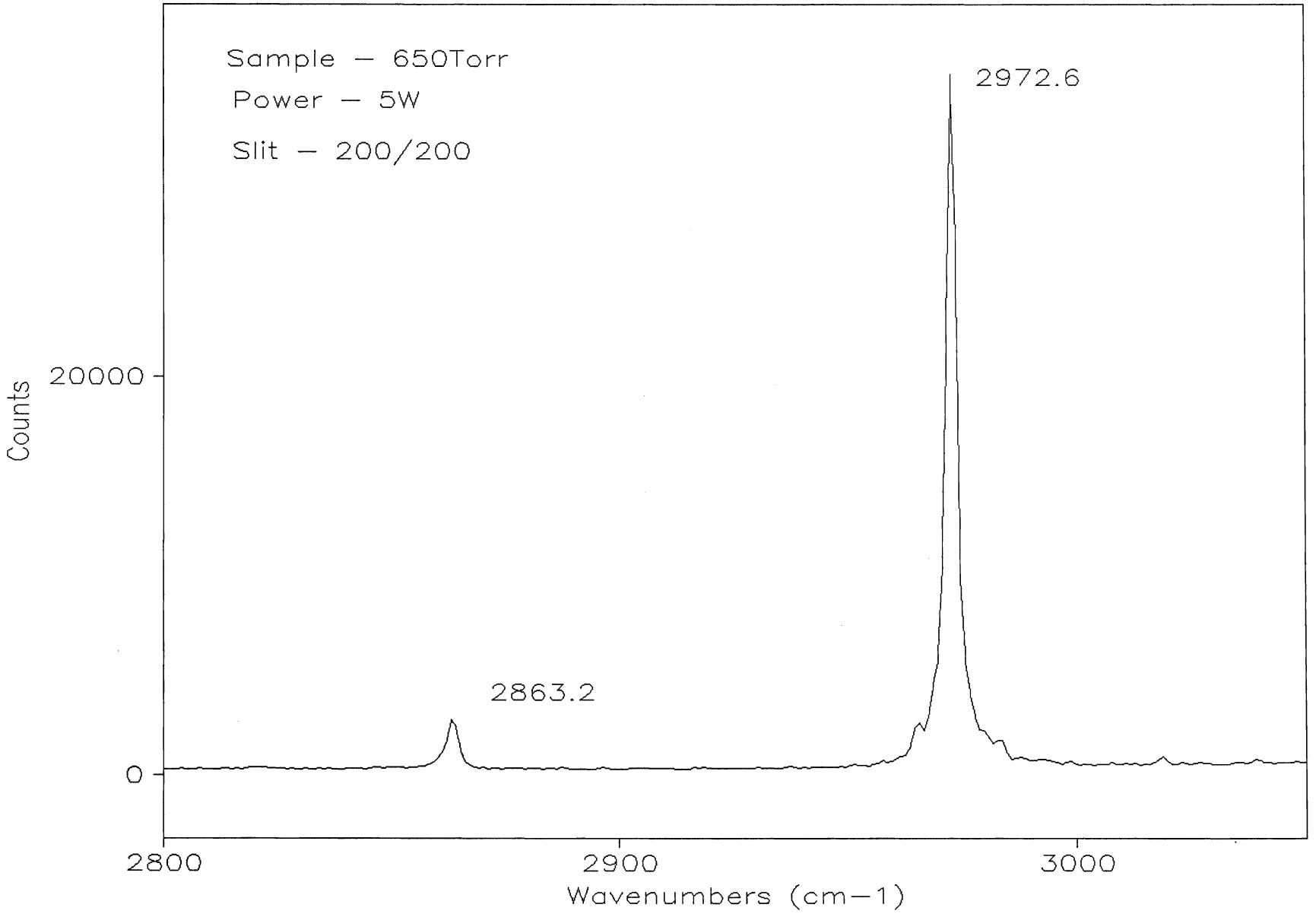

CH3Br(C—H stretch)

Fig. 6.1

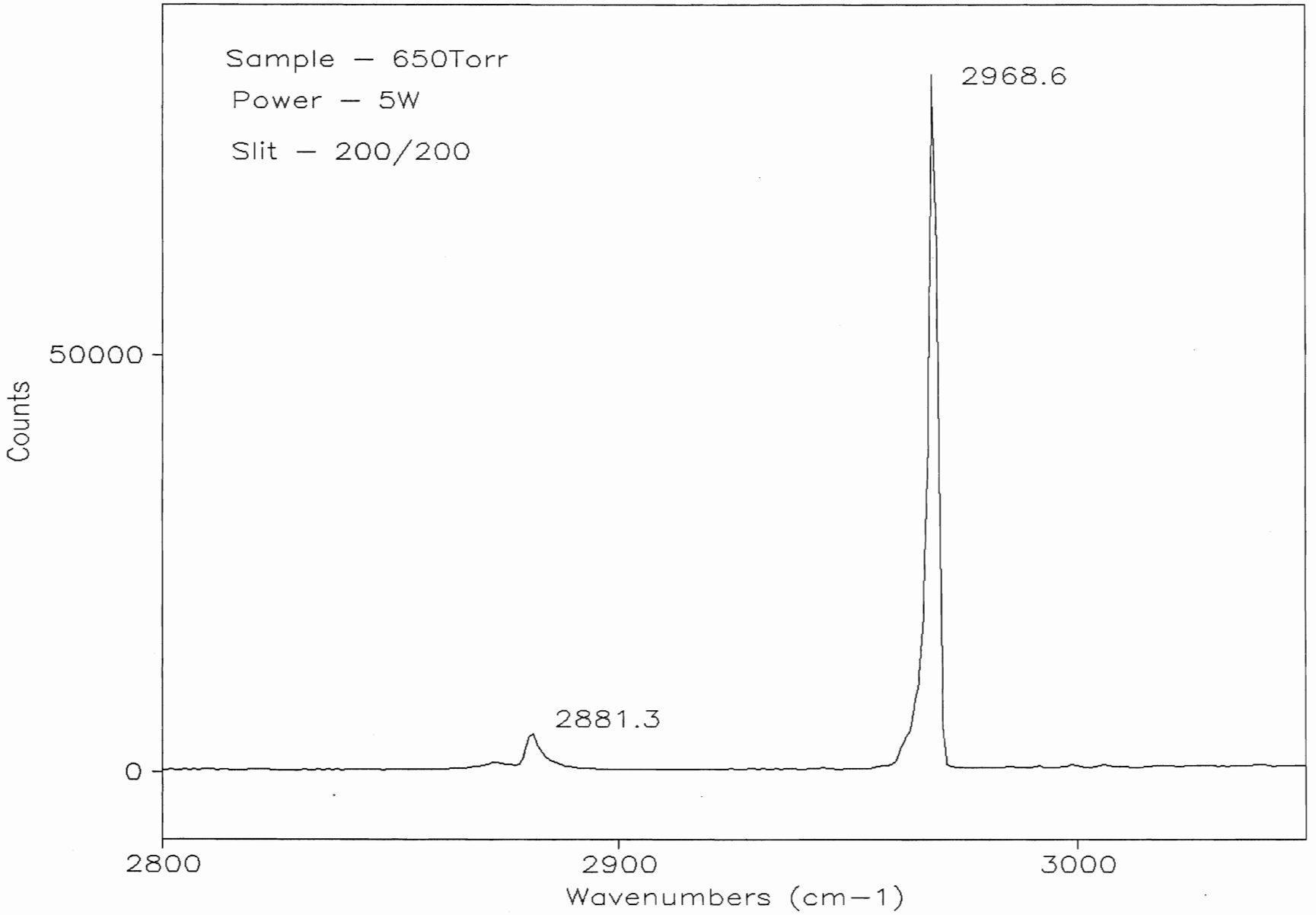

CH3Cl(C—H stretch)

Fig. 6.2

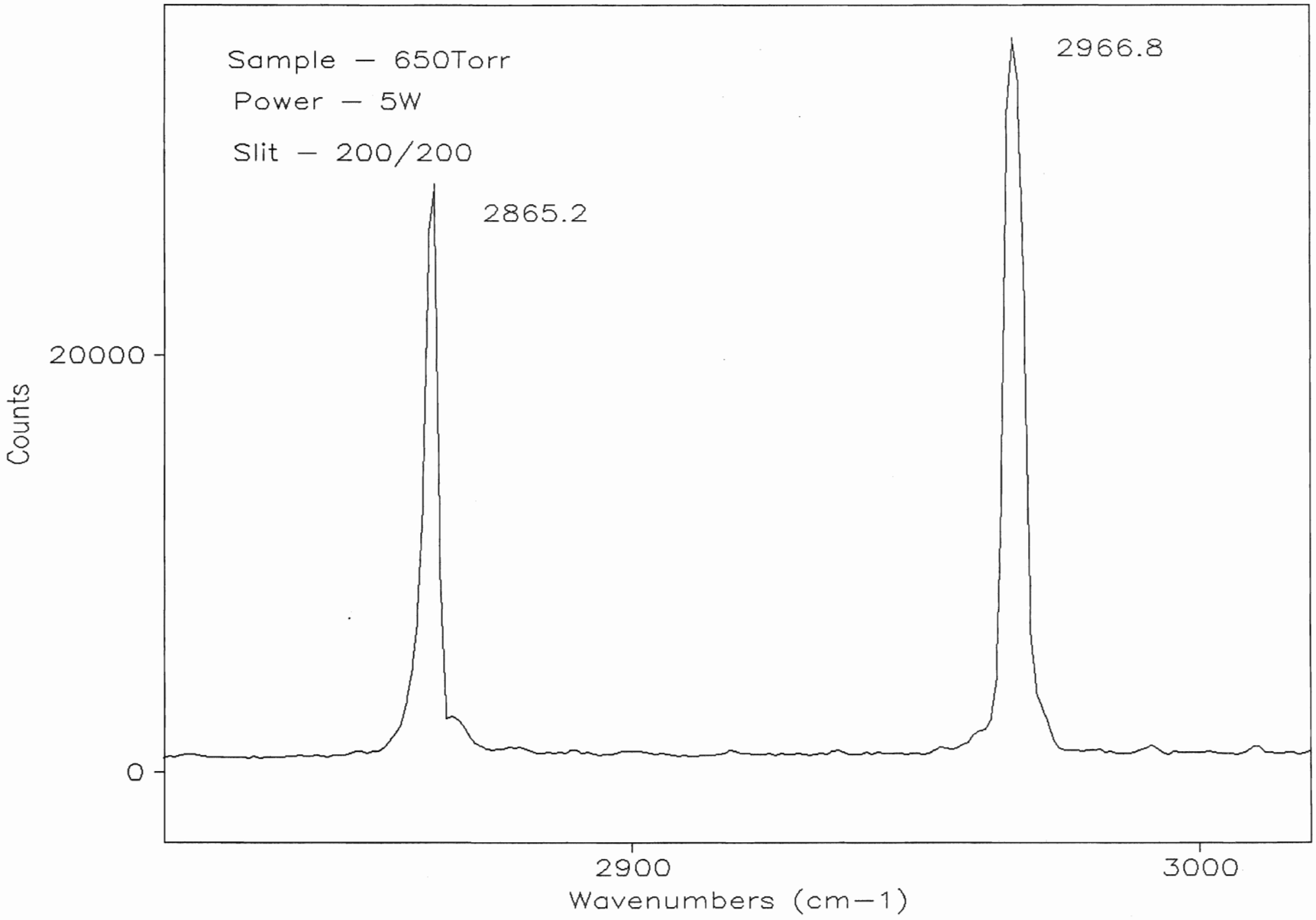

CH3F(C—H stretch)

Fig. 6.3

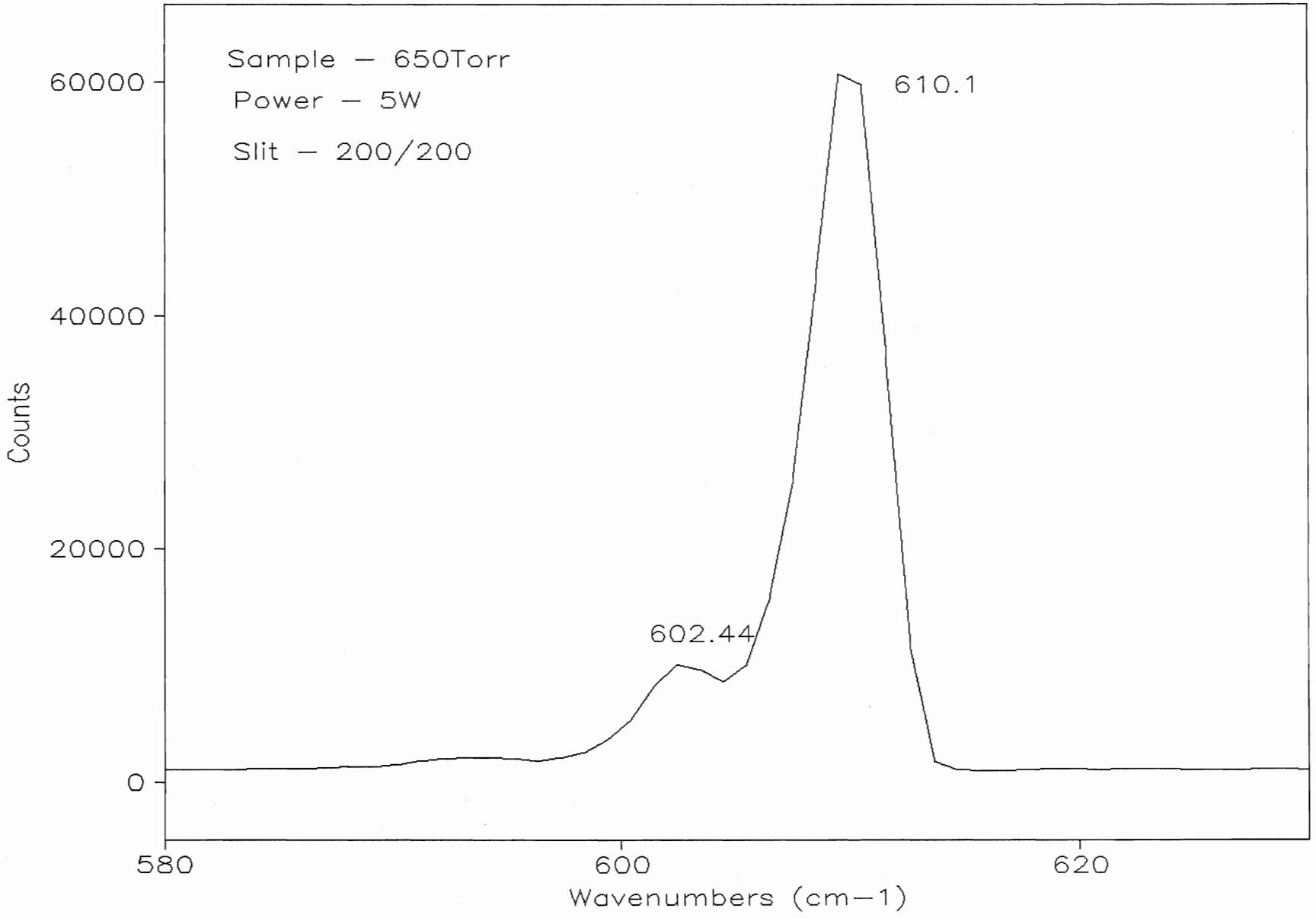

CH3Br(C–Br stretch)

Fig. 6.4

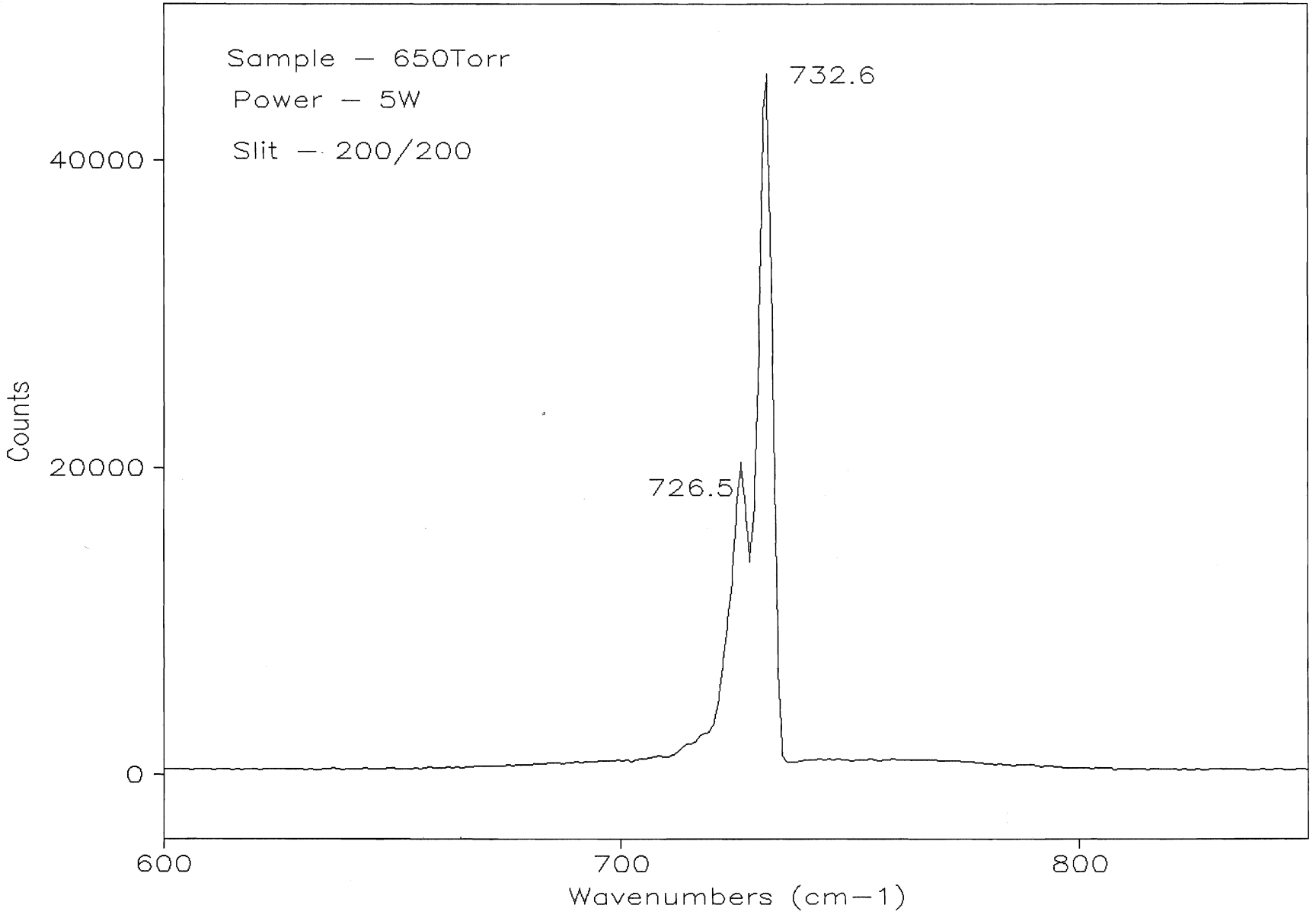

CH3Cl(C—Cl stretch)

Fig. 6.5

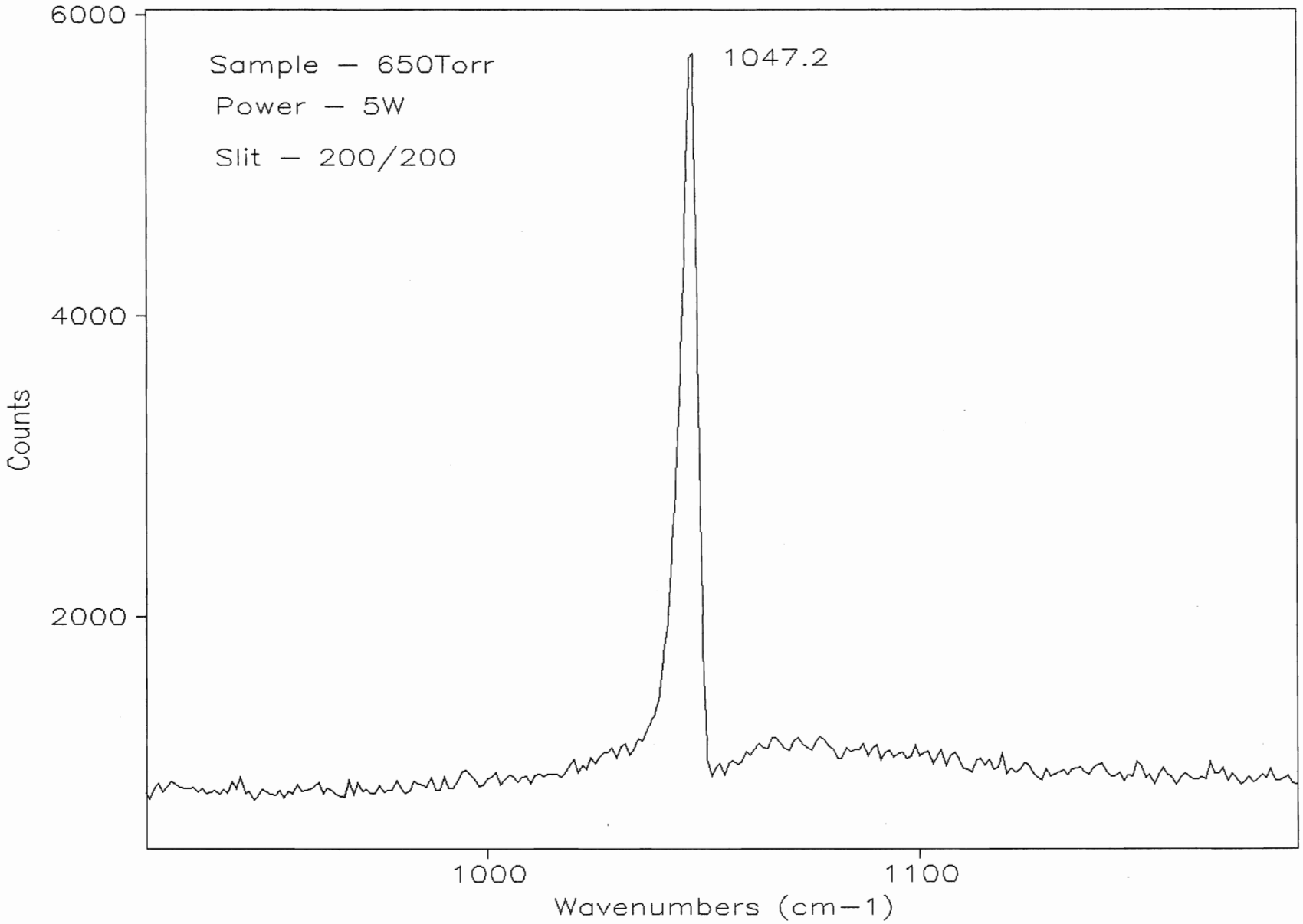

CH3F(C—F stretch)

Fig. 6.6

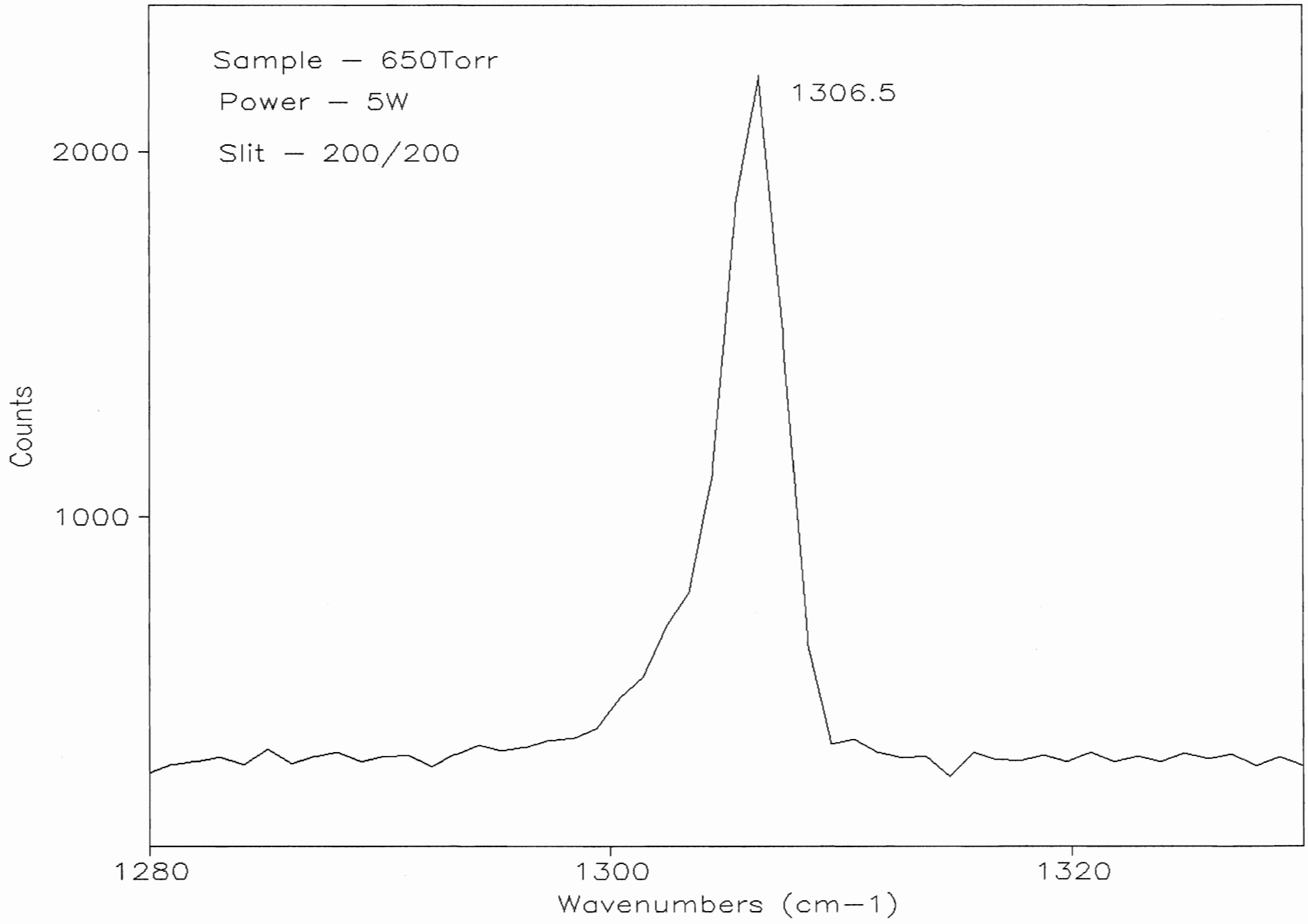

CH3Br(C–H deformation) Fig. 6.7

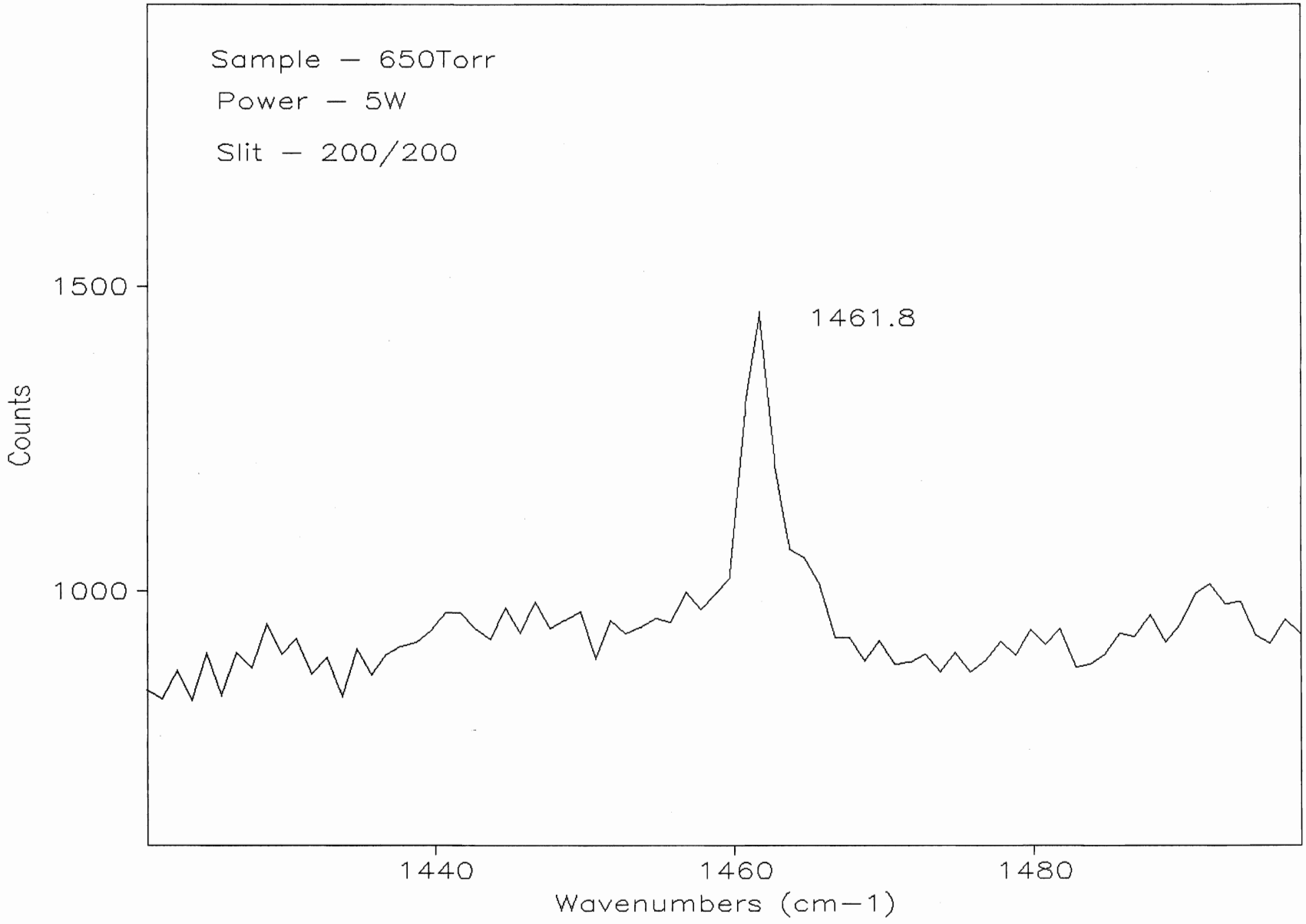

CH3F(C—H deformation) Fig. 6.8

uncertain to specifically what it could be. The FTIR data, for the ν_2, was very similar to the literature value.

As already stated above the degenerate modes were not observed for any of the molecules. A suitable explanation could be the extremely weak intensities for these modes and the literature observations[37] that these modes do not have a distinct Q branch but are broad bands with a significant amount of rotational structure superimposed on them.

However, this is an unsatisfactory explanation, as previously these modes have been observed. The fact should not be ignored, that all literature results were in the "pre-laser era", and it would be thought that spectra recorded with laser as source should provide results similar to those observed if not improved. This is a disappointing observation, and it may be stated that when spectra are re-recorded these degenerate modes might be observed. The errors in the experimental data are provided in Sec. 6.3, and could be the main reason.

Relative Raman and infra-red intensities were obtained from the theoretical calculation, for all modes, and are given in Tables 6.4-{a, b, c}, along with Raman depolarization ratios. Depolarization values obtained give insight as to the type of vibration occurring i.e., symmetric or asymmetric (Sec. 2.5).

For the methyl bromide (Table 6.4c) the LANL1DZ basis does not give Raman intensities and depolarization ratios. The STO-3G* basis does give Raman intensities and depolarization ratios. It would be considered highly inappropriate, to take results of two different basis sets and to try and discuss them would become even more difficult. Hence, it may be stated that there exist no acceptable theoretical intensities and depolarization ratios for the methyl bromide.

Comparing our experimentally obtained symmetric frequencies with those theoretically computed we make the following observations, only for the methyl chloride and fluoride.

The C-H stretch intensities are the most intense and were easily observed. The symmetric deformation has very low intensity for methyl fluoride. This mode was not

seen for the methyl chloride. There is however an uncertainty if this mode was observed for the methyl fluoride or not. The symmetric carbon-halogen stretch intensity is lower for the methyl fluoride than the methyl chloride. Further, from the computation the C-X stretch does not have intensity of great significance, but was easily observed for all molecules.

The depolarization ratio for the ν_1 and ν_3 symmetric modes indicate strongly polarized bands, which were easily observed in the respective experimental spectra. The symmetric deformation, ν_2 was computed to be less polarized than the other two symmetric modes.

For the degenerate modes the intensities fall off as the frequency of the mode decreases. From the depolarization ratios it is seen that these bands are completely depolarized, which could be included as one of the reasons for difficulty in experimental observation.

TABLE 6.4

Theoretical intensities and depolarization ratios

a}

Molecule	Symmetry of vibration	Mode	HF/D95** (cm^{-1})	Intensities Raman (A^4/amu)	Intensities Infrared (km/mole)	Depolariz - ation Ratio
CH_3F	A_1	ν_1	3219.9	130.14	43.3	0.04
		ν_2	1623.6	3.3	8.0	0.67
		ν_3	1176.7	6.4	149.4	0.44
	E	ν_4	3313.8	47.2	60.8	0.75
		ν_5	1619.8	13.1	2.6	0.75
		ν_6	1300	5.9	2.6	0.75

b}

Molecule	Symmetry of vibration	Mode	HF/D95** (cm^{-1})	Intensities Raman (A^4/amu)	Intensities Infrared (km/mole)	Depolariz - ation Ratio
CH_3Cl	A_1	ν_1	3251.59	128	40	0.013
		ν_2	1514.4	0.46	2 8.9	0.72
		ν_3	787	26.06	47.7	0.3
	E	ν_4	3314.9	54.5	18.8	0.75
		ν_5	1604.9	12.4	5.2	0.75
		ν_6	1116.1	6.39	1.91	0.75

TABLE 6.4

Theoretical intensities and depolarization ratios

c}

Molecule	Symmetry of vibration	Mode	LANL1DZ (cm^{-1})	Intensities Raman (A^4/amu)	Intensities Infrared (km/mole)	Depolarization Ratio
CH_3Br	A_1	ν_1	2973.2	-	37.03	-
		ν_2	1306.1	-	41.4	-
		ν_3	609.4	-	25.5	-
	E	ν_4	3060	-	11.2	-
		ν_5	1414.1	-	7.2	-
		ν_6	956.5	-	14.66	-

The normal mode analysis provides an insight to the part played by the other atoms during a specific vibration. From a study of the normal modes, obtained with respect to the Cartesian coordinates, the following observation was made.

From the Gaussian 90 normal mode analysis obtained for displacements of all atoms along Cartesian coordinates, in units of Å, the following observations are made for the three symmetric modes.

1} The symmetric C-H stretch is denoted as ν_1. For all three molecules, this stretch is observed to be in the region 2900-3000 cm^{-1}. From Fig. 6.9, it is observed that this mode is distinctly a carbon hydrogen stretch and there is maximum displacement for these atoms. The halogen displacement is small, and is found to decrease as the halogen atomic number increases i.e., $CH_3F \approx 0.002$ and for CH_3Cl and CH_3Br the atoms do not move at all. The carbon displacement is nearly consistent across the molecules, with a value of approximately 0.04. The hydrogens show the greatest displacement which is 0.44 for CH_3F and 0.58 for CH_3Cl and CH_3Br.

2} For the symmetric deformation (Fig. 6.10) denoted as ν_2 , the trend observed for the three molecules is as follows. This is primarily a methyl deformation with minimal halogen displacements. The displacements of all atoms for all three molecules are nearly identical.

3} Considering the symmetric carbon halogen stretch (Fig. 6.11) which is denoted as ν_3, the range for the halogen stretch frequency is greater than that for the symmetric C-H stretch and deformation. The wave number decreases as the halogen atomic number increases. On inspecting calculated G90 individual atomic displacements, it is seen that the hydrogen displacement is significant for all molecules. This displacement remains nearly constant with a value of 0.44. The carbon displacement is maximum with a slight increase in value as the halogen size increases and is along negative z direction. The halogen displacement falls off significantly as the halogen size increases.

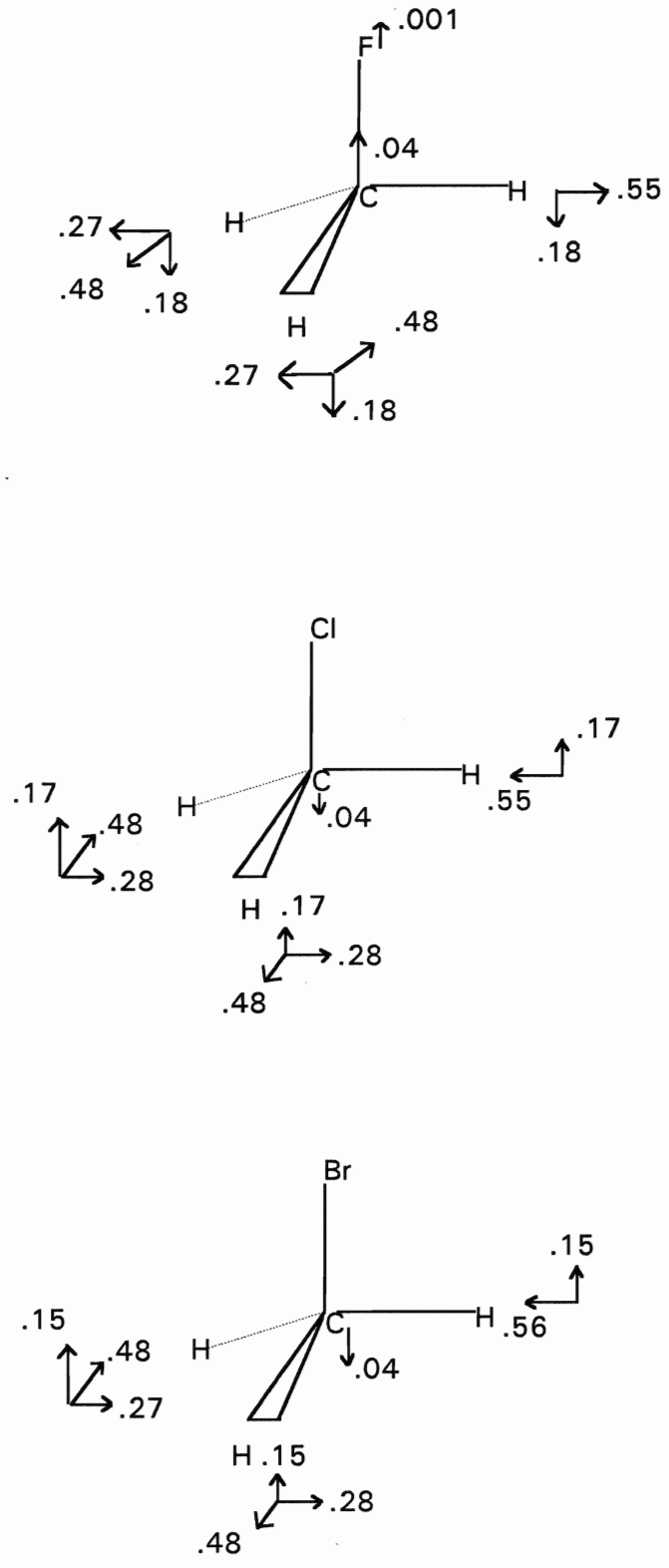

Fig. 6.9- Normal mode displacements along Cartesian coordinates for the symmetric C-H stretch (units Å)

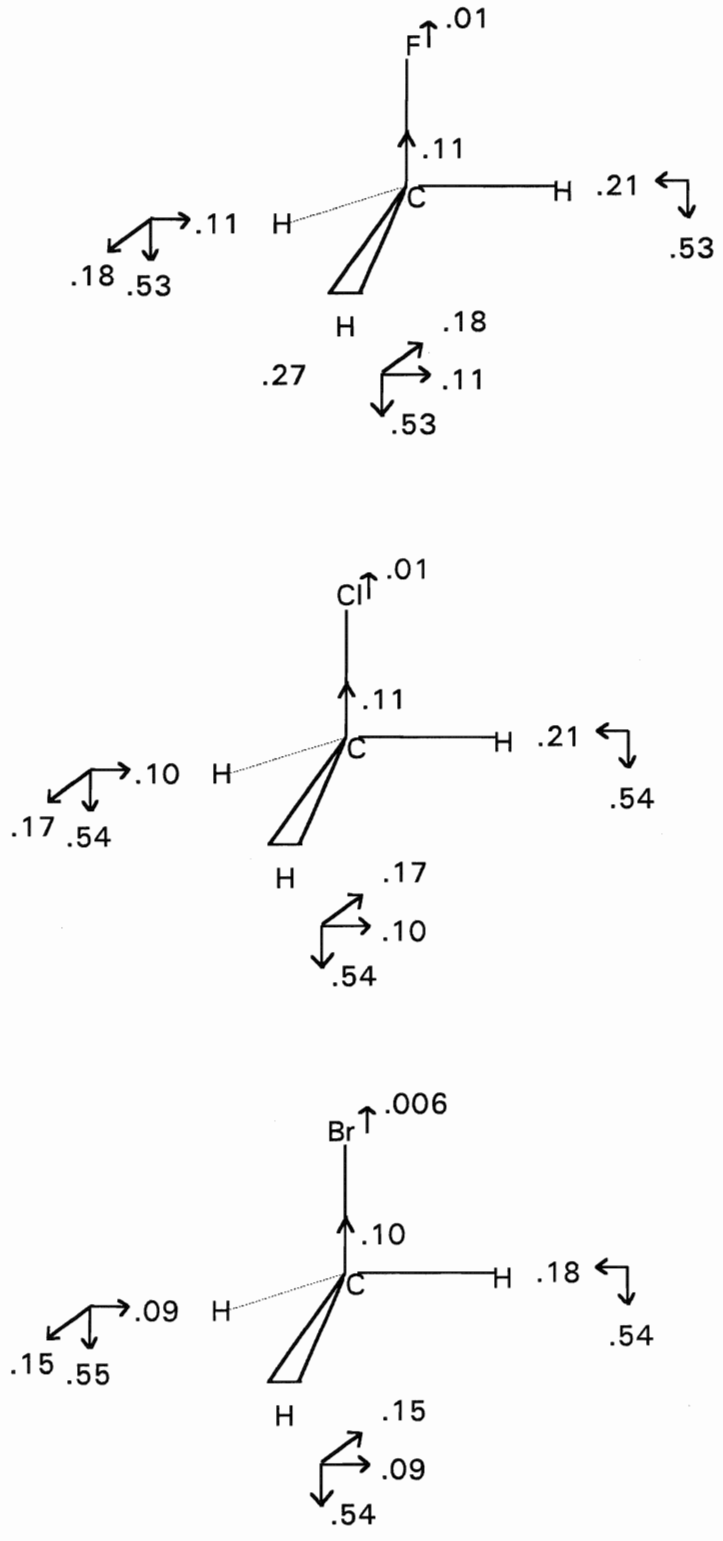

Fig, 6.10 -Normal mode displacements along Cartesian coordinates for the symmetric C-H deformation (units Å)

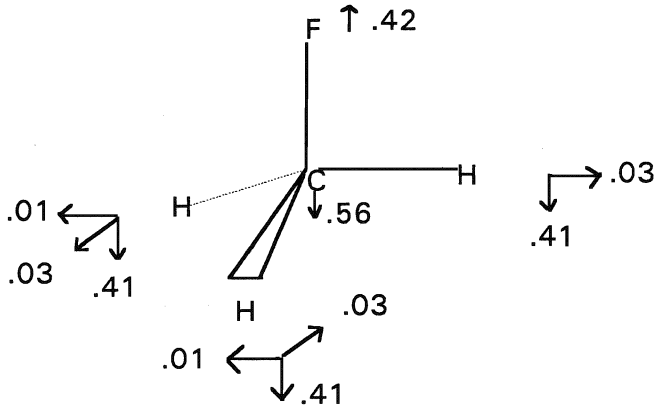

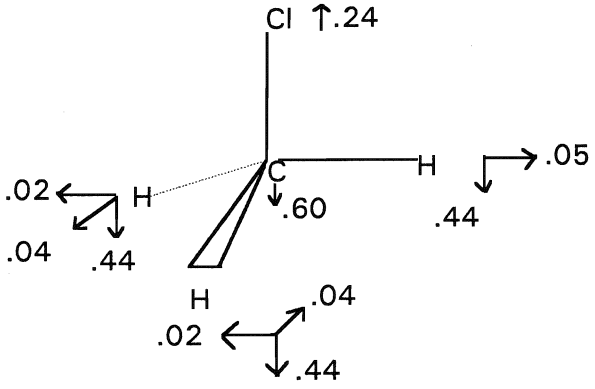

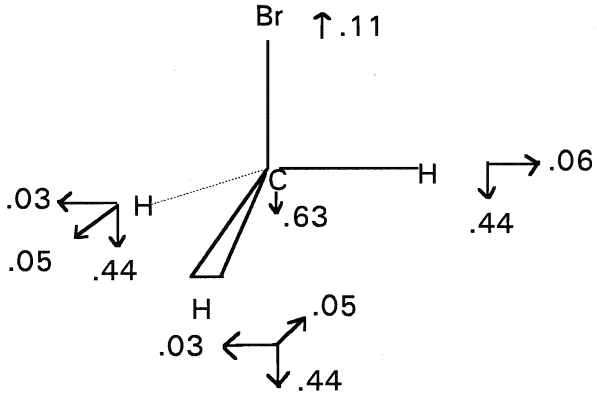

Fig. 6.11- Normal mode displacements along Cartesian coordinates for the symmetric C-X stretch (units Å)

From the preceding normal modes description, an attempt is made to relate this with the experimentally observed spectra. The following discussion is primarily qualitative. The C-H frequency and intensity falls as the halogen atomic number decreases. This can be explained in the following way: From Fig. 6.9 this symmetric stretch is primarily a displacement of the carbon and hydrogen atoms. Further the low intensity for methyl fluoride can be related to the weak polarization ability of the fluorine atom. The methyl chloride and bromide have equal displacement for the hydrogens, but the intensity of methyl chloride is greater than that for the methyl bromide.

Considering the carbon-halogen stretch, the frequency increases as the halogen atomic number decreases. From Fig. 6.11 it is observed that the fluorine and chlorine displacement is much greater than that for the bromine atom, and the hydrogen displacement is nearly identical in all three molecules. This variation in the frequencies is primarily due to the type of halogen atom. The frequencies are seen to decrease as the halogen atomic number increases. This is primarily due to the small size and high electronegativity of the fluorine atom. However, the intensity is seen to be significantly greater for the bromine relative to the chlorine and the fluorine is the least. These observations are again, primarily due to the size of atoms.

The above observations will be kept in mind and returned to when we consider the experimentally measured absolute intensities.

6.1.4: POLARIZABILITIES-

The calculated molecular polarizabilities are observed to be significantly lower than the experimental values (Table 6.5). There is an increase in error as the atomic number of the halogen increases i.e., F, Cl, Br. Previous[22] calculations of the polarizabilities for methyl fluoride and methyl chloride gave values with 25% error.(Table 6.5). These

TABLE 6.5

Comparison of Experimental and Calculated Polarizabilities (units $10^{-40}Cm^2/V$)

Molecule	Experimental[63]	Calculated	Calculated[22]
CH_4	2.85	2.04[23]	1.95
CH_3F	2.93	1.98	2.02
CH_3Cl	5.10	3.23	3.31
CH_3Br	6.30	3.38[a]	-

[a] LANLIDZ basis set

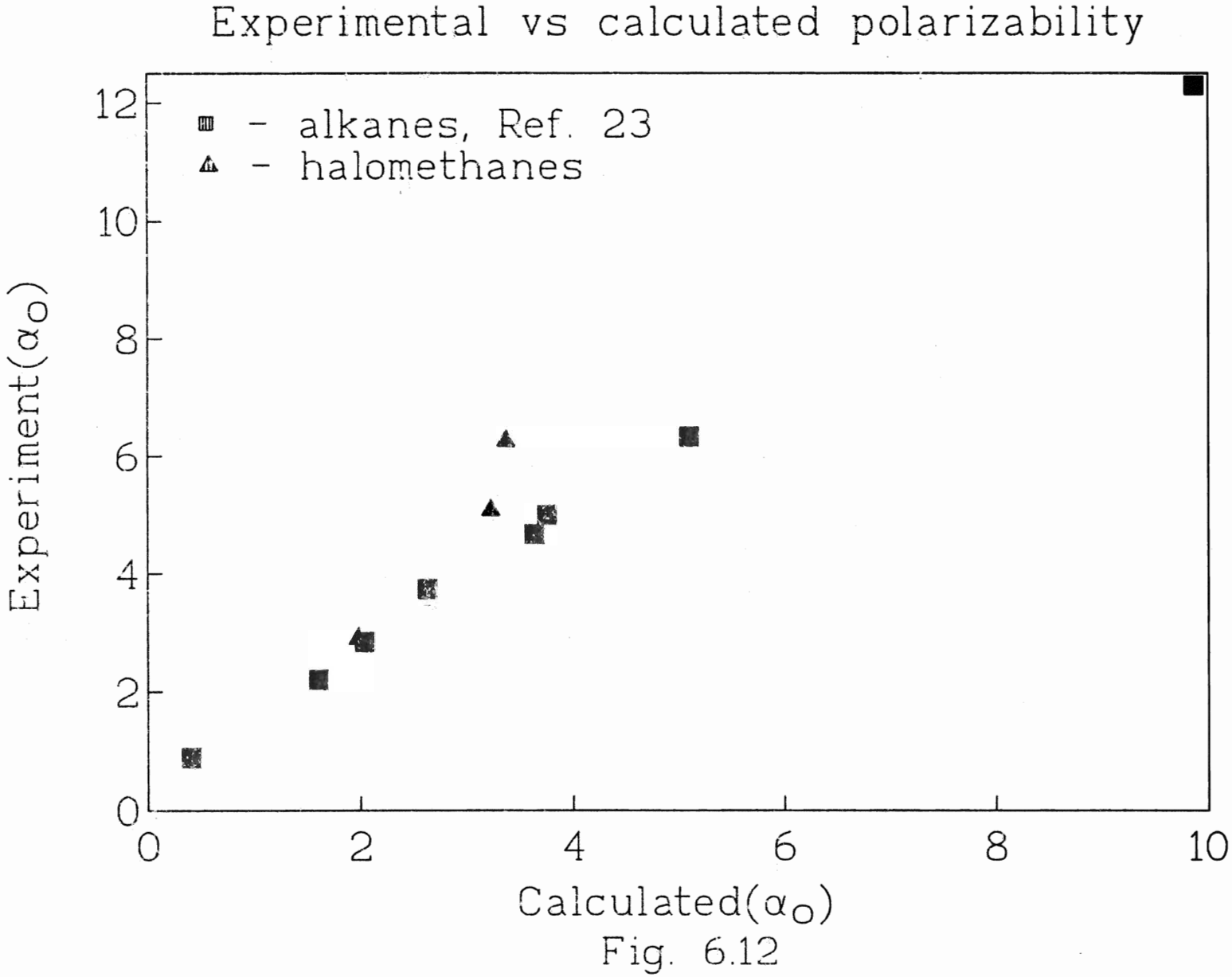
Experimental vs calculated polarizability
- alkanes, Ref. 23
- halomethanes
Experiment(α_o)
Calculated(α_o)
0
2
4
6
8
10
12

Fig. 6.12

calculations were performed at the HF level with the Dunning basis (spd) incorporating polarization functions.

For methyl bromide, the LANL1DZ basis resulted in the largest value of the polarizability (Table 6.2) i.e., least error compared to experiment relative to the other two basis sets, and it was the LANL1DZ which was used for further computations, namely polarizability derivatives and AIM analysis. A large error still exists, but of more importance is to obtain a qualitative description with the AIM analysis. This will be considered in detail later in the discussion.

However, at this point it is important to point out that the primary reason for performing an AIM computation is not to obtain different polarizabilities. We obtain polarizabilities satisfactorily from an *ab initio* MO computation. With the AIM analysis we gain insight to the main factors contributing to the molecular polarizability and the polarizability derivatives i.e., charge transfer and atomic dipole. This analysis will be considered in Sec. 6.2.2.

The main factors influencing a polarizability calculation include flexibility of basis set and extent of electron correlation.

The large error in the calculated polarizabilites is undesirable, however, as already stated, it is the trend which is of more significance (Fig. 6.12). The plot of experimental versus theoretical polarizabilities, for the hydrocarbons and the methyl halides depicts a linear relationship. The polarizabilities for the hydrocarbons were obtained from Ref. 23.

The trace values of the molecular polarizabilities are now considered, which are as given in Tables 6.6-{a, b, c}. The values are given for the equilibrium geometry and for the geometry when a particular bond was changed. We have ±0.005 Å for the C-H and ± 0.01 Å for the C-X (X= F, Cl, Br) bond. Due to the molecular orientation (Fig. 4.1), we get, $\alpha_{xx} = \alpha_{yy} < \alpha_{zz}$ for methyl chloride and methyl bromide (Tables 6.6-{b.c}), and $\alpha_{xx} = \alpha_{yy} > \alpha_{zz}$ for methyl fluoride (Table 6.6a).

TABLE 6.6

Diagonal elements of the molecular polarizability tensor via *ab initio* G90 and AIM analysis of the MO wave function.all values in units of $10^{-40}Cm^2/V$

CH_3F

a}

	α_{AIM}			α_{G90}		
Geometry	**xx**	**yy**	**zz**	**xx**	**yy**	**zz**
Equilibrium	1.986	1.986	1.954	1.986	1.986	1.965
C-H{+.005}	2.005	2.017	1.961	2.005	2.005	1.965
C-H{-.005}	1.966	1.978	1.949	1.966	1.966	1.957
C-F{+.01}	1.983	1.995	1.978	1.983	1.983	1.989
C-F{-.01}	1.987	1.998	1.929	1.988	1.988	1.940

CH_3Cl

b}

	α_{AIM}			α_{G90}		
Geometry	**xx**	**yy**	**zz**	**xx**	**yy**	**zz**
Equilibrium	2.583	2.576	4.402	2.624	2.624	4.456
C-H{+.005}	2.632	2.665	4.371	2.643	2.643	4.469
C-H{-.005}	2.569	2.549	4.400	2.606	2.606	4.443
C-Cl{+.01}	2.584	2.616	4.454	2.625	2.625	4.509
C-Cl{-.01}	2.586	2.591	4.349	2.623	2.623	4.403

TABLE 6.6

Trace elements of the molecular polarizability tensor via *ab initio* G90 and AIM analysis of the MO wave function.all values in units of $10^{-40}Cm^2/V$

CH_3Br

Geometry	α_{AIM} xx	α_{AIM} yy	α_{AIM} zz	α_{G90} xx	α_{G90} yy	α_{G90} zz
Equilibrium	1.899	1.897	6.228	1.906	1.906	6.321
C-H{+.005}	1.922	1.917	6.247	1.927	1.927	6.338
C-H{-.005}	1.884	1.879	6.216	1.889	1.889	6.306
C-Br{+.01}	1.896	1.896	6.308	1.904	1.904	6.403
C-Br{-.01}	1.902	1.898	6.148	1.908	1.908	6.238

c}

This might be expected to be true from a basic knowledge of the atoms' electronegativities. The fluorine atom is much smaller than the chlorine and bromine atoms. It is also more electronegative and has electrons bound much more tightly to it, resulting in polarizability being much less along the C-F bond than along the C-H bonds. The only exceptional case was when the C-F bond length was increased by +0.01 Å, in this case there was increased polarizability along the C-F bond and we get $\alpha_{xx} = \alpha_{yy} < \alpha_{zz}$. A reason for this observation could be that the polarizability is not only dependent on the atoms forming the bond, but also on the length of the bond. This point will be confirmed later in the discussion (Sec. 6.2.1)

For the chlorine and bromine atoms, being much larger, the electrons are more loosely held and hence there is a much greater polarizability value along the C-Cl and C-Br bonds than along the C-H bonds i.e., in the z direction.(Tables 6.6-{b, c}) For the methyl chloride the contribution along the z direction is nearly double that along the other two directions. For the methyl bromide, the contribution along the z direction is nearly triple relative to the other two directions.

The reason for the above observation is explained as follows: The polarizability is defined as the ease of charge re-distribution, which depends partly on the number of valence electrons and how strongly they are bound to the nucleus. The chlorine atom belongs to the third row of the periodic table, has a total of seventeen electrons surrounding the nucleus. The bromine atom belongs to the fourth row of the periodic table and has a total of thirty five electrons, which contribute to the large polarizability along the z direction. This concept will be kept in mind and returned to in the AIM analysis. The AIM results are also given in Table 6.6-{a, b, c} and will be discussed in Sec. 6.2.1.

6.1.5: POLARIZABILITY DERIVATIVE-

The focus of this work was in the determination of the polarizability derivatives, and the comparison of these derivatives with experiment which is significant. The polarizability derivative was numerically determined by taking the difference between the polarizability at the equilibrium geometry and the polarizability determined when a vibration was simulated in the molecule. The vibration was simulated by stretching and then contracting a particular bond in the molecule. There are only two types of bonds in the molecule, the C-H and C-X (X=F, Cl, Br). For the symmetric C-H stretching vibration the three C-H bonds were simultaneously changed, and for the halogen vibration the carbon and respective halogen bond was changed. The choice of bond change is as follows:

Carbon-hydrogen bond-

The C-H bonds were displaced by $\Delta r = \pm 0.2, \pm 0.1, \pm 0.03, \pm 0.02, \pm 0.01$, and ± 0.005 Å. The importance of varying the bond lengths is the noticeable variation in the polarizability with change in bond length. Further, the polarizability of a molecule does not have a linear dependence on bond length; it is observed that the polarizability deviates from linearity as we move away from the equilibrium position. This non linearity is due to the presence of higher order terms attaining significance. There is a distinct curvature observed in the graphs of polarizability versus bond length. This is of importance when considering which value of bond displacement is appropriate for calculations. The important factor is that the polarizabilities obtained at values different from the equilibrium are significant only if there is not too large a deviation i.e., the linearity is noticeable, nor too diminutive so that the change is not significant. The polarizabilities obtained at the different bond lengths are shown in Tables 6.7, 6.8 and 6.9, for the methyl fluoride, methyl chloride and methyl bromide respectively. Graphs were plotted for polarizability versus bond length and from the graphs, it is easily seen that the polarizability values deviate

TABLE 6.7

Variation in polarizability with change in C-H bond length for CH_3F

Bond length r(Å)	Δr(Å)	Polarizability (α) ($10^{-40}Cm^2/V$)	$\lvert\Delta\alpha\rvert$ ($10^{-40}Cm^2/V$)	Δα/Δr ($10^{-30}Cm/V$)
1.2836	0.20	2.7268	0.7482	3.7410
1.1836	0.10	2.3217	0.3431	3.4312
1.1136	0.03	2.0754	0.0968	3.2279
1.1036	0.02	2.0425	0.0639	3.1959
1.0936	0.01	2.0104	0.0318	3.1779
1.0886	0.005	1.9944	0.0158	3.1611
1.0826	0.00	1.9786	-	-
1.0786	-0.005	1.9629	0.0156	3.1235
1.0736	-0.01	1.9475	0.0311	3.1016
1.0636	-0.02	1.9169	0.0617	3.0838
1.0536	-0.03	1.8868	0.0918	3.0595
0.9836	-0.10	1.6916	0.2869	2.8695
0.8836	-0.20	1.4558	0.5228	2.6138

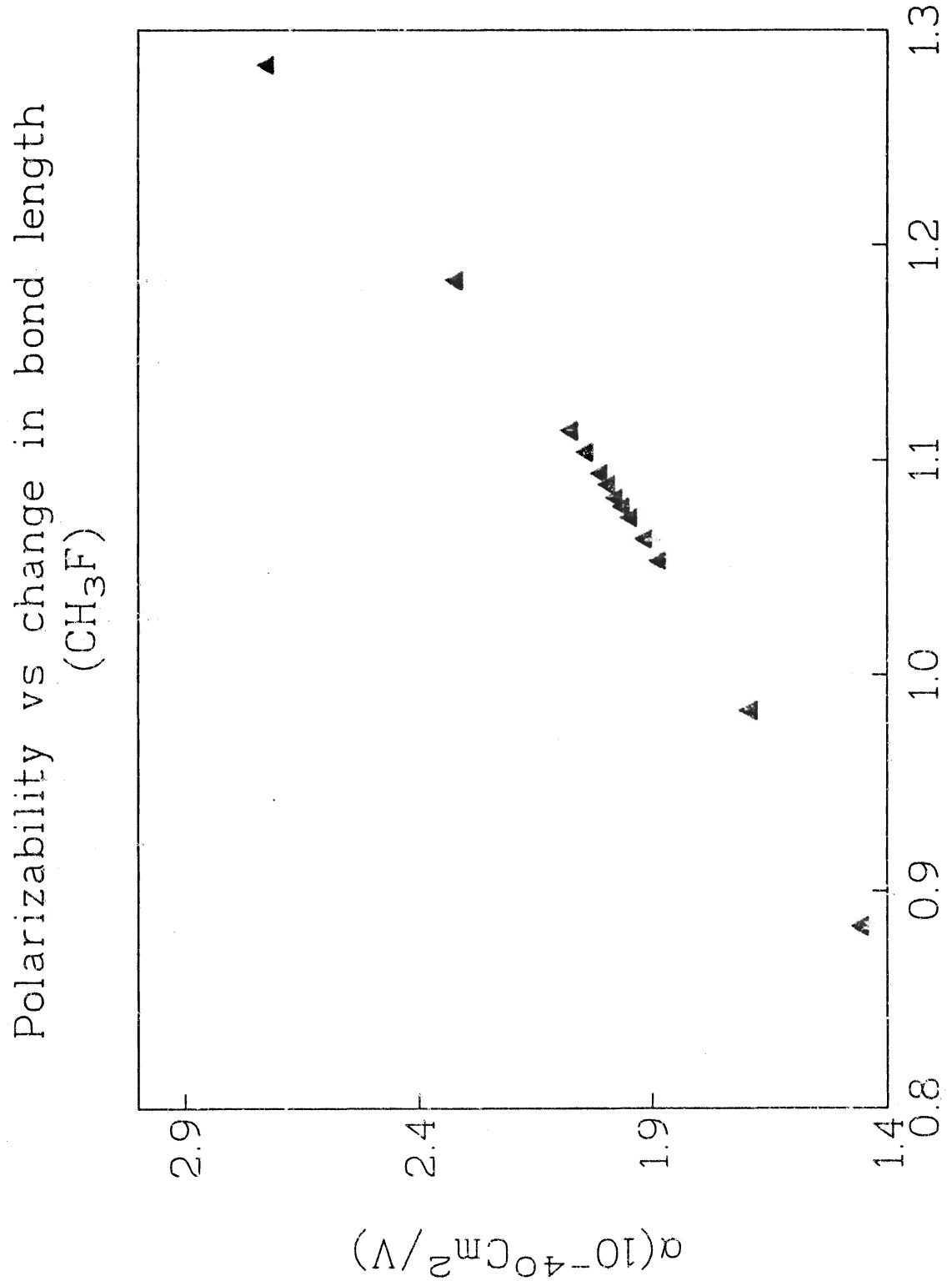
Polarizability vs change in bond length
(CH_3F)
2.9
2.4
1.9
1.4
0.8
0.9
1.0
1.1
1.2
1.3
r(Å)
$\alpha(10^{-40}Cm^2/V)$

Fig. 6.13

TABLE 6.8

Variation in polarizability with change in C-H bond length for CH_3CL

Bond length r(Å)	Δr(Å)	Polarizability (α) ($10^{-40}Cm^2/V$)	$\lvert\Delta\alpha\rvert$ ($10^{-40}Cm^2/V$)	Δα/Δr ($10^{-30}Cm/V$)
1.2789	0.2	4.0217	0.7869	3.9345
1.1789	0.1	3.5956	0.3608	3.6076
1.1089	0.03	3.3368	0.1019	3.3980
1.0989	0.02	3.3021	0.0673	3.3659
1.0889	0.01	3.2681	0.0333	3.3302
1.0839	0.005	3.2513	0.0164	3.2907
1.0789	0.00	3.2348	-	-
1.0739	-0.005	3.2184	0.0164	3.2895
1.0689	-0.01	3.2020	0.0328	3.2834
1.0589	-0.02	3.1698	0.0665	3.2485
1.0489	-0.03	3.1382	0.0966	3.2215
0.9789	-0.1	2.9191	0.3157	3.1572
0.8789	-0.2	2.6833	0.5512	2.7578

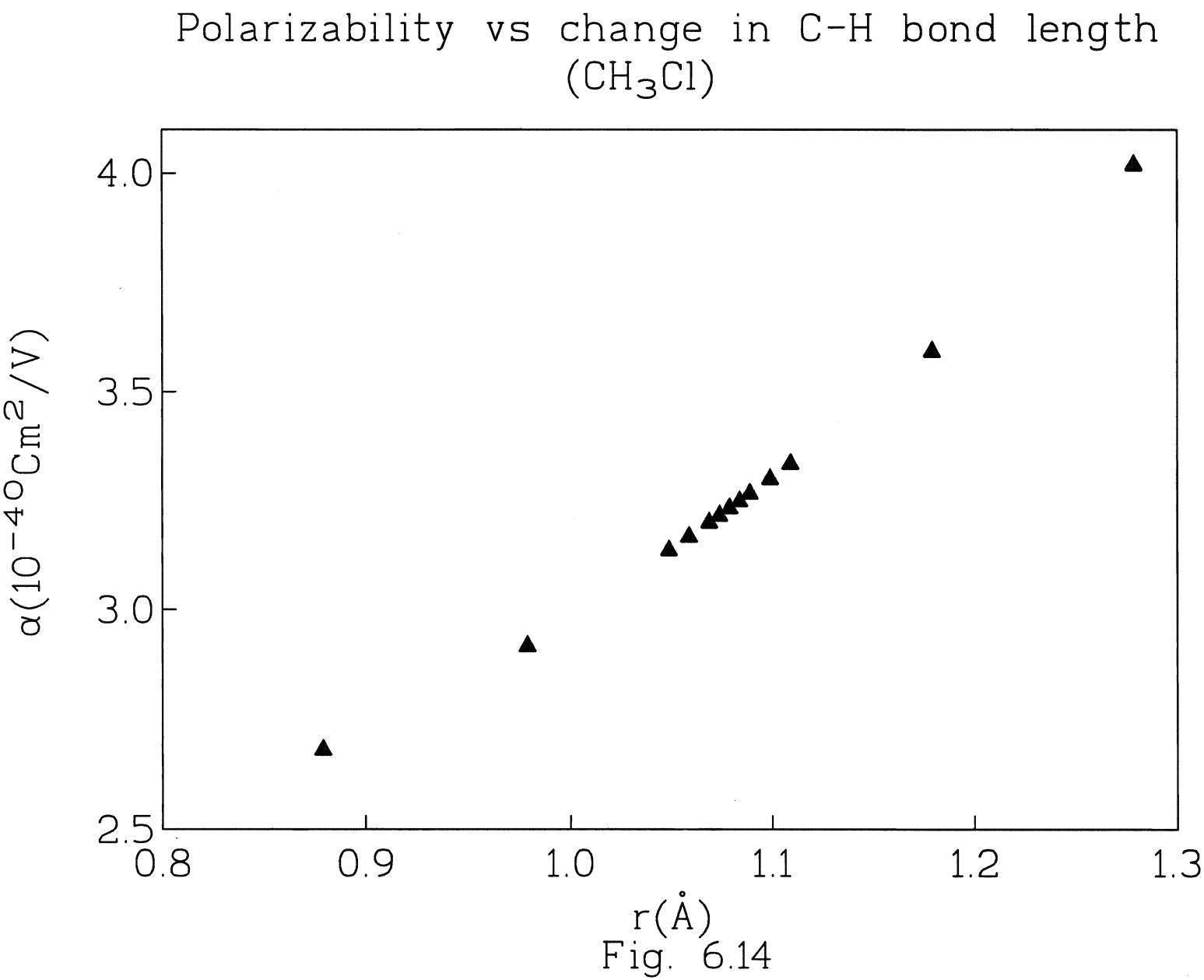
Polarizability vs change in C-H bond length
(CH_3Cl)
$\alpha(10^{-40}Cm^2/V)$
4.0
3.5
3.0
2.5
0.8
0.9
1.0
1.1
1.2
1.3
r(Å)
Fig. 6.14

TABLE 6.9

Variation in polarizability with change in C-H bond length for CH_3Br

Bond length r(Å)	Δr(Å)	Polarizability (α) ($10^{-40}Cm^2/V$)	$\lvert \Delta\alpha \rvert$ ($10^{-40}Cm^2/V$)	Δα/Δr ($10^{-30}Cm/V$)
1.2744	0.2	4.2878	0.9102	4.5512
1.1744	0.1	3.7996	0.4220	4.2201
1.1044	0.03	3.4976	0.1200	4.0000
1.0944	0.02	3.4570	0.0794	3.9695
1.0844	0.01	3.4170	0.0394	3.9386
1.0794	0.005	3.3972	0.0196	3.9241
1.0744	0.00	3.7760	-	-
1.0694	-0.005	3.3616	0.0160	3.2026
1.0644	-0.01	3.3388	0.0388	3.8789
1.0544	-0.02	3.3006	0.0769	3.8489
1.0444	-0.03	3.2630	0.1146	3.8193
0.9744	-0.1	3.0158	0.3618	3.6184
0.8744	-0.2	2.7074	0.6702	3.3512

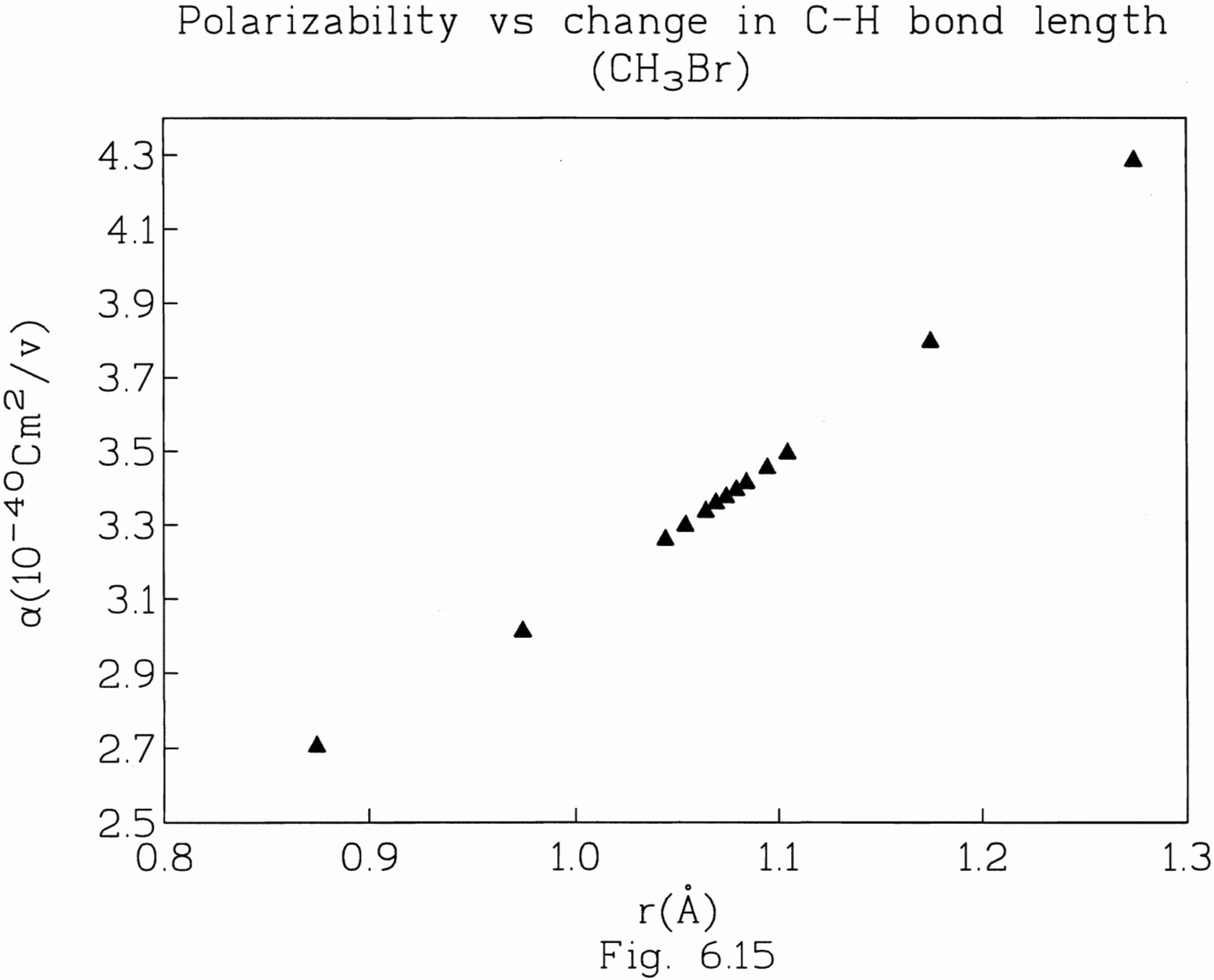
Polarizability vs change in C-H bond length
(CH_3Br)
$\alpha(10^{-40}Cm^2/v)$
4.3
4.1
3.9
3.7
3.5
3.3
3.1
2.9
2.7
2.5
0.8
0.9
1.0
1.1
1.2
1.3
r(Å)
Fig. 6.15

largely from linearity at distances ±0.1 and ±0.2 Å from equilibrium bond length (Figs. 6.13, 6.14, 6.15). Further, for ±0.03, ±0.02, and ±0.01 Å the error was greater than 2% for polarizability and polarizability derivative, hence these values are not used and only variation of the bond length by ±0.005 Å is found to be appropriate, satisfying the requirements outlined above. This value for the C-H bond is identical with the value opted for the hydrocarbons (methane, ethane, propane), as has been shown in Ref. 23.

Carbon- halogen bond-

The C-X (X = F, Cl, Br) bond lengths were displaced by Δr = ±0.2, ±0.1, ±0.03, ± 0.01, ±0.005, ±0.002, and ±0.001 Å, to obtain the most suitable value which might then be employed for further computations. As these bonds had not been studied before, unlike the C-H bonds, it was necessary to calculate the polarizability for small deviations such as ±0.001, and ±0.002 Å. The increase and decrease in bond lengths corresponded to a bond stretch and a bond contraction respectively. The polarizabilities were determined and are as depicted in Tables 6.10, 6.11, and 6.12, for the methyl fluoride, methyl chloride and methyl bromide, respectively The deviation from linearity is visible from the plots of polarizabilities versus bond length (Figs. 6.16, 6.17, 6.18) for the values greater than +0.01 and less than -0.01. There is a distinct curvature in the line and it is essential for our computations that linearity is maintained as the primary focus is to simulate a vibration at the equilibrium geometry. A 1% error was observed corresponding to ±0.01 for the methyl fluoride, and errors of 2-3% for the methyl chloride and bromide. Nevertheless this value was taken to represent the C-X symmetric vibration.

Further calculations, i.e., polarizability derivatives and AIM analysis, were computed, using ±0.01 Å representing the bond displacement for the C-X (X=F, Cl, Br) and ±0.005 Å, representing bond displacement for C-H bonds.

The polarizabilities were computed for the equilibrium geometry and for geometries corresponding to displacements of the bonds by values stated above (Tables 6.13-{a, b,

TABLE 6.10

Variation in polarizability with change in C-F bond length for CH_3F

Bond length r(Å)	Δr(Å)	Polarizability (α) ($10^{-40}Cm^2/V$)	$\lvert\Delta\alpha\rvert$ ($10^{-40}Cm^2/V$)	Δα/Δr ($10^{-30}Cm/V$)
1.5667	0.20	2.1636	0.1851	0.9253
1.4667	0.10	2.0589	0.0804	0.8041
1.3967	0.03	2.0010	0.0214	0.7142
1.3867	0.02	1.9926	0.0140	0.7007
1.3767	0.01	1.9854	0.0069	0.6873
1.3717	0.005	1.9819	0.0034	0.6805
1.3687	0.002	1.9799	0.0014	0.6765
1.3677	0.001	1.9792	0.0007	0.6751
1.3667	0.00	1.9786	-	-
1.3657	-0.001	1.9779	0.0007	0.6726
1.3647	-0.002	1.9772	0.0013	0.6647
1.3617	-0.005	1.9752	0.0033	0.6670
1.3567	-0.01	1.9720	0.0066	0.6603
1.3467	-0.02	1.9656	0.0129	0.6466
1.3367	-0.03	1.9596	0.0189	0.6328
1.2667	-0.1	1.9252	0.0534	0.5337
1.1667	-0.2	1.9022	0.0768	0.3840

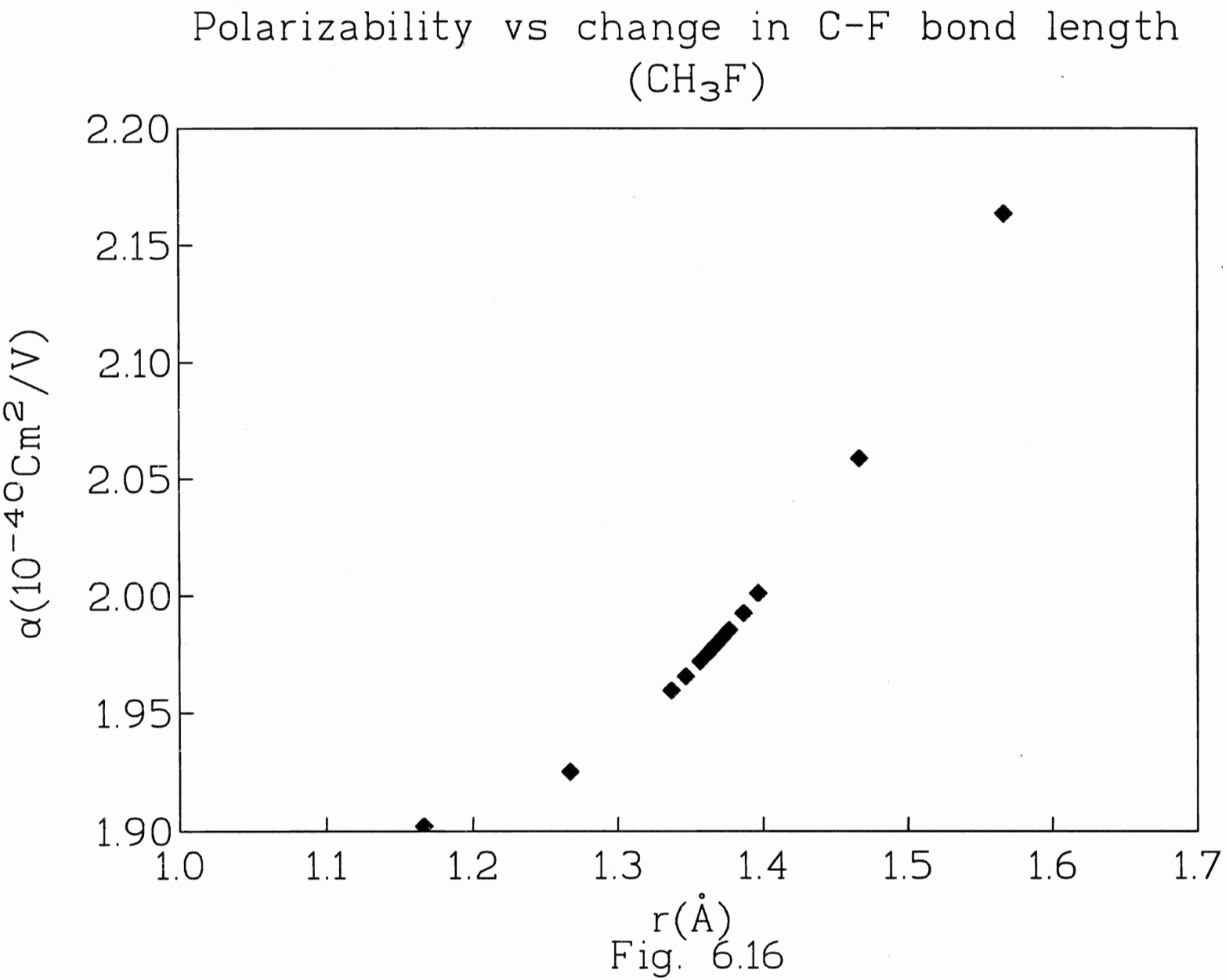
Polarizability vs change in C-F bond length
(CH_3F)
2.20
2.15
2.10
2.05
2.00
1.95
1.90
$\alpha(10^{-40}Cm^2/V)$
1.0
1.1
1.2
1.3
1.4
1.5
1.6
1.7
r(Å)
Fig. 6.16

TABLE 6.11

Variation in polarizability with change in C-Cl bond length for CH_3Cl

Bond length r(Å)	Δr(Å)	Polarizability (α) ($10^{-40}Cm^2/V$)	$\lvert\Delta\alpha\rvert$ ($10^{-40}Cm^2/V$)	Δα/Δr ($10^{-30}Cm/V$)
1.9902	0.20	3.6573	0.4225	2.1123
1.8902	0.10	3.4319	0.1971	1.9714
1.8202	0.03	3.2906	0.0558	1.8588
1.8102	0.02	3.2719	0.0370	1.8526
1.8002	0.01	3.2532	0.0184	1.8374
1.7952	0.005	3.2440	0.0091	1.8297
1.7922	0.002	3.2385	0.0036	1.8250
1.7912	0.001	3.2366	0.0018	1.8234
1.7902	0.00	3.2348	-	-
1.7892	-0.001	3.2329	0.0018	1.8209
1.7882	-0.002	3.2312	0.0036	1.8191
1.7852	-0.005	3.2257	0.0091	1.8144
1.7802	-0.01	3.2168	0.0181	1.8067
1.7702	-0.02	3.1989	0.0358	1.7912
1.7602	-0.03	3.1815	0.0532	1.7756
1.6902	-0.1	3.0684	0.1664	1.6640
1.5902	-0.2	2.9356	0.2992	1.4962

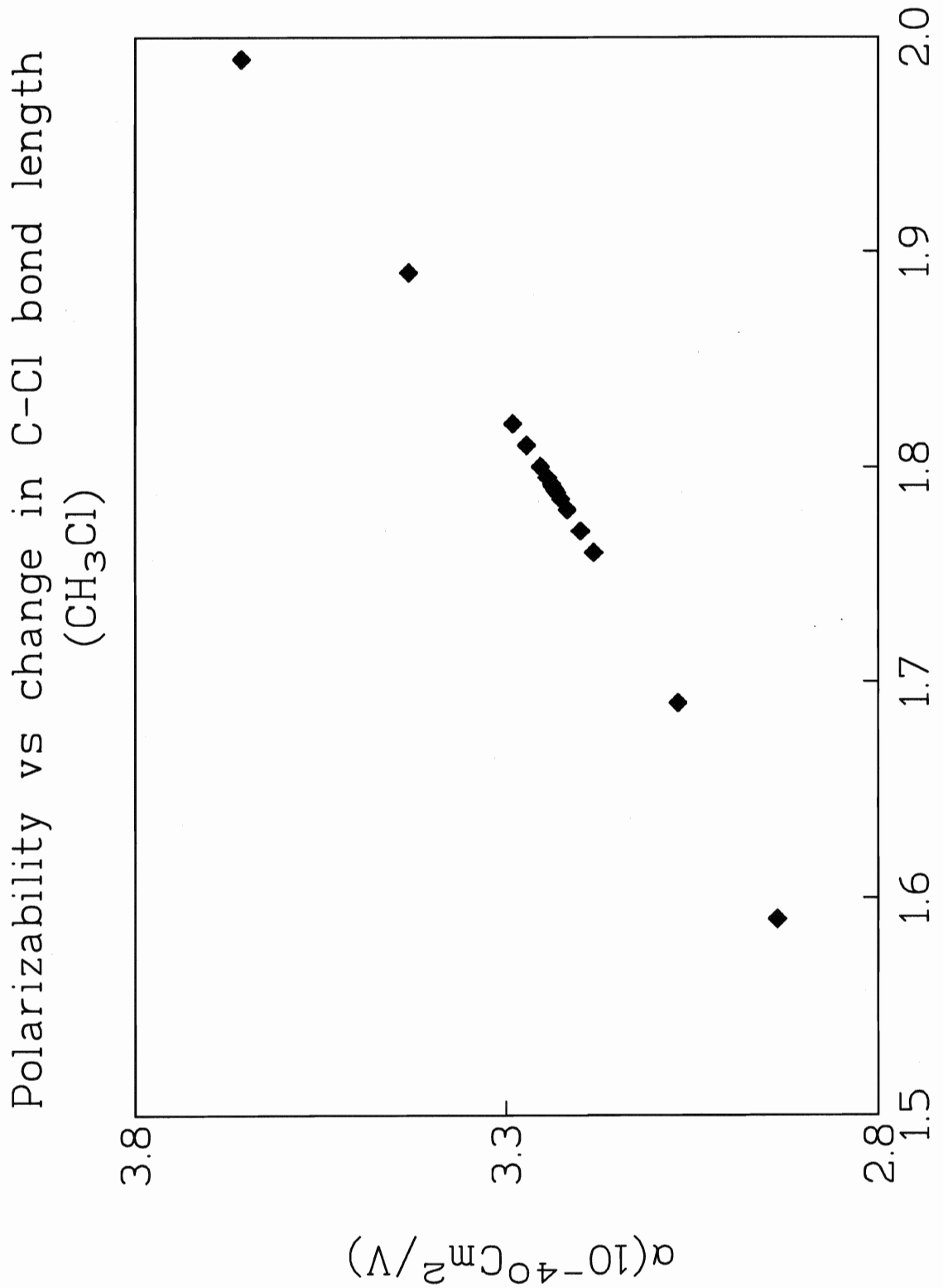
Polarizability vs change in C-Cl bond length
(CH_3Cl)
$\alpha(10^{-40}Cm^2/V)$
3.8
3.3
2.8
1.5
1.6
1.7
1.8
1.9
2.0
r(Å)

Fig. 6.17

TABLE 6.12

Variation in polarizability with change in C-Br bond length for CH_3Br

Bond length r(Å)	Δr(Å)	Polarizability (α) ($10^{-40}Cm^2/V$)	$\lvert\Delta\alpha\rvert$ ($10^{-40}Cm^2/V$)	Δα/Δr ($10^{-30}Cm/V$)
2.2129	0.20	3.9776	0.5999	2.9998
2.1129	0.10	3.6738	0.2962	2.9621
2.0429	0.03	3.4573	0.0797	2.6581
2.0329	0.02	3.4305	0.0529	2.6462
2.0229	0.01	3.4039	0.0263	2.6343
2.0179	0.005	3.3907	0.0131	2.6283
2.0149	0.002	3.3828	0.0052	2.6247
2.0139	0.001	3.3802	0.0262	2.6235
2.0129	0.00	3.3776	-	-
2.0119	-0.001	3.3750	0.0026	2.6211
2.0109	-0.002	3.3724	0.0052	2.6199
2.0079	-0.005	3.3645	0.0131	2.6163
2.0029	-0.01	3.3515	0.0261	2.6102
1.9929	-0.02	3.3256	0.0519	2.5980
1.9829	-0.03	3.3000	0.0776	2.5858
1.9129	-0.1	3.1279	0.2496	2.4969
1.8129	-0.2	2.9054	0.4722	2.3610

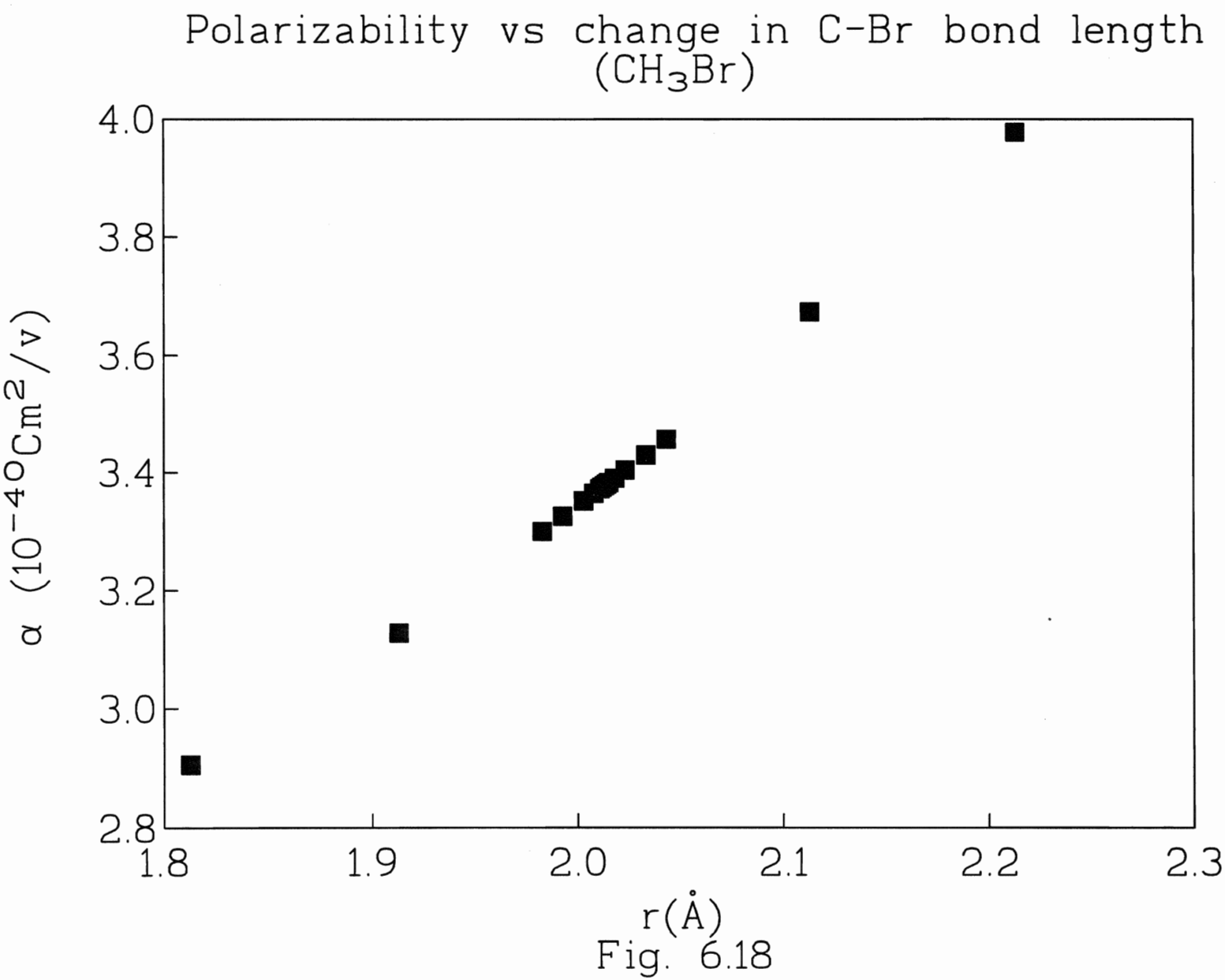
Polarizability vs change in C-Br bond length
(CH_3Br)
4.0
3.8
3.6
3.4
3.2
3.0
2.8
α ($10^{-40}Cm^2/v$)
1.8
1.9
2.0
2.1
2.2
2.3
r(Å)
Fig. 6.18

TABLE 6.13

Comparison of polarizabilities computed via *ab initio* G90 and AIM analysis of the MO wave function.all values in units of $10^{-40}Cm^2/V$

a} CH_3F

Geometry	α_{G90}	α_{AIM}
Equilibrium	1.9786	1.9786
C-H{+.005}	1.9943	1.9943
C-H{-.005}	1.9630	1.9632
C-F{+.01}	1.9854	1.9855
C-F{-.01}	1.9719	1.9716

b} CH_3Cl

Geometry	α_{G90}	α_{AIM}
Equilibrium	3.2348	3.1917
C-H{+.005}	3.2513	3.2330
C-H{-.005}	3.2184	3.1792
C-Cl{+.01}	3.2532	3.2179
C-Cl{-.01}	3.2168	3.1754

TABLE 6.13

Comparison of polarizabilities computed via *ab initio* G90 and AIM analysis of the MO wave function.all values in units of $10^{-40}Cm^2/V$

c} CH_3Br

Geometry	α_{G90}	α_{AIM}
Equilibrium	3.3776	3.3412
C-H{+.005}	3.3972	3.3620
C-H{-.005}	3.3616	3.3263
C-Br{+.01}	3.4039	3.3664
C-Br{-.01}	3.3515	3.3160

TABLE 6.14

Comparison of polarizability derivatives computed via *ab initio* G90 and AIM analysis on the MO wave function all values in units of 10^{-30}Cm/V

CH_3F

Molecule	$(\Delta\alpha/\Delta r)_{G90}$	$(\Delta\alpha/\Delta r)_{AIM}$
C-H{+.005}	1.0537	1.0457
C-H{-.005}	⇒1.047 1.0412	⇒1.036 1.0271
C-F{+.01}	0.6873	0.6873
C-F{-.01}	⇒0.6738 0.6603	⇒0.6928 0.6982

CH_3Cl

Molecule	$(\Delta\alpha/\Delta r)_{G90}$	$(\Delta\alpha/\Delta r)_{AIM}$
C-H{+.005}	1.0965	2.7547
C-H{-.005}	⇒1.086 1.0763	⇒2.011 1.2673
C-Cl{+.01}	1.8374	2.6297
C-Cl{-.01}	⇒1.822 1.8067	⇒2.128 1.6255

CH_3Br

Molecule	$(\Delta\alpha/\Delta r)_{G90}$	$(\Delta\alpha/\Delta r)_{AIM}$
C-H{+.005}	1.3078	1.3818
C-H{-.005}	⇒1.188 1.0675	⇒1.188 0.9942
C-Br{+.01}	2.6343	2.5169
C-Br{-.01}	⇒2.622 2.6102	⇒2.518 2.5199

c}). The polarizability increases on increasing the particular bond, and decreases on decreasing it. The derivatives calculated were then divided by the amount the bond was changed i.e., 0.005 Å for C-H and 0.01 Å for C-X (X=F, Cl, Br), and also by the number of bonds changed i.e., 3 for C-H and 1 for C-X (X=F, Cl, Br). Polarizability derivatives with respect to internal coordinate i.e., bond length, are thus obtained. The mean derivative value was taken for each bond type, and is as depicted in Table 6.14.

From the values calculated, it is observed that the derivatives for the bond increase are slightly larger than those for the bond decrease. However, there is close agreement between values for the bond stretch and bond contract. The mean values are also depicted, and it is a comparison of these values which will be made with the AIM computation and then with experiment.

From the derivatives computed, the following observations are made: For the methyl fluoride the derivative computed for C-F vibration is less than that for the C-H. This is attributed to the small size and high electronegative character of the fluorine atom. For the methyl chloride and bromide the halogen derivative is predicted to be greater than the hydrogen derivative. In fact, the C-Cl is nearly double that for the C-H in methyl chloride, and the C-Br is triple the C-H in methyl bromide. These observations for the derivative values are similar to that of the molecular polarizability, preceding section, wherein the contribution along the z direction was double for the methyl chloride and triple for the methyl bromide relative to the x and y directions. The above discussion may be summarized in the form:

$$\left(\frac{\Delta\alpha}{\Delta r(C-F)}\right)_{CH_3F} < \left(\frac{\Delta\alpha}{\Delta r(C-H)}\right)_{CH_3F} < \left(\frac{\Delta\alpha}{\Delta r(C-H)}\right)_{CH_3Cl} < \left(\frac{\Delta\alpha}{\Delta r(C-H)}\right)_{CH_3Br} < \left(\frac{\Delta\alpha}{\Delta r(C-Cl)}\right)_{CH_3Cl}$$

$$< \left(\frac{\Delta\alpha}{\Delta r(C-Br)}\right)_{CH_3Br}$$

6.2: AIM ANALYSIS-

The AIM analysis, as discussed in Sec. 4, was performed on the wave function obtained by the *ab initio* MO calculation. The following is a discussion of the results obtained from the AIM computation i.e., the polarizability and polarizability derivative. Comparison will be made with G90 computation to check the recovery of the data by the AIM computation. A detailed description of the contributions to the polarizability and polarizability derivatives for the methyl halides will be individually considered. Further, a comparison will also be made with the methane molecule to observe the significant changes. A description of molecular volumes, obtained by summation of atomic volumes, will also be considered.

6.2.1: POLARIZABILITY-

The following is a comparison of the molecular polarizability as computed via G90 and then as recovered by the AIM analysis. Though a different basis set was used for methyl bromide, it is not the reliability of the basis, but the trend in the results which is significant. From the AIM analysis, the main factors of interest include: 1} The recovery by the AIM computation relative to the G90, and 2} A pictorial description of the main factors contributing to the polarizability and the polarizability derivative.

There is observed to be good reproducibility for the methyl fluoride (Table 13a), but consistent error of 1-1.3% for the methyl chloride and bromide (Tables 13-{b, c}), relative to the G90 value. Therefore it may be stated from the above that the AIM computation successfully recovers the information contained in the G90 wave function file. The total polarizability increases on stretching of the bond and decreases on bond contraction. This observation, as stated earlier Sec. 6.1.4, was due to the dependence of the polarizability on bond length.

On observing the contributions of the trace elements for the molecular polarizability (Tables 6-{a, b, c}), the following trend is observed:

1} From G90 computation we have xx = yy, but from AIM we get xx ≈ yy, which is due to a built in asymmetry of the AIM code. This asymmetry does not have a significant error in the final values, but it depends on the type of atom and the integration being carried out at that atom.

2} For the methyl fluoride there is smaller contribution along the z direction as compared with x and y directions.(Table 6.6{a}). An obvious reason, as stated, is that the fluorine atom not only is small in size but is the most electronegative and this results in the charge being concentrated more on the atom than being distributed along the bond. For the methyl chloride, the polarizability along the z direction is nearly double that in the other two directions and for methyl bromide it is nearly triple (Tables 6.6-{b, c}). The reasons for this were stated above and was due to the sizes of the atoms, the number of electrons and the atom electronegativity.

6.2.2:CONTRIBUTIONS OF CHARGE TRANSFER AND ATOMIC DIPOLE TO THE TOTAL POLARIZABILITY FOR THE EQUILIBRIUM GEOMETRY-

The following is an observation of the factors contributing to the molecular polarizability. The charge transfer and the atomic dipole terms sum to give the total polarizability (Eqn. 5.11). The methyl halides will be individually considered, along with a description of the contributions made by each atom. The trend in the halides as the atomic size increases will be examined.

Methyl Fluoride-(Table 6.15a)

Charge transfer: (CT)

The greatest contribution to the CT is from the three hydrogens, which contribute positive charge transfer, the maximum being along the x and y directions. The carbon and

fluorine atoms have zero contribution along x and y direction. Carbon has negative contributions for CT along the z direction

Atomic dipole: (AD)

The carbon has the maximum dipole contribution, though it has a negative value along the x and y direction and a small positive contribution along the z direction. The fluorine atom makes a positive contribution along all three directions, and is of the form: $x=y<z$. The hydrogens have positive contribution along all three directions with the greatest along the z direction.

Methyl Chloride-(Table 6.15b)

Charge transfer: (CT)

The main contributions to the charge transfer arise from the hydrogens which have $x \approx y<z$. The carbon and chlorine have zero contribution in x and y direction, further the carbon has negative contribution and the chlorine a small positive value, along the z direction.

Atomic dipole: (AD)

The carbon makes the largest negative contribution in all directions. There is a positive contribution from the hydrogen and the chlorine atoms, wherein we get $x=y<z$ and $x=y>z$, respectively.

Methyl Bromide-(Table 6.15c)

Charge transfer:(CT)

The carbon and bromine have zero contribution in the x and y direction. In the z direction the carbon has a negative value and the bromine a positive value. The main contribution is from the hydrogens, which exhibit positive value in all directions, with maximum along z axis.

TABLE 6.15

Trace elements of the charge transfer and atomic dipole contributions to the molecular polarizability for the optimized equilibrium geometry, units $10^{-40}Cm^2/V$

a} CH_3F

	Charge Transfer			Atomic Dipole		
Atoms	**xx**	**yy**	**zz**	**xx**	**yy**	**zz**
C	0.0	0.0	-0.710	-0.836	-0.828	+0.003
F	0.0	0.0	+0.378	+0.297	+0.297	+0.435
H	+2.326	+2.338	+1.588	+0.199	+0.161	+0.259

b} CH_3Cl

	Charge Transfer			Atomic Dipole		
Atoms	**xx**	**yy**	**zz**	**xx**	**yy**	**zz**
C	0.0	0.0	-0.466	-0.829	-0.839	-0.651
Cl	0.0	0.0	+1.347	+0.989	+0.989	+0.376
H	+2.253	+2.264	+3.474	+0.169	+0.162	+0.322

c} CH_3Br

	Charge Transfer			Atomic Dipole		
Atoms	**xx**	**yy**	**zz**	**xx**	**yy**	**zz**
C	0.0	0.0	+0.698	-0.533	-0.539	-0.771
Br	0.0	0.0	+1.223	+0.229	+0.229	+0.525
H	+1.982	+1.990	+4.277	+0.221	+0.221	+0.275

Atomic dipole:(AD)

The carbon has the largest negative value, with maximum along the z direction. The bromine and hydrgens exhibit positive values for all directions and further we get x =y <z.

6.2.3: GENERAL TRENDS-

From the preceding discussion, for all the molecules we observe the following: the carbon and halogen have zero charge transfer contribution along the x and y direction. This observation is similar to that in Ref. 13, and this was stated to occur in the case when the atom lies in a plane perpendicular to the field direction. Hence there are zeros for the carbon and respective halogen in x and y directions, and for one of the hydrogens, in the x direction. For the z direction the carbon has a negative contribution for the methyl fluoride and chloride but a positive contribution for the methyl bromide. The halogens make positive contributions along z direction, for all three molecules. The hydrogens contribute significantly in all three directions, with maxima along the z axis. Further the contribution shown for the hydrogens in Table 6.15 is a summation of the charge transfer term for all three hydrogens. This contribution, along the z direction, increases as the size of the halogen atom increases.

The atomic dipole contribution, which is a displacement of charge within the atomic basin in response to the electric field is considered next. The carbon makes the largest negative contribution for all molecules, the only exception being for the methyl fluoride, wherein there is a small positive contribution along the z direction. The negative value of atomic dipole is in agreement with results previously obtained[13]. This was stated to be because the carbon lies in the interior of the molecule and experiences a field that has been modified by the depolarizing field of the hydrogen atoms. The hydrogen and halogen atoms lie on the exterior surface of the molecule and hence experience the external field. Thus they make a positive contribution in all three directions. For the halogen atomic dipole contribution we have x≈y <z for the methyl fluoride and bromide, and x=y>z for

the methyl chloride. No suitable explanation of this observation can be given, but it would be suggested that the contribution should be greater along the z direction and further this value should increase as the halogen size increases.

6.2.4: POLARIZABILITY DERIVATIVES-

The derivatives were numerically determined from the difference in the equilibrium and the distorted polarizabilities. The derivatives were obtained for each type of bond change i.e., C-H and C-X (X=F, Cl, Br). On dividing by the value of change i.e., 0.005 Å for C-H and 0.01 Å for C-X (X=F, Cl, Br), we obtain the polarizability derivative with respect to the symmetry coordinates (Table 6.14).

The values of the results obtained via G90 and AIM are given in Table 6.14. The polarizability derivatives are obtained for the carbon-hydrogen and carbon-halogen simulated vibration. Considering each molecule individually, the observations are as follows.

Methyl Fluoride:

The AIM results are 99% of those obtained via G90 computation. The derivative for the C-H is lower than that for the C-F vibration.

Methyl Chloride:

There is observed a large error in the derivatives obtained with the AIM computation for the C-H and C-Cl vibrations. A suitable explanation for this will be provided when we observe the individual atom contributions to the polarizability derivatives Sec. 6.2.5.

Methyl Bromide:

The results from G90 and AIM are identical for the C-H, but there is a slight difference for the C-Br vibration. Further the halogen derivative is triple that for the hydrogen derivative.

From the preceding observation it may be stated again that in almost all cases the AIM computation successfully recovers the information contained in the G90 read/write file. (Table 6.13). The trend exhibited by the AIM computation for the polarizability and polarizability derivatives is similar to that exhibited in the G90 results Sec. 6.1.4 and 6.1.5. The only exception was the methyl chloride which will be considered shortly.

The theoretical computations predict that the carbon-hydrogen stretch intensity will be less than the respective carbon-halogen stretch intensity. The only exception was for the methyl fluoride wherein the carbon-hydrogen intensity is greater than that of the carbon-fluorine. The reasons for this disparity have already been stated earlier (Sec. 6.1.4), and will not be repeated. Further the carbon-chlorine intensity is double and the carbon-bromine is triple that of the respective carbon-hydrogen value (Sec. 6.1.5).

The additional information provided by the AIM analysis is the break up of the total molecular polarizability into charge transfer and atomic dipole terms.

6.2.5: CHARGE TRANSFER AND ATOMIC DIPOLE CONTRIBUTIONS TO THE POLARIZABILITY DERIVATIVES-

Individual atomic contributions to charge transfer and atomic dipole are now considered. The contributions for each molecule will be considered, following which the general trend will be discussed.

It will be stated in the beginning, that due to symmetry the carbon and respective halogen have zero contributions along the x and y directions. This has been explained in Sec. 6.2.3, and will not be repeated. One of the hydrogens, numbered as three (H3), has zero contribution along the x direction for similar reasons.

The three hydrogens are indistinguishable, however because they are treated differently in the AIM analysis and to clarify discussion of the computation understanding, they were labeled as H3, H4 and H5 (Fig. 4.1). The hydrogens were labeled according to their z matrix orientation which was used in the G90 computation Sec. 4.6. The changes in CT and AD are strongly dependent on the position of the hydrogens relative to the direction of electric field. This point will be discussed later on when the trends are considered.

methyl fluoride-

The changes which occur when the C-H bond is increased and decreased by 0.005Å. Considering the average changes as they are nearly identical when the bond is contracted and when it is increased (Tables 6.16-{a, b}). Small differences if present are because the calculations were performed at the limits of the integration precision. The carbon has the largest change in CT directed along the positive z direction. The fluorine change is smallest relative to other atoms, and is directed along positive z direction. The three hydrogen changes are individually shown and it is seen that H3 values are slightly different relative to H4 and H5, because of the different orientation to the field. These differences are however summed to yield $\Delta\alpha_{xx} = \Delta\alpha_{yy}$. For the z direction, the three hydrogens have similar change along negative z direction. The carbon atomic dipole change is the largest and is positive for all directions, with x=y>z. The fluorine change is negligible for x and y directions, but larger and positive in the z direction. The hydrogen atomic dipoles are large and positive in the x-y plane, small and positive in the z direction.

The changes in the CT and AD for the C-F bond change as shown in Tables 6.16-{c, d}). The carbon has some charge transferred in the negative z direction. The fluorine exhibits maximum charge transfer relative to other atoms, directed along the positive z direction. The three hydrogens show changes in the negative x and y direction and the largest positive change in the z direction. The atomic dipole changes for all atoms are not

Table 6.16

Charge transfer and atomic dipole contributions to the polarizability derivative for each atom type(CH_3F)units of $10^{-40}Cm^2/V$

a} CH {+0.005-equi.}

	ΔCharge Transfer			ΔAtomic Dipole		
Atoms	**xx**	**yy**	**zz**	**xx**	**yy**	**zz**
C	0.0	0.0	0.0078	0.0071	0.0075	0.0054
F	0.0	0.0	0.0008	-0.0001	-0.0001	0.00091
H3	0.0	0.0024	-0.0030	0.0004	0.0058	0.0005
H4	0.0017	0.0006	-0.0030	0.0041	0.0016	0.0005
H5	0.0018	0.0006	-0.0030	0.0044	0.0016	0.0005
ΣH	0.0035	0.0036	-0.0090	0.0089	0.0090	0.0015

b} CH{-0.005- equi.}

	ΔCharge Transfer			ΔAtomic Dipole		
Atoms	**xx**	**yy**	**zz**	**xx**	**yy**	**zz**
C	0.0	0.0	0.0084	0.0075	0.0077	0.0051
F	0.0	0.0	0.0008	-0.0001	-0.0001	0.0009
H3	0.0	0.0018	-0.0031	0.0003	0.0060	0.0005
H4	0.0013	0.0004	-0.0031	0.0043	0.0016	0.0005
H5	0.0014	0.0004	-0.0031	0.0046	0.0016	0.0005
ΣH	0.0027	0.0026	-0.0093	0.0092	0.0092	0.0015

Table 6.16

Charge transfer and atomic dipole contributions to the polarizability derivative for each atom type(CH_3F)units of $10^{-40}Cm^2/V$

c} C-F {+0.01- equi. }

	ΔCharge Transfer			ΔAtomic Dipole		
Atoms	**xx**	**yy**	**zz**	**xx**	**yy**	**zz**
C	0.0	0.0	-0.0029	0.0012	0.0014	-0.0011
F	0.0	0.0	0.0137	0.0004	0.0005	-0.0008
H3	0.0	-0.0018	0.0061	-0.0011	0.0002	-0.0006
H4	-0.0013	-0.0004	0.0060	-0.0001	-0.0007	-0.0007
H5	-0.0013	-0.0004	0.0060	-0.0001	-0.0008	-0.0006
ΣH	-0.0026	-0.0026	0.0181	-0.0013	-0.0017	-0.0019

d} C-F{-0.01- equi.}

	ΔCharge Transfer			ΔAtomic Dipole		
Atoms	**xx**	**yy**	**zz**	**xx**	**yy**	**zz**
C	0.0	0.0	-0.0032	0.0014	0.0015	-0.0008
F	0.0	0.0	0.0131	0.0007	0.0006	-0.0005
H3	0.0	-0.0017	0.0060	-0.0011	0.0001	-0.0006
H4	-0.0013	-0.0004	0.0060	-0.0002	-0.0007	-0.0006
H5	-0.0013	-0.0004	0.0060	-0.0001	-0.0008	-0.0006
ΣH	-0.0026	-0.0025	0.0180	-0.0014	-0.0016	-0.0018

very significant. Further, the changes for all atoms are identical along the negative z direction.

methyl chloride-

The changes in charge transfer and atomic dipole terms when a carbon hydrogen vibration was simulated in the molecule are given in Tables 6.17-{a, b}. There is seen to be a large difference in CT values when the bond is streched and when it is contracted. For the bond contraction the values are nearly double those for the C-H stretch, for all atoms. This could be stated to be an integration error for the instance when the bond was contracted.

The carbon has the least change in charge transfer and then the chlorine, directed along positive z direction for both atoms. The hydrogens have maximum transfer along negative z direction, and equal changes in x and y directions i.e., summation values. The carbon atomic dipole change is maximum relative to other atoms, and is seen to be greater along the y direction. The chlorine has a small negative change in all directions which is of the form x=y > z. The change in the hydrogen atomic dipoles is large in the x-y plane and smaller fot the z direction.

Considering the carbon-chlorine stretch, the changes are as depicted in Tables 6.17-{c, d}. The changes are nearly identical for the bond stretch and contract, hence, an average change will be considered. The carbon atom has maximum charge transferred in the negative z direction. The chlorine has a small change along the positive z direction. The hydrogens have a maximum change along the positive z direction and very small change along the x and y directions. The carbon has the greatest change in atomic dipole along the positive y direction. However, for the carbon-chlorine contraction (Table 6.17d), the carbon has a maximum along the positive z direction and small changes along the negative x and y directions. The chlorine atom atomic dipole change is positive in all directions, with maximum in the z direction. The three hydrogens have very small changes for all

Table 6.17

Charge transfer and atomic dipole contributions to the polarizability derivative for each atom type(CH_3Cl) units of $10^{-40}Cm^2/V$

a} C-H {+0.005-equi.}

	ΔCharge Transfer			ΔAtomic Dipole		
Atoms	**xx**	**yy**	**zz**	**xx**	**yy**	**zz**
C	-0.0	0.0	0.0015	0.0395	0.0641	0.0143
Cl	0.0	0.0	0.0035	-0.0011	-0.0012	-0.0008
H3	0.0	0.0022	-0.0071	0.0003	0.0053	0.0009
H4	0.0016	0.0005	-0.0071	0.0038	0.0014	0.0009
H5	0.0017	0.0005	-0.0071	0.0040	0.0015	0.0009
ΣH	0.0033	0.0032	-0.0213	0.0081	0.0082	0.0027

b} C-H {-0.005-equi.}

	ΔCharge Transfer			ΔAtomic Dipole		
Atoms	**xx**	**yy**	**zz**	**xx**	**yy**	**zz**
C	0.0	0.0	0.0089	0.0041	0.0315	0.0123
Cl	0.0	0.0	0.0070	-0.0012	-0.0012	-0.0008
H3	0.0	0.0017	-0.0148	0.0003	0.0055	0.0009
H4	0.0012	0.0004	-0.0148	0.0039	0.0014	0.0009
H5	0.0013	0.0004	-0.0148	0.0042	0.0015	0.0009
ΣH	0.0025	0.0025	-0.0444	0.0084	0.0084	0.0027

Table 6.17

Charge transfer and atomic dipole contributions to the polarizability derivative for each atom type(CH_3Cl) units of $10^{-40}Cm^2/V$

c} C-Cl {+0.01-equi.}

	ΔCharge Transfer			ΔAtomic Dipole		
Atoms	**xx**	**yy**	**zz**	**xx**	**yy**	**zz**
C	0.0	0.0	-0.0179	0.0	0.0244	0.0073
Cl	0.0	0.0	0.0079	0.0013	0.0013	0.0209
H3	0.0	0.0002	0.0118	-0.0006	0.0002	-0.0004
H4	0.0001	0.0001	0.0118	0.0	-0.0004	-0.0004
H5	0.0011	0.0001	0.0119	0.0001	-0.0004	-0.0004
ΣH	0.0012	0.0004	0.0345	-0.0005	-0.0006	-0.0012

d} C-Cl{-0.01-equi.}

	ΔCharge Transfer			ΔAtomic Dipole		
Atoms	**xx**	**yy**	**zz**	**xx**	**yy**	**zz**
C	0.0	0.0	-0.0199	-0.0045	-0.0018	0.0084
Cl	0.0	0.0	0.0070	0.0016	0.0014	0.0217
H3	0.0	0.0003	0.0121	-0.0006	+0.0002	-0.0004
H4	0.0003	0.0001	0.0121	0.0	-0.0004	-0.0004
H5	0.0003	0.0	0.0120	0.0001	-0.0004	-0.0004
ΣH	0.0006	0.0004	0.0362	-0.0005	-0.0006	-0.0012

directions and all changes are directed along negative directions. The only exception was for the H3 which has a small change along positive y direction.

methyl bromide-

Considering the changes which occur in charge transfer and atomic dipole terms when a carbon-hydrogen vibration is simulated in the molecule. Individual atom changes are as shown in Tables 6.18-{a, b}. The carbon has the greatest change, relative to the other atoms, directed along positive z direction. The bromine charge transferred is the least and is along the positive z direction. The hydrogens show a slight variation for the instance when the C-H bond is stretched and when it is contracted, particularly along the z direction. In both instances, it is maximum along the negative z direction for H4 and H5. H3 has maximum change along positive y direction. On summation we get $\Delta x = \Delta y$.

The atomic dipole change is largest along the negative z direction, for the carbon atom. The bromine atom has the largest change directed along the negative y direction for the C-H stretch. For the C-H contraction the amount of change is similar in all directions. The three hydrogens have positive change in all three directions, and the change is of equal magnitude for the z direction.

The carbon-bromine vibration simulated in the molecule wherein the bond was increased and then decreased by $\pm$ 0.01Å is considered next. The individual atomic contributions are as in Tables 18-{c, d}. The charge transfer is significant along the positive z direction for all atoms. The changes along the x and y direction are zero for all atoms. Further the carbon shows the greatest change and the bromine and hydrogens show changes of equal magnitude.

The carbon has negative change in the x direction and positive along y and z, for the atomic dipole. Bromine has the maximum change along positive z direction, and small changes along negative x and y directions. The three hydrogens have very small changes, which are negative for the x and y directions and positive for the z direction.

Table 6.18

Charge transfer and atomic dipole contributions to the polarizability derivative for each atom type(CH_3Br) units of $10^{-40}Cm^2/V$

a} C-H {+0.005-equi.}

	ΔCharge Transfer			ΔAtomic Dipole		
Atoms	**xx**	**yy**	**zz**	**xx**	**yy**	**zz**
C	0.0	0.0	0.0155	-0.0059	0.0022	0.0011
Br	0.0	0.0	0.0025	-0.0008	-0.0078	0.0007
H3	0.0	0.0092	-0.0010	0.0006	0.0028	0.0007
H4	-0.0064	0.0022	-0.0010	0.0022	0.0011	0.0007
H5	-0.0068	0.0022	-0.0010	0.0023	0.0011	0.0007
ΣH	-0.0132	0.0136	-0.0030	0.0051	0.0050	0.0021

b} C-H {-0.005-equi.}

	ΔCharge Transfer			ΔAtomic Dipole		
Atoms	**xx**	**yy**	**zz**	**xx**	**yy**	**zz**
C	0.0	0.0	0.0236	-0.0018	0.0020	0.0011
Br	0.0	0.0	0.0016	-0.0014	-0.0014	0.0001
H3	0.0	0.0092	-0.0091	0.0008	0.0020	0.0007
H4	-0.0064	0.0022	-0.0092	0.0017	0.0011	0.0007
H5	-0.0068	0.0022	-0.0092	0.0017	0.0011	0.0007
ΣH	-0.0132	0.0136	-0.0275	0.0042	0.0042	0.0021

Table 6.18

Charge transfer and atomic dipole contributions to the polarizability derivative for each atom type(CH_3Br) units of $10^{-40}Cm^2/V$

c} C-Br {+0.01-equi.}

	ΔCharge Transfer			ΔAtomic Dipole		
Atoms	**xx**	**yy**	**zz**	**xx**	**yy**	**zz**
C	0.0	0.0	0.0098	-0.0008	0.0006	0.0009
Br	0.0	0.0	0.0151	-0.0015	-0.0015	0.0076
H3	0.0	0.0001	0.0154	-0.0004	-0.0	0.0002
H4	-0.0	-0.0	0.0154	-0.0001	-0.0003	0.0002
H5	-0.0	-0.0	0.0154	-0.0001	-0.0003	0.0002
ΣH	-0.0	-0.0	0.0462	-0.0006	-0.0006	0.0006

d} C-Br{-0.01-equi.}

	ΔCharge Transfer			ΔAtomic Dipole		
Atoms	**xx**	**yy**	**zz**	**xx**	**yy**	**zz**
C	0.0	0.0	0.0091	-0.0009	0.0013	0.0014
Br	0.0	0.0	0.0147	-0.0016	-0.0016	0.0080
H3	0.0	0.0	0.0153	-0.0004	-0.0	0.0002
H4	-0.0	-0.0	0.0152	-0.0001	-0.0003	0.0002
H5	0.0	-0.0	0.0152	-0.0001	-0.0003	0.0002
ΣH	0.0	-0.0	0.0457	-0.0006	-0.0006	0.0006

6.2.6: GENERAL TRENDS-

From the preceding observations a pattern is observed for the three methyl halides, when a vibration is simulated in the molecule. As stated earlier, it is the CT and AD which combine to give the total polarizability of the molecule. This provides a pictorial description of the effects which occur when a molecule vibrates. We will try to relate this to the observed intensity variations. In nearly all instances the significant changes occur along the z direction for the three molecules. Hence comparison of changes occurring specifically along the z direction will be made.

The contributions of CT and AD to the polarizability derivative for the simulated C-H vibration are considered first. For all three molecules the charge is transferred in the positive z direction for the carbon and halogen. The carbon charge transfer is the maximum relative to all atoms. The only exception is for the methyl chloride, wherein the change is the least at the carbon, which could be a minor integration error over the carbon atom. The hydrogens have charge of equal magnitude transferred along the negative z direction. Further the magnitude of transfer increases from methyl fluoride to chloride but decreases for the bromide. This could be due to the different basis set used for the methyl bromide.

The change in the atomic dipole is positive for all atoms, in all molecules, along the z direction. The only exception was for the methyl chloride, wherein the chlorine atom shows a transfer along the negative z direction. For all molecules the carbon atom shows the greatest change, and further this change is more along the x and y directions. The magnitude of this change increases from fluorine to chlorine but decreases for the bromide. This fact could be attributed to the basis set. The hydrogens have greater change along the x and y and the smallest along z direction. Further, this change is positive and nearly similar for all molecules

For the instance when the carbon and halogen vibration was simulated in the molecule we make the following observations. There is not a general trend exhibited for the three molecules, but the similarities and differences will be considered. The CT change for the carbon is along the negative z direction for the methyl fluoride and chloride but along the positive z direction for the methyl bromide. The halogens exhibit transfer along the positive z direction, and the magnitude is nearly consistent for all three halides. The three hydrogens exhibit maximum transfer along positive z direction, which is of equal magnitude for all three molecules. Further, for the x and y directions the charge transferred is very small, nearly zero.

The carbon atomic dipole change is not very consistent across the three molecules. Of importance is that the change is along the negative z direction for the methyl fluoride and positive for the other two halides. The halogen atomic dipole change, along z direction, increases as the halogen size increases. For the methyl chloride and bromide it is along the positive z direction and for the methyl fluoride it is along the negative z direction. This change for all molecules is nearly identical along the x and y directions. The hydrogens do not show a change of any significance, for all molecules.

From the above observation of trends we can state in general: in the instance when a carbon-hydrogen vibration is simulated in the molecule the changes in polarizability derivatives are primarily from a change in charge transfer. Further this change should increase as the atomic size of halogen increases. For the carbon-halogen vibration, the changes in polarizability derivatives are primarily from the atomic dipole. Also for the bond type it is the atoms which make up the bond that show greater changes.

6.2.7: COMPARISON OF POLARIZABILITY AND POLARIZABILITY DERIVATIVES BETWEEN METHANE AND HALO SUBSTITUTED (F,Cl, Br)-

To observe the significant changes produced in the methane molecule, on substitution of one hydrogen by a heavy atom such as, F, Cl, and Br, a comparison of results obtained

for the methyl halides, will be made with those previously obtained for the methane molecule. As a different basis was used for the methyl bromide there are seen to be large differences. However, we could state what we expect to observe based on changes observed from methane to methyl fluoride to methyl chloride.

REVIEW OF METHANE RESULTS-

From previous calculations[13] performed on the methane molecule, we consider contributions of CT and AD to the polarizability and polarizability derivatives. Considering the molecular polarizability; the carbon atom has zero contributions in all directions and the four hydrogens have x=y=z (2.435), for the CT. The atomic dipole of the carbon is the largest (-0.771), but is of negative value and is equal in all directions. The hydrogen atoms have a smaller positive contribution of equal magnitude for all directions (0.333). The molecular polarizability was 1.997, and further there was excellent recovery by the AIM computation. Units for above quoted values are $10^{-40}Cm^2/V$.

The polarizability derivatives were numerically determined by the procedure outlined for the methyl halides. The only difference was that to simulate a vibration, the C-H bonds were only stretched by 0.005 Å and not contracted. The hydrogens show a small change in the CT term. The main contribution is from the changes in the atomic dipole, which is greater for the carbon relative to the hydrogens. The total polarizability derivative value was calculated to be 1.04 ($10^{-30}Cm/V$).

METHANE AND HALOMETHANE-

When one of the hydrogens is substituted by a halogen atom i.e., fluorine, chlorine or bromine, the following changes are observed. We consider first the distinct changes occurring in the molecule i.e., methane, on substitution. These differences can be stated to have a profound effect on the polarizabilities and polarizability calculations.

The methane has spherical symmetry and belongs to the T_d point group. All hydrogens are symmetrically oriented around the carbon, and are indistinguishable. The methyl halides belong to the C_{3v} point group and the three hydrogens have different orientations with respect to the applied field direction. However, these differences cancel on summation and we obtain equal changes for the x and y directions. The spherical symmetry of the molecule is lost, however the tetrahedral structure is maintained.

The carbon for methane was taken at the origin and hence has zero charge transfer for all directions. In the methyl halides, the carbon is directed along the negative z axis. There is however a significant difference in the orientations of the methane and methyl halides. The comparison would have been more appropriate if the orientations had been similar, none the less a comparison will be made.

The molecular polarizability increases as the atomic number and size increases. All charge transfer terms are not positive, the carbon has zero transfer along the x and y direction and a negative contribution along the z axis (exception was methyl bromide). Both the halogen atom and the hydrogens have positive contribution. Further the atomic dipole contribution is greatest for the carbon, though it makes a negative contribution, which is similar for the methane (exception was z direction in methyl fluoride). The hydrogens make positive contributions in all directions(exception was methyl fluoride).

The polarizability derivative for methane is nearly identical with that of methyl fluoride 1.05 (10^{-30}Cm/V). Significant differences are present in the two molecules, and this similarity in the derivative is suprising. We consider the results obtained from G90 for the derivatives and we observe that there is an increase in the C-H derivatives as the substituted atom size and charge increases. The order of increasing derivative value, in units of 10^{-30}Cm/V, may be written in the form:

$$\{1.04\}_{CH_4} < \{1.05\}_{CH_3F} < \{1.09\}_{CH_3Cl} < \{1.19\}_{CH_3Br}$$

Hence, from the above observation it can correctly be stated that for a particular type of vibration the neighbouring atoms also contribute to the intensity. Further the polarizability derivatives for the C-H bonds are not transferable but are characteristic of the molecule.

6.2.8: MOLECULAR VOLUMES-

The importance of molecular volumes has been explicitly described elsewhere. We consider in the following whether the results previously observed are reproduced. The molecular volumes are obtained in the AIM computation by summation over atomic volumes. The atomic volume is determined, in the AIM analysis, as the region of space formed by the union of the atomic surface with an envelope of the charge density (Sec. 5.1). For interior atoms, the atomic surfaces are bounded by other atoms, hence the above definition is primarily for exterior atoms i.e., hydrogens and halogen. In the PROAIM input (Sec. 5.4), two values of the charge density were quoted namely, 0.001 and 0.002 a.u. It has been found that this value, 0.001 a.u. envelope[13, 56], for the entire molecule gives good agreement with the van der Waals shapes and sizes of molecules. Hence the volumes obtained with the extreme outer surface cut off in the charge density of 0.001 a.u. are only discussed.

A linear relationship was shown to exist between polarizabilities and volumes for methane, ethane, propane and butane. In Table 6.19 are shown the total molecular volumes, obtained by a summation of the atomic volumes, for the methyl halides. The molecular volumes are given for the different geometries i.e., equilibrium, C-H ±0.005Å and C-X ±0.01Å, and for the field applied in different directions.

The molecular volume is seen to increase as the halogen size increases. This is analogous with the increase in polarizability, and hence the above stated linear relationship is observed (Fig. 6.19). Further as the halogen size increases there is a noticeable difference in the volume, charge and energy of all atoms. Though exact values are not quoted, the trend exhibited is stated. There is an increase in carbon charge, volume and

stability. The hydrogens have a decrease in charge, volume and stability. The only exception was for the methyl bromide wherein the hydrogens have increased stability in energy. There is a significant increase in volume of the halogen atom as the size increases, hence an increase in the overall volume. As expected, when the respective bond was stretched i.e., C-H or C-X, the total molecular volume increases, and decreases when the bond is contracted, relative to equilibrium values. This is again analogous with the observations made for the polarizabilities (Tables 13-{a, b, c}). However the increase and decrease in volume was of very small magnitude ≈ 1-2 a.u., for each molecular geometry.

We next consider the instance when a field of magnitude 0.009449 a.u. is applied in the x, y and z directions. The changes in the total molecular volume are as follows, and all changes are relative to the instance when no field is applied i.e., E_0. For the methyl fluoride and chloride, and the different geometries we observe that for a field applied in the x and y directions there is an increase in the total molecular volume. However for a field applied in the z direction there is a decrease in the total molecular volume. The methyl bromide showed the reverse effect i.e., an increase in volume for the field applied in the z direction and a decrease in volume for the x and y directions.

We could go into great detail and consider the effects on individual atoms i.e., charge, volume and stability for a field applied in the x, y and z directions. Further the analysis may be considered for the C-H bond change and respective C-X bond. However it was not thought appropriate to include that analysis in this discussion. Of importance was that from the above analysis we have shown the linear relationship to exist between molecular volume and polarizability. But this was not found in the case of the polarizability derivatives, and we may conclude that the molecular volumes may be appropriately applied only to the molecular polarizabilities.

TABLE 6.19

Molecular volumes, in atomic units, for different geometries and for different field directions

Geometry	E_0	E_x	E_y	E_z
$CH_3F_{(equi.)}$	303.25	303.33	303.06	301.65
$CH_3F_{(C\text{-}H\{+.005\})}$	304.43	304.39	304.60	302.82
$CH_3F_{(C\text{-}H\{-.005\})}$	301.98	302.17	301.97	300.40
$CH_3F_{(C\text{-}F\{+.01\})}$	303.57	304.40	303.39	301.17
$CH_3F_{(C\text{-}F\{-.01\})}$	303.17	303.45	302.20	302.30
$CH_3Cl_{(equi.)}$	424.16	424.62	424.78	423.21
$CH_3Cl_{(C\text{-}H\{+.005\})}$	425.19	425.99	425.74	424.93
$CH_3Cl_{(C\text{-}H\{-.005\})}$	423.19	423.44	423.46	422.17
$CH_3Cl_{(C\text{-}Cl\{+.01\})}$	424.92	425.48	425.59	423.70
$CH_3Cl_{(C\text{-}Cl\{-.01\})}$	422.90	423.78	423.88	422.75
$CH_3Br_{(equi.)}$	482.03	482.29	482.30	474.24
$CH_3Br_{(C\text{-}H\{+.005\})}$	483.21	484.12	483.30	484.86
$CH_3Br_{(C\text{-}H\{-.005\})}$	481.18	481.38	481.46	483.12
$CH_3Br_{(C\text{-}Br\{+.01\})}$	483.34	483.91	483.93	485.30
$CH_3Br_{(C\text{-}Br\{-.01\})}$	480.66	480.62	480.57	482.18

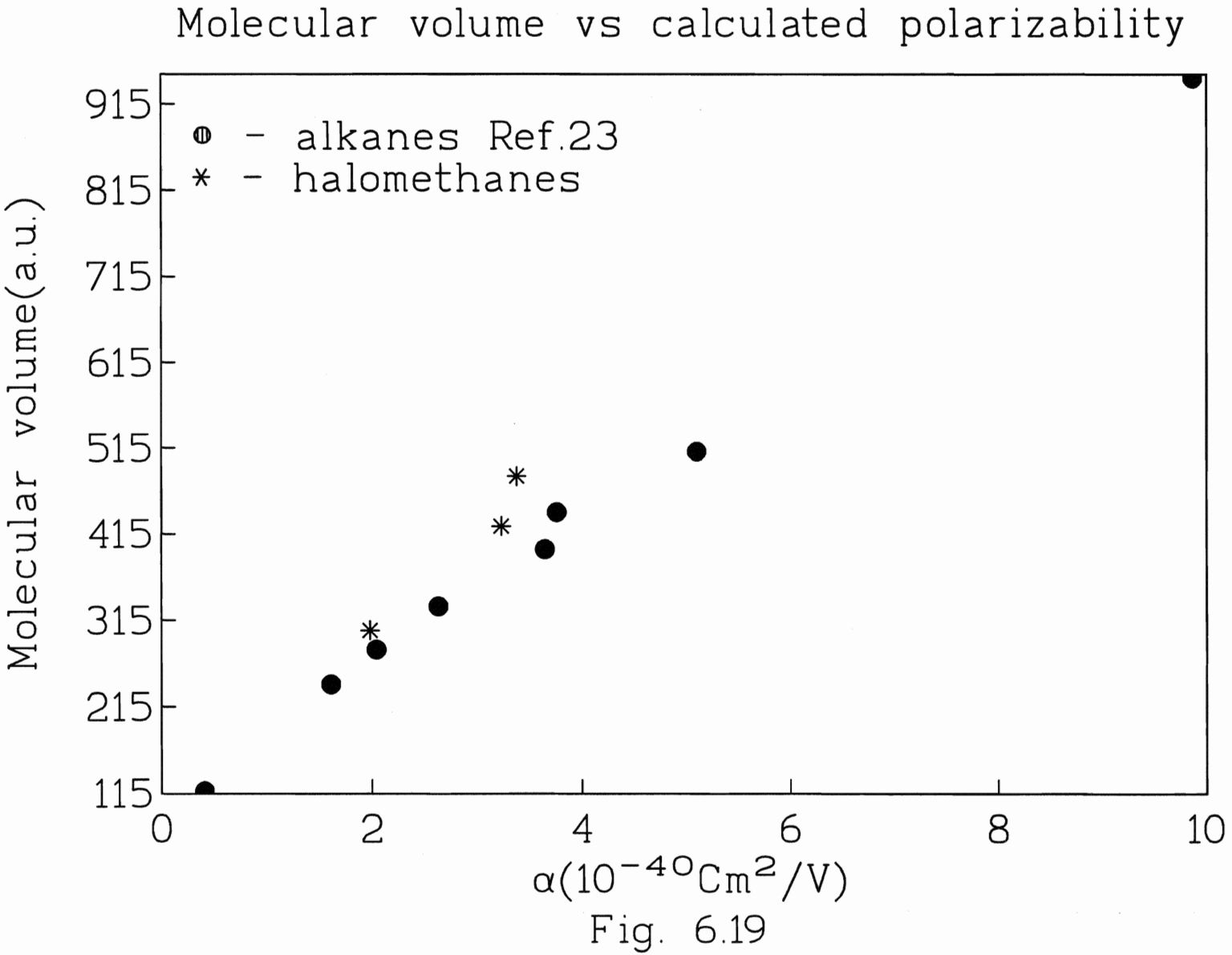
Molecular volume vs calculated polarizability
915
815
715
615
515
415
315
215
115
Molecular volume(a.u.)
- alkanes Ref.23
* - halomethanes
0
2
4
6
8
10
α(10⁻⁴⁰Cm²/V)

Fig. 6.19

6.3:EXPERIMENTAL RESULTS-

The procedure opted for instrument standardization, recording spectra and measuring absolute intensities for the symmetric vibrations has been explained in Secs-3.1.0, 3.1.1, and 3.1.2. We consider in the following results obtained along with a suitable explanation wherever necessary.

6.3.1: STANDARDIZATION RESULTS-

The instrument calibration was carried out following the procedure stated in Sec. 3.1.1, and from the results obtained we draw the following conclusion: There exist flaws in the calibration procedure which are sequentially outlined below.

1} In all standard lamp spectra recorded there was superimposed an interference pattern, which can result in an error of approximately 10% to the intensity measurement. This interference was observed to be due to defective optics: a pin-hole in the polarizer and the presence of a wedge of 1° in the quartz scrambler.

2} The optics were not consistent with those used to record the actual sample spectra. This is the basic requirement of any calibration so that the response of the instrument may be obtained under conditions pertaining to the actual experiment. The changes in optics were thought to be eliminated, however an error was significant. Primarily, changes occurred relative to polarizer and scrambler orientations. This was observed when depolarization ratios were calculated.

3} As stated earlier (Sec. 3.1.1), the output from the standard lamp was different for the two orientations of the polarizer i.e., parallel and perpendicular. However correction factors were obtained with respect to both orientations and appropriately applied.

Although there exist highly disagreeable errors in the calibration procedure, as stated above, absolute intensity values were obtained applying procedure in Sec. 3.1.2. This was thought to be suitable for a qualitative analysis though inappropriate on a quantitative basis. The errors being consistent for all sample spectra could be thought to be

eliminated. This persistent error eliminates a comparison with theory, which is significantly dissatisfactory, however a qualitative analysis will be included.

6.3.2: ABSOLUTE INTENSITIES-

The following is an observation of the results, which are as depicted in Table 6.20, wherein absolute intensities for each molecule, will be individually considered.

methyl bromide-

The carbon-bromine stretch is seen to be the most intense followed by the carbon-hydrogen stretch and the carbon-hydrogen deformation.

methyl chloride-

Only two of the symmetric modes were observed, and this has already been discussed in Sec. 6.1.3. It is seen that the carbon-hydrogen stretch is less intense than the carbon-chlorine stretch.

methyl fluoride-

The carbon-hydrogen stretch is more intense than the carbon-fluorine stretch. The carbon-hydrogen deformation, though there is uncertainty in its assignment, is extremely weak.

6.3.3: COMPARISON WITH THEORY (G90 and AIM)-

From the preceding observation made on the experimentally measured intensities we compare the results for the three methyl halides and draw a general conclusion based on theoretical intensities.

The theoretical intensities were determined, as stated previously (Sec.-4.10 and 5.3), and the results have been discussed in Sec. 6.2.4. An important difference exists between the theory and experimental intensities: the theoretical intensities correspond to the derivative of the polarizability with respect to internal coordinates and the experimental

Table 6.20

Experimental and theoretical absolute intensities for the symmetric vibrations

Molecule/ Mode		$(\frac{\partial\sigma}{\partial\Omega}\times10^{-36})\frac{m^2}{sr}$	$(\frac{\Delta\alpha}{\Delta r}\times10^{-30})$Cm / V	
			G90	AIM
CH_3Br	C-H (stretch)	104.7	1.188	1.188
	C-H(deformation)	3.764	-	-
	C-Br(stretch)	126.9	2.622	2.622
CH_3Cl	C-H (stretch)	200.2	1.086	2.011
	C-H(deformation)	-	-	-
	C-Cl(stretch)	122.0	1.822	2.128
CH_3F	C-H (stretch)	12.50	1.047	1.036
	C-H(deformation)	0.058	-	-
	C-F(stretch)	1.403	0.6738	0.6928

derivatives are with respect to normal coordinates. The values for the C-H stretch correspond to the stretching of the three hydrogens. For each molecule the total intensity will be divided by three, to make a qualitative comparison with theory.

The methyl fluoride has the lowest intensity relative to the other two molecules, which corresponds to the theoretical prediction. From theoretical derivatives Table 6.14, it is observed that the carbon-hydrogen intensities are less than those for the respective halogen stretch. The exception was for the carbon-fluorine intensity which was lower than that for the carbon-hydrogen. This is based on the high electronegativity and small size of the fluorine atom. Experimentally these observations are correctly accounted for in all three molecules.

The only difference, as compared with the theory, was that the carbon-hydrogen stretch is of greater intensity for the methyl chloride relative to the methyl bromide, carbon-hydrogen stretch.

An explanation for the above disagreement is suggested. The experimentally observed intensities corresponding to the symmetric vibrations, though are denoted to be specifically related to a particular bond, are in reality a combination of nuclear displacements. This was clearly depicted in the normal modes obtained with respect to Cartesian coordinates Figs.- 6.9, 6.10, 6.11. Hence, when we consider the symmetric C-H stretch, it is primarily the hydrogens which are displaced, for all molecules. The chlorine and bromine are not displaced at all. Thus the carbon-hydrogen stretch is nearly identical for the methyl chloride and methyl bromide, relative to atomic displacements.

Our theoretical analysis is correct in the observation that the intensity for methyl bromide is greater than for methyl chloride. This is because even though the bromine atom is not displaced, it plays a significant contribution to the intensity, due to its ease of polarization. With this argument, the chlorine atom also contributes to the C-H intensity, but its size and ease of polarization is less than for the bromine atom, and accordingly the intensity of C-H for methyl chloride should be less than methyl bromide. This is correctly

stated as we observe via theory and experiment that the intensity for the C-Br stretch is greater than for the C-Cl stretch.

We thus observe, from the preceding, that a good qualitative comparison between our experiment and theory results is obtained.

A comparison was not made with the avaliable experimental literature data. The main reason was that the intensities measured for the symmetric stretches were total intensities i.e., the trace and anisotropic Eqns. (2.15) and (2.16). The primary focus of our work, as stated earlier, was to measure absolute trace scattering intensities Eqn. (2.17).

7: CONCLUSION-

In the preceding section we considered the results and discussed the trends exhibited. We now conclude the work, and state the flaws and achievements of the research undertaken. Future work which may be undertaken, using this work either as a reference or as a comparison is also outlined.

From the computations earlier performed and the observations made, it may be pointed out that the D95** or D95(p,d), basis set employed here has been shown to produce good reproducibility between G90, AIM and experiment, for the series of hydrocarbons.

The results obtained for the molecules studied i.e., the methyl fluoride, methyl chloride and methyl bromide, it may be inferred that: There is good reproducibility between G90 and AIM for the methyl fluoride. The basis set (D95**) was appropriate for the methyl fluoride as the fluoride atom belongs to the same row of the periodic table as the carbon, and the addition of the d functions on the p function accounts for the charge polarizability suitably.

However, for the methyl chloride where the chlorine atom belongs to the third row of the periodic table, this basis set contains no provision for polarization of the d orbitals present on the chlorine atom. Hence the reproducibility is greatly diminished. It would be necessary, to obtain good reproducibility, to include additional orbitals (f orbital), to allow for the charge polarization.

For the methyl bromide the LANL1DZ basis set resulted in good agreement between G90 and AIM. This basis incorporates D95V (Dunning/Huzinaga valence double zeta) on the first two rows of the periodic table i.e., for the carbon and the hydrogens, and ECP + DZ for the fourth row i.e., for the bromine. We consider if our choice of basis was appropriately made for the methyl bromide. All along it has been stated that even though the theoretical polarizability was extremely low, it was the trend exhibited along with

qualitative description with the AIM which was more important. With this in mind it would have been more appropriate to have used the STO-3G*, basis set as there are advantages with this basis set, namely: The least deviation of geometric parameters compared to experiment, relative with the other two bases sets. The computation with this basis gives Raman intensities and depolarization ratios, though frequencies are greatly deviated compared with experiment. Further the STO-3G* incorporates all 35 electrons of the bromine atom. The LANL1DZ basis, uses only the valence electrons i.e., 7. This may not be a significant problem as the AIM results obtained with the LANL1DZ were comparable with the G90 results.

It is extremely unfortunate that the experimental data is plagued with errors. The data obtained was seen to be not suitable on a quantitative basis. A qualitative analysis was appropriately made with the theory results. However more favourable would have been a quantitative analysis, which will be undertaken in the future. Further, the data obtained could definitely be used as a check when spectra are recorded and measurements made. With a knowledge of the errors known by this work there is a high probability of them not being repeated. Due to insufficient time available the measurements could not be repeated, but we are certain that the work done henceforth will be much improved.

Finally, it seems that there exists a high probability of the work being repeated. The main question than to be asked is, what then have I achieved besides significant errors. I will now focus on the positive aspects of this work.

No previous calculations of the polarizability derivatives have been undertaken for the methyl halides. The methodology used to theoretically simulate a particular vibration in the molecule i.e., by stretching and contracting, has not been performed before. Although no experiment work supports the theory, the results obtained provide a good qualitative picture.

The AIM analysis has successfully reproduced G90 polarizability and polarizability derivatives. The exception was the methyl chloride, wherein a large deviation in the

polarizability derivatives was obtained. With the AIM analysis we can ascertain how the two factors, namely the charge transfer and the atomic dipole significantly contribute to the polarizability and the polarizability derivatives of the molecule. Further the atom size and electronegativity plays a significant role in the intensity variations.

We have successfully reproduced the previous observations obtained with the AIM analysis. Also the correlation between molecular volumes and polarizabilitites was observed.

The experimental values may be used as preliminary data for future work undertaken for the methyl halides.

The work that may be undertaken in the future is as out lined below:

1} Incorporating computations on other molecules, namely molecules where one hydrogen is substituted by either nitrogen or oxygen group. Hence if the reliability of this basis set is to be further enhanced it would be necessary to study the series of molecules which incorporate atoms of the first two rows of the periodic table.

2} To include other elements of the periodic table with suitable changes performed on the basis set and preferentially a basis set which is suitable for the molecules studied.

3} To perform theoretical computations on other modes of vibration namely the bending vibrations.

4} Repeat experimental measurements with proper instrument calibration, wherein results of this work may be used as a check for the appropriateness of the new results.

REFERENCES-

1} E. N. Svenderson, *Dissertation* Odense University (1980).

2} M. Wolkenstein, *Compt. Rend. Acad. Sci.*(USSR), **30**, 791 (1941).

3} L. Silberstein, *Lond. Edinb. Dubl. Phil. Mag.*, **33**, 92 (1917)

4} J. Applequist, J.R. Carl, and K.K. Fang, *J. Am. Chem. Soc.*, **94**, 295 (1972)

5} M. Gussoni, in "ADVANCES IN INFRARED AND RAMAN SPECTROSCOPY", {ed.R.J.H.Clark and R.E.Hester, Heyden, London (1979).}

6} R.E. Hester, in "RAMAN SPECTROSCOPY", {ed.H.A.Szymanski, Plenum Press, New York (1970).}

7} M. Eliashevich and M. Wolkenstein, *J. Phys* .(USSR), **9**, 101 (1945).

8} D.A. Long, *Proc .Roy .Soc. (London)*, **A217**, 203 (1953).

9} J. Tang and A.C. Albrecht, in "RAMAN SPECTROSCOPY" (vol 2), {ed. H.A.Szymanski, Plenum Press, New York (1970)}.

10} S. Montero and G. del. Rio, *Mol. Phys.*, **31**, 357 (1976).

11} W. Holzer, *J. Mol. Spectroscopy.*, **25**, 123 (1968).

12} W. Holzer, *J. Mol. Spectroscopy.*, **27**, 522 (1968).

13} K. M. Gough, H. K. Srivastava and K. Belohorcova, *J. Chem. Phys.*, **98**, 9669 (1993).

14} W.F. Murphy, W. Holzer, and H.J. Berstein, *Appl. Spectrosc.*, **23**, 211 (1969).

15} H. L. Welsh, M. F. Crawford, T. R. Thomas, and G. R. Love, *Can. J. Phy.*, **30** ,577 (1952).

16} H. W. Schrotter, and H. J. Bernstein, *J. Mol. Spectroscopy.*, **12**, 1 (1964).

17} T. Yoshino, and H. J. Bernstein, *J. Mol. Spectroscopy.*, **2**, 213 (1958).

18} G. Placzek, U.S. Atomic Energy Commission, UCRL-Trans, 524(L) (1962) [translated *Handebuch der Radiologie*, 2nd ed., edited by E.Marx, (Akademisch, Leipzig, 1934) Vol. 6, part II, 205-374].

19} J. Morca, C. Domingo, R. Escribano and S. Montero, *J. Raman. Spetrosc.*, **10**, 215

(1981).

20} A. D. Dickson, I. M. Mills, and B. Crawford, Jr., *J. Chem. Phys.*, **27**, 445 (1957).

21} A. J. van Straten and W. M. A. Smit, *J. Chem. Phys.*, **67**, 970 (1977).

22} A. Hinchliffe, "*Ab Initio* DETERMINATION OF MOLECULAR PROPERTIES", (IOP Publishing Ltd 1987).

23} K.M.Gough, *J. Chem. Phys.*, **91(4)**, 2424 (1989).

24} K. M. Gough, H. Srivastava and K. Belohorcova, *J. Chem. Phys. in print.*

25} R. J. Puddephatt and P. K. Monaghan, "THE PERIODIC TABLE OF THE ELEMENTS", {Claredon Press, Oxford (1986).

26} P.R. Griffiths and J.A. de Haseth, "FOURIER TRANSFORM INFRARED SPECTROMETRY", {John Wiley and Sons, Inc. New York (1986) }.

27} A.G. Marshall and F.R. Verdun,"FOURIER TRANSFORMS IN NMR,OPTICAL AND MASS SPECTROMETRY", { Elsevier, New York (1990) }.

28} T. H. Dunning, *J. Chem. Phys.* **53**, 2823 (1970); **55**, 716 (1971).

29} S. Huzinaga, *J. Chem. Phys.*, **42**, 1293 (1965).

30} P. J. Hay and W. R. Wadt, *J. Chem. Phys.*, **82**, 270 (1985).

31} W. R. Wadt and P. J. Hay, *J. Chem. Phys.*, **82**, 284 (1985).

32} Gaussian 90, M.J. Frisch, M. Head-Gordon, G.W. Trucks, J.B. Foresman, H.B. Schlegel, K. Ragavachari, M.A. Robb, J.S. Binkley, C. Gonzalez, D.J. Defrees, D.J. Fox, R.A. Whiteside, R. Seeger, C.F. Melius, J. Baker, R.L. Martin, L.R. Kahn, J.J.P. Stewart, S. Topiol and J.A. Pople, {Gaussian, Inc., PittsburghP.A., (1990).}

33} AIMPAC, McMaster University (1990) C.W. Biegler-Konig, R.F.W. Bader, and Ting-Hua Tang, *J. Comp. Chem.*, **3**, 317 (1982).

34} L.A. Woodward in "RAMAN SPECTROSCOPY",{ed. H.A.Szymanski, Plenum Press New York (1970).}

35} G.W. Chantry in, "THE RAMAN EFFECT"(vol1), {ed. A.Anderson, Marcel Dekker,Inc. New York (1971).}

36} L. A. Woodward, "INTRODUCTION TO THE THEORY OF MOLECULAR VIBRATIONS AND VIBRATIONAL SPECTROSCOPY"{Oxford University Press (1972) }

37} G. Hertzberg, "MOLECULAR SPECTRA AND MOLECULAR STRUCTURE: POLYATOMIC MOLECULES" {Van Nostrand, Princeton, 1955}

38} W.F. Murphy in " ANALYTICAL RAMAN SPECTROSCOPY "{ed. J.G.Grasselli and B.J.Bulkin, John Wiley and Sons, INC.New York (1991).}

39} J. R. Scherer, S. Kint, and G. F. Bailey, *J. Mol. Spectrosc.* **39**, 146 (1971).

40} K. M. Gough and W. F. Murphy, *J. Chem. Phys.*, **87**, 1509 (1987)

41} W. Kiefer, H.J. Bernstein, H. Wieser, and M. Danyluck, *J.Mol.Spectrosc.*, **43**, 393, (1972).

42} F.A. Jenkins and H.E. White, " FUNDAMENTALS OF OPTICS", { McGraw-Hill Book Company, INC.New York (1957).}

43} G.F. Bailey and J.R. Scherer, *Spectrosc.Lett.*, **2**, 261, (1969).

44} R. Scherer and S. Kint, *Applied Optics*, **9**, 1615, (1970).

45} H.W. Schrotter and H.W. Klockner, in "RAMAN SPECTROSCOPY OF GASES AND LIQUIDS", {ed A.Weber,Springer-Verlag Berlin Heidelberg, New York (1979).}

46} Spectra Calc "Galactic Industries Corporation", {Copy right 1990}

47} W.J. Hehre, L. Radom, P.v.R. Schleyer, and J.A. Pople, "AB INITIO MOLECULAR ORBITAL THEORY",{ John Wiley and Sons, New York. (1986).}

48} J.P. Lowe, "QUANTUM CHEMISTRY", {Academic Press, Inc., San Diego, California (1978).}

49} W.G. Richards and J.A. Horsley, "AB INITIO MOLECULAR ORBITAL CALCULATIONS FOR CHEMISTS", {Clarendon Press.Oxford (1970).}

50} R.C. Binning Jr., L.A. Curtiss, *J. Comput. Chem.*, **10**, 1206 (1990).

51} R. F. W. Bader and P. M. Beddall, J. Chem. Phys., **56**, 3320 (1972).

52} E.W. Ignacio and H.B. Schlegel, *J. Phy. Chem.*, **96**, 5830 (1992).

53} S. Glasstone, "TEXT BOOK OF PHYSICAL CHEMISTRY", {Van Nostrand, New York (1946)}

54} R.F.W. Bader," ATOMS IN MOLECULES- A QUANTUM THEORY ", {Claredon-press, Oxford, New York (1990).}

55} R. F. W. Bader, T. T. Ngyen-Dang and Y. Tal., *Rep. Prog. Phys.*, **44**, 893 (1981).

56} R.F.W. Bader, M.T. Carrol, J.R. Cheeseman, and Cheng Chang, *J. Am. Chem. Soc.*, **109**, 7968 (1987).

57} K. Collard and G.G. Hall, *Int. J. Quantum Chem.*, **12**, 623 (1977).

58} R. F. W. Bader, W. H. Henneker and P. E. Cade, *J. Phys. Chem.*, **46**, 341 (1967).

59} R.F.W. Bader, *J.Chem. Phys.*, **91**, 6989 (1989).

60} R.F.W. Bader, T.A. Keith, K.M. Gough and K.E. Laidig, *Mol. Phys.*, **75**, 1167 (1992).

61} R. F. W. Bader and K. E. Laidig, *J. Chem. Phys.*, **93**, 7213 (1990).

62} ALPHA (2.0), H.K. Srivastava and K.M. Gough, Brock University, (1991).

63} M. P. Boggard, A. D. Buckingham, R. K. Pierens and A. H. White, *Faraday Trans.* **I 74**, 3008 (1978).